REPORT ON A HELICOPTER-BORNE Z-AXIS TIPPER ELECTROMAGNETIC (ZTEM) AND AEROMAGNETIC GEOPHYSICAL SURVEY

Alum, Barren Hills, Silver Peak and Pearl Blocks

Yerington & Tonopah, Nevada

For:

Sierra Geothermal Power Corp.

By:

Geotech Ltd.
245 Industrial Parkway North
Aurora, Ont., CANADA, L4G 4C4
Tel: 1.905.841.5004
Fax: 1.905.841.0611
www.geotech.ca
Email: info@geotech.ca

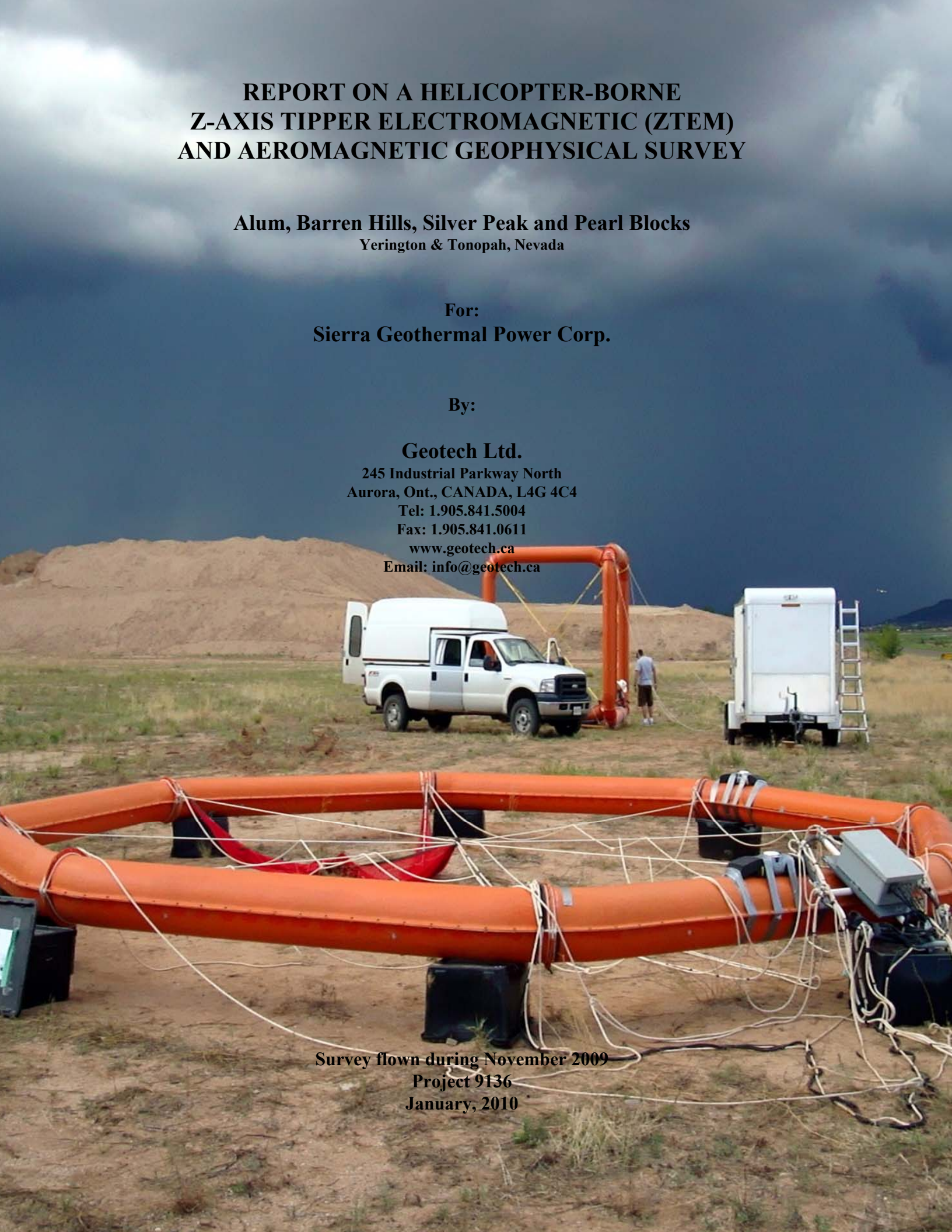

Survey flown during November 2009
Project 9136
January, 2010

TABLE OF CONTENTS

LIST OF FIGURES

LIST OF TABLES

APPENDICES

REPORT ON A HELICOPTER-BORNE Z-AXIS, TIPPER ELECTROMAGNETIC GEOPHYSICAL SURVEY

Alum, Barren Hills and Silver Peak and Pearl Blocks
Yerington and Tonopah, Nevada

Executive Summary

During November 6th to 15th, 2009 Geotech Ltd. carried out a helicopter-borne geophysical survey for Sierra Geothermal Power Corp over the Alum, Barren Hills and Silver Peak and Pearl Block situated near Yerington and Tonopah, Nevada U.S.A.

Principal geophysical sensors included a Z-Axis Tipper electromagnetic (ZTEM) system, and a caesium magnetometer. Ancillary equipment included a GPS navigation system and a radar altimeter. A total of 622 line-kilometres were planned to be flown.

The survey operations were based out of the town of Yerington and Tonopah, Nevada. In-field data quality assurance and preliminary processing were carried out on a daily basis during the acquisition phase. Preliminary and final data processing, including generation of final digital data and map products were undertaken from the office of Geotech Ltd. in Aurora, Ontario.

The survey report describes the procedures for data acquisition, processing, final image presentation and the specifications for the digital data set. There is no formal interpretation presented in this report, however, 2D Inversions are presented in Appendix F.

1. INTRODUCTION

1.1 General Considerations

These services are the result of the Agreement made between Geotech Ltd. and Sierra Geothermal Power Corp. to perform a helicopter-borne geophysical survey over the Alum, Barren Hills and Silver Peak and Pearl blocks located near Yerington and Tonopah Nevada, U.S.A. (Figure 1).

Jeff Witter acted on behalf of Sierra Geothermal Power Corp. during the data acquisition and data processing phases of this project.

The geophysical surveys consisted of helicopter borne AFMAG Z-axis Tipper electromagnetic (ZTEM) system and aero magnetics using a caesium magnetometer. A total of 628 line kilometres of geophysical data were acquired during the survey. The survey area is shown in Figure 2.

In a ZTEM survey, a single vertical-dipole air-core receiver coil is flown over the survey area in a grid pattern, similar to regional airborne EM surveys. Two orthogonal, air-core horizontal axis coils are placed close to the survey site to measure the horizontal EM reference fields. Data from the three coils are used to obtain the Z/X and Z/Y Tipper (Vozoff, 1972) components at six frequencies in the 30 to 720 Hz band. The ZTEM was used to map geology using resistivity contrasts and magnetometer data were also collected to help map geology using magnetic susceptibility contrasts.

Figure 1 -Property Location

The crew was based in Yerington and Tonopah, Nevada, for the acquisition phase of the survey. Survey flying started on November 6th and was completed on November 16th, 2009.

Data quality control and quality assurance, and preliminary data processing were carried out on a daily basis during the acquisition phase of the project. Final reporting, data presentation and archiving were completed from the Aurora office of Geotech Ltd. in January, 2010.

1.2 Survey Location

The Barren Hills Block is located approximately 18 kilometres to the South of Yerington and the Alum and Silver Peak & Pearl Blocks are located approximately 37 kilometres southwest of Tonopah, Nevada as shown in Figure 2.

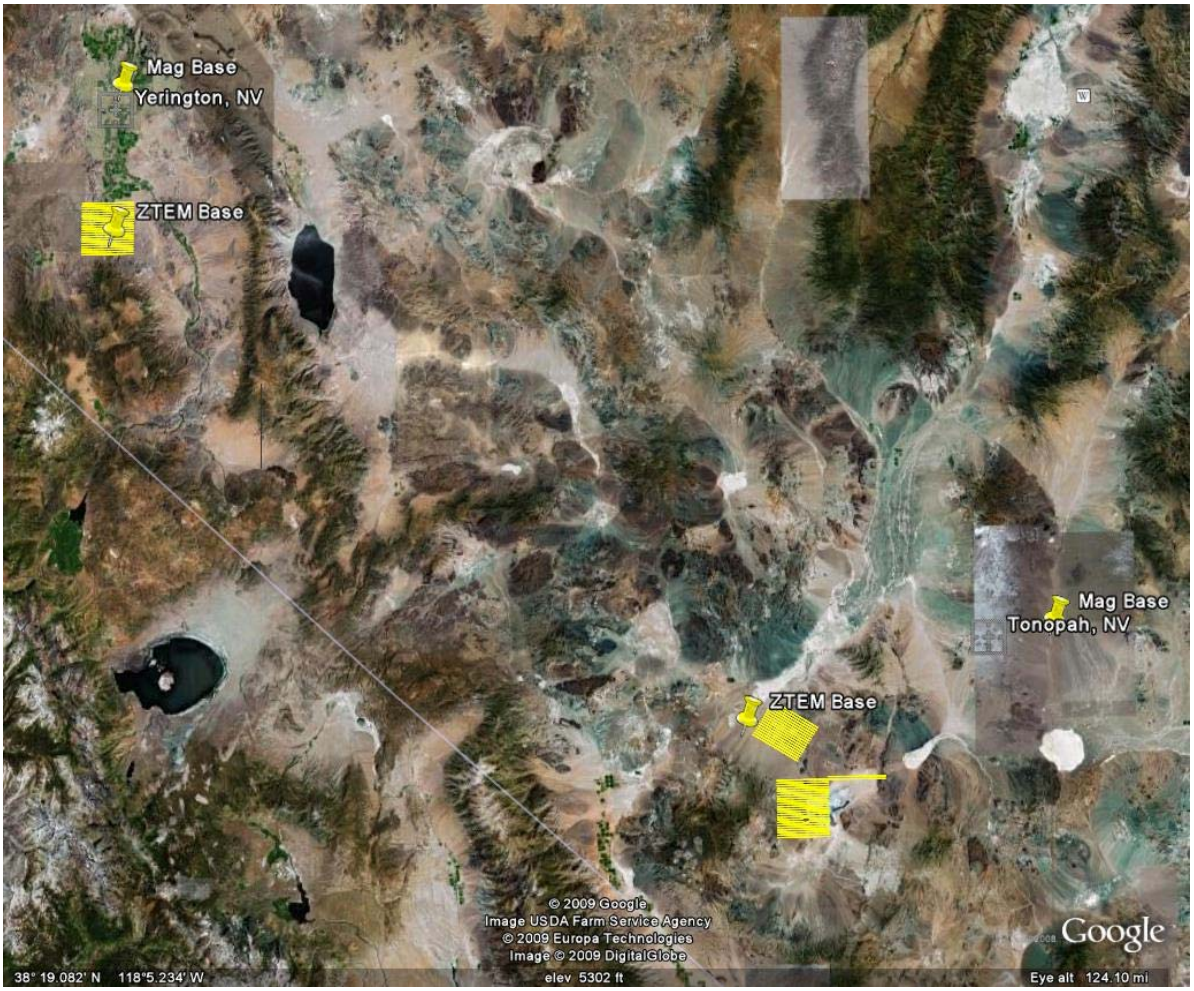

Figure 2 – The Blocks, with ZTEM and Magnetic Base Station Locations

The Barren Hills and Silver Peak & Pearl blocks were flown in an East to West (N 90° E / N 270° E) direction, with a flight line spacing of 500 metres, as depicted in Figure 3 & 4. The Alum block was flown in a Southeast to Northwest (N 122° E / N 302° E) direction, with a flight line spacing of 500 metres, as depicted in Figure 5 Tie lines were neither planned nor flown for this survey block. For more detailed information on the flight spacing and direction see Table 1.

1.3 Topographic Relief and Cultural Features

The Barren Hills Block exhibits a high relief covering 102.3 square kilometres, with an elevation ranging from 1374 to 1890 meters above sea level (see Figure 3). The survey area has visible signs of culture such as, roads and trails running through the survey. The most notable road is highway 208 which runs across the northwest corner of the block. Special care is recommended in identifying any other potential cultural features from other sources that might be recorded in the data.

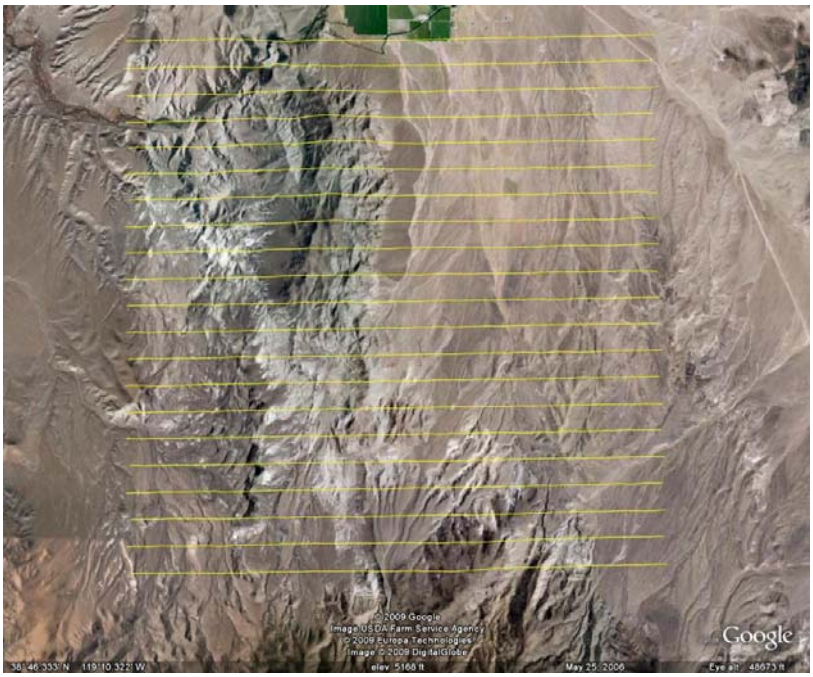

Figure 3 – Google Earth image of the Barren Hills Block.

The Silver Peak & Pearl Block exhibits a high relief covering 122.3 square kilometres, with an elevation ranging from 1289 to 2115 meters above sea level (see Figure 4). The Alum Block exhibits a high relief covering 76.8 square kilometres, with an elevation ranging from 1442 to 1725 meters above sea level (see Figure 5). Both of the survey areas have visible signs of culture such as, roads and trails running through the survey. There are Power lines which cross both blocks. The most notable road is Nivloc Road which runs through the centre of the Silver Peak block and continues through the Alum block to the north. In the Silver Peak Block Silverpeak road runs through the southeast corner of the block ending at the Silver Peak Elementary school located inside the block at the south end. Special care is

recommended in identifying any other potential cultural features from other sources that might be recorded in the data.

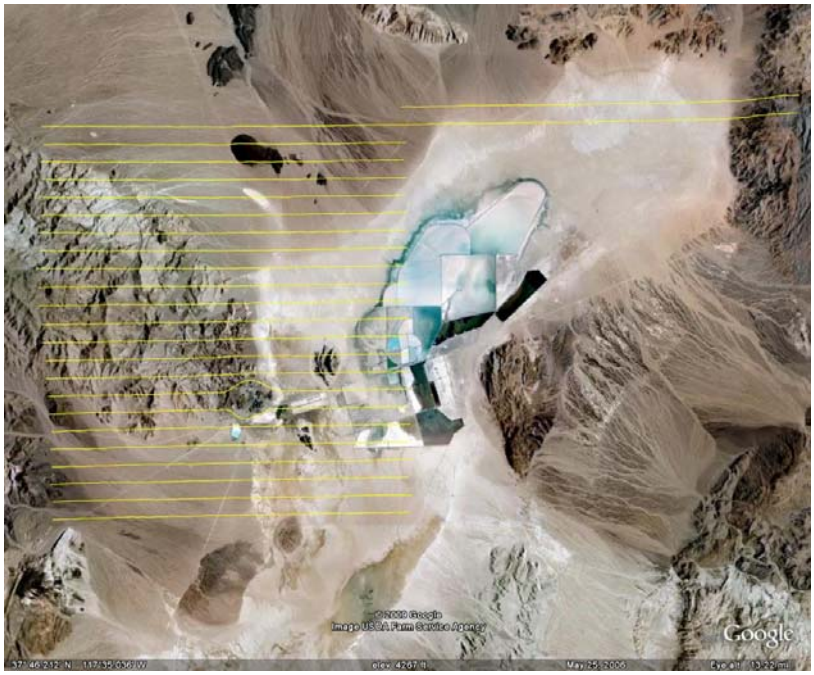

Figure 4 - Google Image of the Silver Peak & Pearl Block

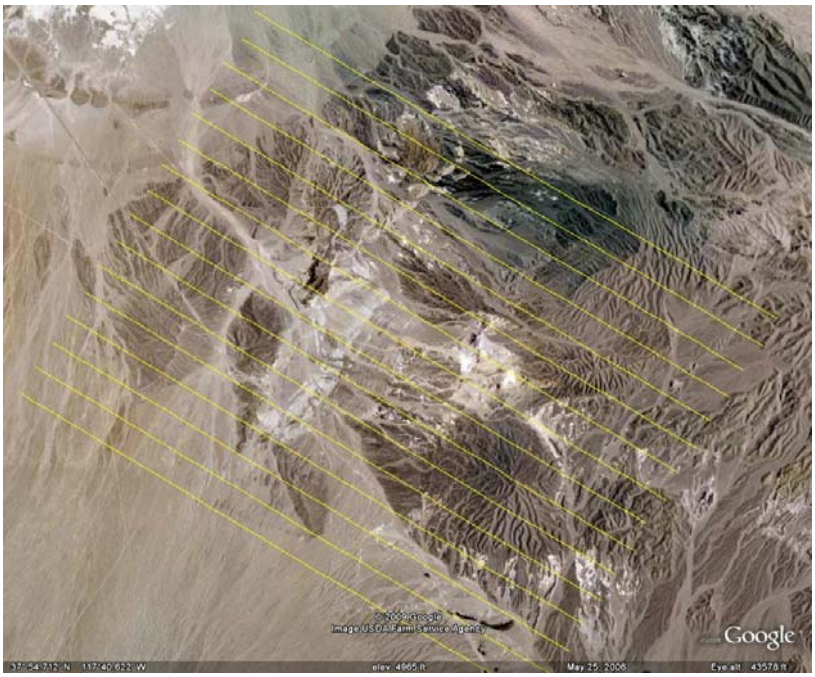

Figure 5 - Google Image of the Alum Block

2. DATA ACQUISITION

2.1 Survey Area

The survey blocks (see Location map in Appendix A and Figure 2) and general flight specifications are as follows:

Table 1 - Survey Specifications

Survey block	Traverse Line spacing (m)	Area (Km^2)	Planned Line-km	Actual[1] Line-km	Flight direction	Line numbers
Alum Block	Traverse: 500	76.8	160	161.8	N 122° E / N 302° E	L 1000- L1150
SilverPeak Block	Traverse: 500	122.3	252	254.9	N 90° E / N 270° E	L 2000- L2230
Barren Block	Traverse: 500	102.3	210	212.2	N 90° E / N 270° E	L 3000- L3200
TOTAL		**301.4**	**622**	**628.9**		

Survey block boundaries co-ordinates are provided in Appendix B.

2.2 Survey Operations

Survey operations were based out of Yerington Nevada, on November 6th to November 11th, 2009 and Tonopah Nevada, on November 12th to November 15th, 2009. The following table shows the timing of the flying.

Table 2 - Survey schedule

Date	Flight #	Flown km	Block	Crew location	Comments
11-06-2009				Yerington Nevada	System Installation
11-07-2009				Yerington Nevada	System Installation
11-08-2009				Yerington Nevada	System Installation
11-09-2009				Yerington Nevada	System Installation
11-10-2009	1,2,3	210	Barren	Yerington Nevada	Production
11-11-2009				Yerington Nevada	Moved to Tonopah
11-12-2009	4,5,6	412	S/B, S/A, A/P	Tonopah Nevada	Production
11-13-2009	7,8,9	270	SP/A	Tonopah Nevada	Re-flights Production
11-14-2009	10	130	S/P	Tonopah Nevada	Re-flights Production
11-15-2009				Tonopah Nevada	Job complete

[1] Actual line-km represents the total line-km contained in the final databases. These line-km normally exceed the Planned line-km's, as indicated in the survey NAV files. Table two shows a large number of kms flown because there were a number of re-flights

2.3 Flight Specifications

During the survey the helicopter was maintained at a mean height of 169 metres above the ground with a nominal survey speed of 80 km/hour for the survey block. This allowed for a nominal EM sensor terrain clearance of 95metres and a magnetic sensor clearance of 111 metres.

The output data sampling rate from the acquisition program was 0.4 second for electromagnetics, 0.1 second for magnetometer and 0.2 second for altimeter and GPS. This translates to electromagnetic readings at approximately 10m intervals and magnetic readings roughly every 2 to 5 metres along flight track. Navigation was assisted by a CDGPS receiver and data acquisition system, which reports GPS co-ordinates as latitude/longitude and directs the pilot over a pre-programmed survey flight path.

The operator was responsible for monitoring of the system integrity. He also maintained a detailed flight log during the survey, tracking the times of the flight as well as any unusual geophysical or topographic feature.

On return of the aircrew to the base camp the survey data was transferred from a compact flash card (PCMCIA) to the data processing computer. The data were then uploaded via ftp to the Geotech office in Aurora for daily quality assurance and quality control by trained personnel, operating remotely.

2.4 Aircraft and Equipment

2.4.1 Survey Aircraft

The survey was flown using a Eurocopter Aerospatiale (Astar) 350 B3 helicopter, registration number N354SH. The helicopters were owned and operated by Sinton Helicopters Ltd. Installation of the geophysical and ancillary equipment was carried out by Geotech Ltd.

2.4.2 Airborne Receiver

The airborne ZTEM receiver coil measures the vertical component (Z) of the EM field. The receiver coil is a Geotech Z-Axis Tipper (ZTEM) loop sensor which is isolated from most vibrations by a patented suspension system and is encased in a fibreglass shell. It is towed from the helicopter using a 90 metre long cable as shown in Figure 6. The cable is also used to transmit the measured EM signals back to the data acquisition system.

The coil has a 7.4 metre diameter with an orientation to the Vertical Dipole. The digitizing rate of the receiver is 2000 Hz. Attitudinal positioning of the receiver coil is enabled using 3 GPS antennas mounted on the coil. The output sampling rate is 0.4 seconds (see Section 2.4.7)

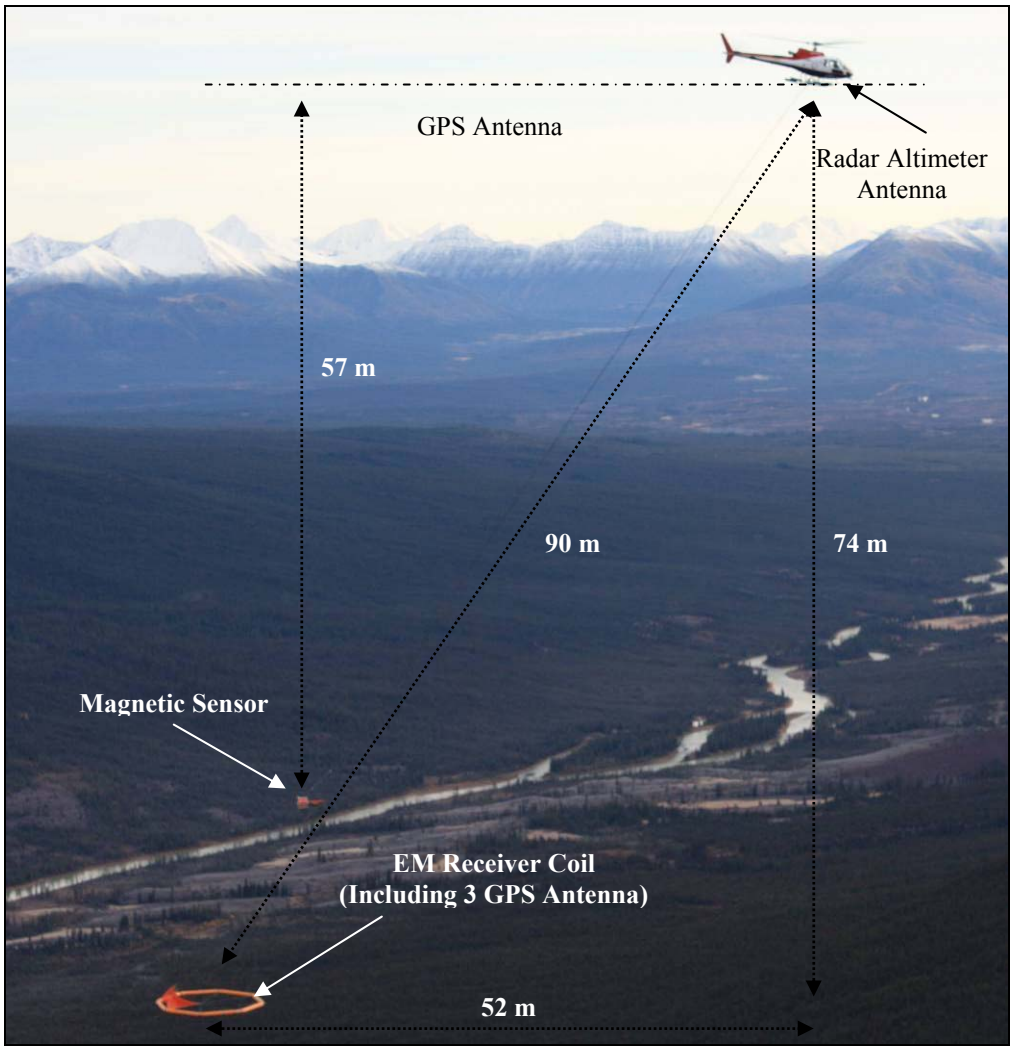

Figure 6 - ZTEM System Configuration

2.4.3 Base Station Receiver

The two Geotech ZTEM base station receiver coils measure the orthogonal, horizontal X and Y components of the EM reference field. They are set up perpendicular to each other and roughly oriented according to the flight line direction. The orientation of both units is not critical as the horizontal field can be further decomposed into the two orientations of the survey flight. The orientation of the base stations were measured using a compass.

The base station coils each have a diameter of 3.5 meters, with the coil orientations to the horizontal dipole, as shown in Figure 7.

The Barren Block base station receiver coils were installed in a remote area inside the survey block (38 44.860 N, 119 10.289 W). The coils were oriented perpendicular to each other: Coil A was oriented at an N 340° E direction, with coil B oriented at an N 250° E direction.

The Alum and Sliver Peak Blocks base station receiver coils were installed in a remote area 3 kilometres west of the Alum the survey block (37 54.094N, 117 46.535 W). The coils were

oriented perpendicular to each other: Coil A was oriented at an N 80° E direction, with coil B oriented at an N 350° E direction.

Figure 7 - ZTEM base station receiver coils.

2.4.4 Airborne magnetometer

The magnetic sensor utilized for the survey was a Geometrics split-beam optically pumped caesium vapour magnetic field sensor, mounted in a separate bird, and towed on a cable at a mean distance of 57 metres below the helicopter (Figure 6). The sensitivity of the magnetic sensor is 0.02 nanoTesla (nT) at a sampling interval of 0.1 seconds. The magnetometer will perform continuously in areas of high magnetic gradient with the ambient range of the sensor approximately 20k-100k nT. The Aerodynamic magnetometer noise is specified to be less than 0.5 nT. The magnetometer sends the measured magnetic field strength as nanoTesla to the data acquisition system via the RS-232 port.

2.4.5 Radar Altimeter

A Terra TRA 3000/TRI 40 radar altimeter was used to record terrain clearance. The antenna was mounted beneath the bubble of the helicopter cockpit.

2.4.6 GPS Navigation System

The navigation system used was a Geotech PC104 based navigation system utilizing a NovAtel CDGPS (Canada-Wide Differential Global Positioning System Correction Service) enabled Propak V3-RT20 GPS receiver. Geotech's Navigate software, using a full screen display with controls in front of the pilot, allows him to direct the flight.

5 NovAtel GPS antennas are utilized during the survey; one is mounted on the helicopter tail (Figure 6), one installed with the Receiver Base Station (Figure 7) and three are mounted on the airborne receiver (Figure 6). As many as 14 GPS and two CDGPS satellites may be monitored at any one time. The horizontal positional accuracy or circular error probability (CEP) is 1.8 m, with CDGPS active, it is 0.6 m. The co-ordinates of the block were set-up prior to the survey and the information was fed into the airborne navigation system.

2.4.7 Digital Acquisition System

The power supply and the data acquisition system are mounted on an equipment rack which is installed into the helicopter. Signal and power wires are run through the helicopter to connect on to the tow cable outside. The tow cable supports the ZTEM and magnetometer birds during flight via a safety shear pin connected to the helicopter hook. The major power and data cables have a quick disconnect safety feature as well. The installation was undertaken by the Geotech Ltd. crew and was certified before surveying.

A Geotech data acquisition system recorded the digital survey data on an internal compact flash card. Data is displayed on an LCD screen as traces to allow the operator to monitor the integrity of the system. The data type and sampling interval as provided in Table 3.

Table 3 - Acquisition and Processing Sampling Rates

DATA TYPE	ACQUISITION SAMPLING	PROCESSING SAMPLING
ZTEM Receiver	0.0005 sec	0.4 sec
Magnetometer	0.1 sec	0.4 sec
GPS Position	0.2 sec	0.4 sec
Radar Altimeter	0.2 sec	0.4 sec
ZTEM Base station	0.0005 sec	– –

2.4.8 Mag Base Station

A combined magnetometer/GPS base station was utilized on this project. A Geometrics Caesium split-beam vapour magnetometer was used as a magnetic sensor with a sensitivity of 0.001 nT. The base station was recording the magnetic field together with the GPS time at 1 Hz on a base station computer.

The base station magnetometer sensors for the Barren Hills Block (39 00.0789N, 119 09.5063W) and for the Alum and Silver Peak & Pearl Blocks (38 4.082 N, 117 5.724 W) were installed away from electric transmission lines and moving ferrous objects such as motor vehicles. The base station data were backed-up to the data processing computer at the end of each survey day.

3. PERSONNEL

The following Geotech Ltd. personnel were involved in the project.

Field:

Project Manager:	Lee Harper (Office)
Data QA/QC:	Harish Kumar (Office)
Crew chief:	Les Moschuk
System Operators:	Paul Taylor

The survey pilot and the mechanical engineer were employed directly by the helicopter operator – Sinton Helicopters Ltd.

Pilot:	Scott Sinton

Office:

Preliminary Data Processing:	Rafael Coyoli
Final Data Processing:	Rafael Coyoli
Final Data QC:	Biljana Milicevic
Interpretation/2D Inversion:	Eugeme Druker
Reporting/Mapping:	Wendy Acorn

Data acquisition phase was carried out under the supervision of Andrei Bagrianski, P. Geo, Surveys Manager. Processing phase was carried out under the supervision of Gord Smith, Manager of Data Processing. Interpretation 2D Inversion stage was under the supervision of Jean Legault, Chief Geophysicists (Interpretation).The overall contract management and customer relations were by Paolo Berardelli.

4. DATA PROCESSING AND PRESENTATION

Data compilation and processing were carried out by the application of Geosoft OASIS Montaj and programs proprietary to Geotech Ltd.

4.1 Flight Path

The flight path, recorded by the acquisition program as WGS 84 latitude/longitude, was converted into the NAD83, UTM Zone 11 North coordinate system in Oasis Montaj.

The flight path was drawn using linear interpolation between x, y positions from the navigation system. Positions are updated every second and expressed as UTM easting's (x) and UTM northing's (y).

4.2 In-field Processing and Quality Control

In-Field data processing and quality control are done on a flight by flight basis by a qualified data processor (see Section 3.0). Processing steps and check up procedures are designed to assure the best possible final quality of ZTEM survey data. A general overview of those steps is presented in the following paragraphs.

The In-Field quality control can be separated into several phases:

a. GPS Processing Phase: GPS Data are first examined and evaluated during the GrafMov processing.
b. Raw data, ZTEM viewer phase:

   Data can be viewed, examined for consistency, individual channel spectra examined and overall noise estimated in the viewer provided by the ZTEM proprietary software, on the raw flight data and raw base station data separately, on the merged data, and finally on the data that have undergone ZTEM processing.
c. Field Geosoft phase:

   Magnetic data, Radar altimeter data, GPS positioning data are re-examined and processed in this phase. Prior to splitting the lines EM data are examined flight by flight and the effectiveness of applying the attitude correction evaluated. After splitting the lines, a set of grids are generate for each parameter and their consistency evaluated. Data profiles are also re-evaluated on a line to line basis. A power line monitor channel is available in order to identify power line noise.

4.3 GPS Processing

Three GPS sensor (mounted on the airborne receiving loop) measurements were differentially corrected using the Waypoint GrafMov^{TM} software in order to yield attitude corrections to recorded EM data.

4.4 ZTEM Electromagnetic Data

The ZTEM data were processed using proprietary software. Processing steps consist of the following preliminary and final processing steps:

4.4.1 Preliminary Processing (AFMAG)

a. Airborne EM, Mag, radar altimeter and GPS data are first merged with EM base station data into one file.
b. Merged data are viewed and examined for consistency in an incorporated viewer
c. In the next, processing phase, the following entities are taken into account:
   - the Base station coils orientation with respect to the Magnetic North,
   - the Local declination of the magnetic field,
   - Suggested direction of the X coordinate (North or line direction),
   - Sensitivity coefficient that compensates for the difference in geometry between the base station and airborne coils.
   - Rejection filters for the 60 Hz and helicopter generated frequencies.
d. Six frequencies (In phase and Quadrature components) are extracted from the airborne EM coil response in the windows of 0.4 seconds and the base station coils in the windows of 1.0 seconds (30, 45, 90, 180, 360, and 720 Hz).
e. The ratios between the real parts (in phase) of the vertical Z component (airborne) over the horizontal X component (base station), and Z component over horizontal orthogonal Y component, as well as the ratios of their imaginary parts (quadrature), are calculated.
f. Such processed EM data are then merged with the GPS data, magnetic base station data and exported into a Geosoft xyz file.

4.4.2 Geosoft Processing

Next stage of the preliminary data processing is done in a Geosoft ™ environment, using the following steps:

a. Import the output xyz file from the AFMAG processing, as well as the base Mag data into one database.
b. Split lines according to the recorded line channel,
c. GPS processing, flight path recovery (correcting, filtering, calculating Bird GPS coordinates, line splitting)
d. Radar altimeter processing, yielding the altitude values in metres.
e. Magnetic spike removal, filtering (applied to both airborne and base station data). Calculation of a base station corrected mag.
f. Apply preliminary attitude corrections to EM data (In phase and Quadrature), filter and make preliminary grids and profiles of all channels.

4.4.3 Final Processing

Final data processing and quality control were undertaken by Geotech Ltd headquarters in Aurora, Ontario by qualified senior data processing personnel.

A quality control step consisted of re-examining all data in order to validate the preliminary data processing and to allow for final adjustments to the data.

Attitude corrections were re-evaluated, and re-applied, on component by component, flight by flight, and frequency by frequency bases. Any remaining line to line system noise was removed by applying a mild additional levelling correction.

4.4.4 ZTEM Profile Sign Convention

Z/X and Z/Y components do not exhibit maxima or minima above conductors, resistors or at contacts; in fact they produce cross-over type anomalies (Ward, 1959). The crossover polarity sign convention for ZTEM is according to the right hand Cartesian rule (Z positive –up) that is commonly used for multi-component transient electromagnetic methods.

For the East to West lines at the Barren Hills and Silver Peak & Pearl Blocks the sign convention for the Z/X in-line component crossover is positive-negative pointing West to East for tabular conductors perpendicular to the profile (Figure 8). The corresponding Z/Y component in-phase cross-over polarity is positive-negative pointing South to North (90 degrees counter clockwise to Z/X) according to the right hand Cartesian rule.

For the NW to SE lines at the Alum Block the sign convention for the Z/X in-line component crossover is positive-negative pointing NW to SE for tabular conductors perpendicular to the profile (Figure 9). The corresponding Z/Y component in-phase cross-over polarity is positive-negative pointing SW to NE (90 degrees counter clockwise to Z/X) according to the right hand Cartesian rule.

Conversely, tabular resistive bodies produce In-Phase cross-over's that are opposite in sign to conductors. A brief discussion of ZTEM and AFMAG, along with selected forward model responses is presented in Appendix D.

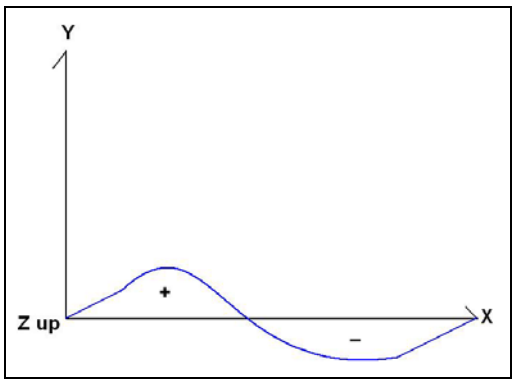

Figure 8 - ZTEM Crossover Polarity Convention for the Barren & Silver Peak Blocks.

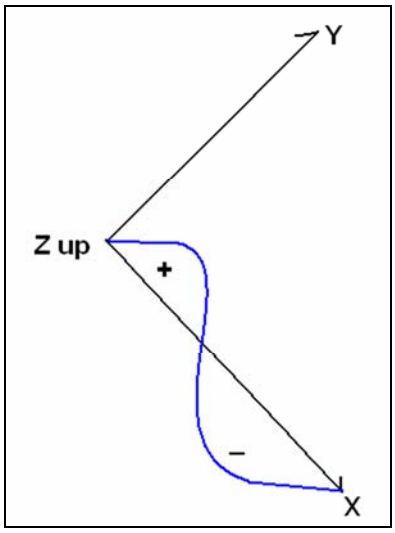

Figure 9 - ZTEM Crossover Polarity Convention of the Alum Block

4.4.5 ZTEM Quadrature Sign Dependence

One important note regarding the sign of the ZTEM Quadrature, relative to the In-Phase component, particularly with regards to computer modeling and inversion.

The sign of the magnetotelluric Quadrature relative to the In-Phase tipper transfer function component pertains to the Fourier transformation of the time series to give frequency domain spectra. There are two widely used conventions for time dependence in the transformations, **exp(+iωt)** and **exp(-iωt)**. That which is implemented largely is a matter of personal preference and precedent. The importance of the In-Phase and Quadrature sign convention is not critical, provided that it is known and documented.

In ZTEM, the data processing code used for the Fourier transformation the time-series data to frequency domain spectra adopts a **exp(-iωt)** time dependence (J. Dodds, Geo Equipment Manufacturing, pers. comm., Nov-2009). Whereas in the forward modeling and inversion program Zvert2d, the sign of the Quadrature relative to the In-Phase transfer function assumes an **exp(+iωt)** dependence[2].

The reasons for adopting $\mathbf{e^{-i\omega t}}$ used in ZTEM are several: a) In-phase and Quadrature profile and contour plan maps can be readily compared, since they are usually in the same-sign and quadrant (i.e.,Figure 10); b) Phase-rotation and Total Divergence (DT) parameters need not be changed when comparing In-Phase versus Quadrature data.

As a result, for users interested in computer modeling and inversion of ZTEM data, the sign of the Quadrature may need to be reversed, relative to the In-Phase component, depending upon the convention in the users modeling software (Figure 10). Indeed this reverse Quadrature polarity convention is assumed in all in-house forward modeling and inversion of

2 Phillip E. Wannamaker (2009): Two-dimensional Inversion of ZTEM data: Synthetic Model Study and Test Profile Images, Internal Geotech technical report by Emblem Exploration Services Inc., January 22, 2009, 32 pp.

ZTEM data, as described in Figures 5-7 in Appendix D.

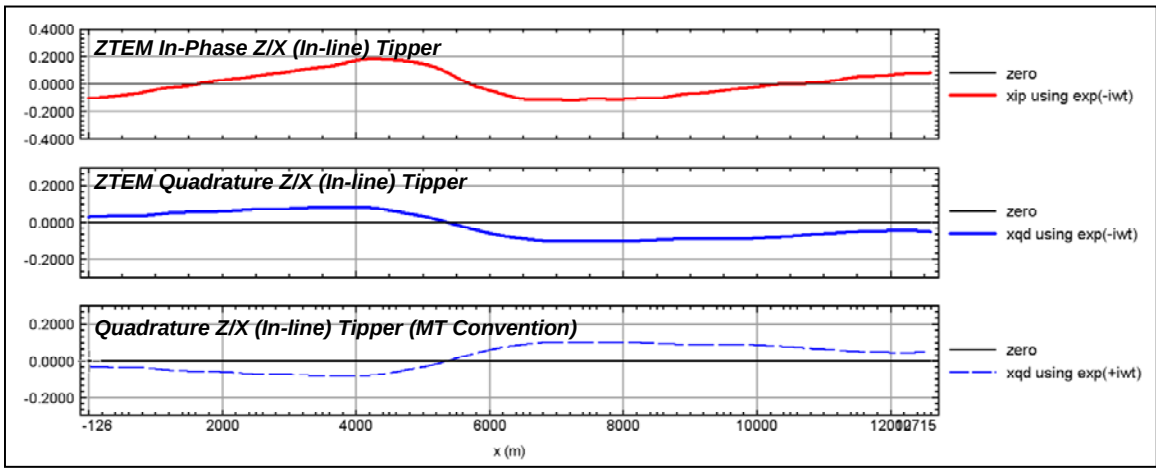

Figure 10 - Illustration of ZTEM In-Phase & Quadrature Tipper transfer function polarity convention (e-iωt) relative to equivalent MT Tipper Quadrature polarity convention (e+iωt) for a graphitic conductor in Athabasca Basin, SK.

4.4.6 Total Divergence and Phase Rotation Processing

In a final processing step DT (Total Divergence) and PR (Phase Rotation) processing are applied to the multi-frequency In-phase and Quadrature ZTEM data. This is due to the crossover nature of the Tipper Responses; these additional processing steps are applied to convert them into local maxima for easier interpretation.

To present the data from both tipper components into one image, the Total Divergence parameter, termed the DT is calculated from the horizontal derivatives of the Z/X and Z/Y tippers (Lo and Zang, 2008). It is analogous to the "Peaker" parameter in VLF (Pedersen, 1998).

Total Divergence DT:	***DT = DIV (Z/X, Z/Y)***
	= d(Z/X)/dx+d(Z/Y)/dy

This DT parameter was introduced by Petr Kuzmin (Milicevic, 2007, p. 13) and is derived for each of the In Phase and Quadrature components at individual frequencies. These in turn allow for minima over conductors and maxima over resistive zones. DT grids for each of the extracted frequencies were generated accordingly, using a reverse colour scheme with warm colours over conductors and cool colours over resistors.

The DT gives a clearer image of conductor's location and shape but, as a derivative, it does not preserve some of the long wavelength information and is also sensitive to noise.

As an alternative, a 90 degree Phase Rotation (PR) technique is also applied to the grids of each individual component (Z/X and Z/Y). It transforms bipolar (cross over) anomalies into single pole anomalies with a maximum over conductors, while preserving long wavelength information (Lo et al., 2009). The two orthogonal grids are then usually added to obtain a Total Phase Rotated grid for the In-Phase and Quadrature.

Total Phase-Rotation:	***= PR (Z/X) + PR (Z/Y)***

A presentation of the ZTEM test survey results over unconformity uranium deposits that illustrates DT and TPR examples, as documented by Lo et al. (2009) is provided in Appendix E.

4.4.7 2D EM Inversion

2d inversions of the ZTEM results were performed over selected lines using the Geotech Zvert2d software developed by Phil Wannamaker, U. of Utah, for Geotech Ltd. The inversion algorithm is based on the 2D inversion code with Jacobians of de Lugao and Wannamaker (1996), the 2D forward code of Wannamaker et al (1987), and the Gauss-Newton parameter step equations of Tarantola (1987). Zvert2d has been developed/modified for use with our ZTEM platform by taking into account the 75-80m air-layer between radar bird and ground surface.

The 2D code only considers the In-Line (Z/X) data and assumes that the strike lengths of bodies are infinite and orthogonal to the profile. The code is designed to account for the ZTEM vertical coil receiver and fixed base station reference measurements – although this option was not used in this study. The inversion uses a model-mesh consisting of 440 cells laterally and 62 cells vertically. Typically the ZTEM data are de-sampled to 180-200 pts, in order to allow the inversion to run in 10minutes or less. Typically, between 1-2% errors are added to the In-line in-phase (XIP) and Quadrature (XQD) data obtained at 30,45,90,180,360 & 720Hz. Errors are adjusted until numerical convergence (<1.0 rms) is attained in 8 iterations or less. All inversions are based on a 1k ohm-m homogeneous starting half-space model. For Alum and Silver Peak Blocks, 30 ohm-m start models utilized; for Barren Hills, a 100 ohm-m start model was utilized.

4.5 Magnetic Data

The processing of the total magnetic field intensity (TMI) data involved the correction for diurnal variations by using the digitally recorded ground base station magnetic values. The base station magnetometer data was edited and merged into the Geosoft GDB database on a daily basis. The aeromagnetic data was corrected for diurnal variations by subtracting the observed magnetic base station deviations.

Due to the absence of tie-lines, further tie-line or micro levelling were not applied to the magnetic data.

The corrected magnetic data was interpolated between survey lines using a random point gridding method to yield x-y grid values for a standard grid cell size of approximately 0.50 cm at the mapping scale. The Minimum Curvature algorithm was used to interpolate values onto a rectangular regular spaced grid.

5. DELIVERABLES

5.1 Survey Report

The survey report describes the data acquisition, processing, and final presentation of the survey results. The survey report is provided in two paper copies and digitally in PDF format.

5.2 Maps

Final maps were produced at scale of 1:20,000. The coordinate/projection system used was NAD83, UTM Zone11 North. All maps show the flight path trace and topographic data; latitude and longitude are also noted on maps.

The preliminary and final results of the survey are presented as profile plans for the EM data that were generated for individual real (In-Phase) and imaginary parts (Quadrature) of the Z/X and Z/Y components. Colour contour maps of the corresponding DT (Total Divergence) Grids for five of the six frequencies, (30, 45, 90, 180, 360 and 720Hz[4]), as well as for corresponding Phase Rotated Grids for individual components.

3D views have been constructed by plotting the DT grids at their respective penetration depths using a 1000 ohm-m half space, using the Bostick skin depth rule (Murakami, 1985) see Appendix D.

Final maps were chosen, in consultation with the client, to represent all collected data, are listed in Section 5.3.

Sample maps of the related 3D view, Magnetic, Total Divergence and Digital Elevation Model are included in this report and presented in Appendix C.

5.3 Digital Data

- Two copies of the data and maps on DVD were prepared to accompany the report. Each DVD contains a digital file of the line data in GDB Geosoft Montaj.
- DVD structure.

  There are two (2) main directories;
  Data contains databases, grids and maps, as described below.
  Report contains a copy of the report and appendices in PDF format.

  Databases in Geosoft GDB format, containing the channels listed in Table 4.

Table 4 - Geosoft GDB Data Format.

Column	Description
Lines	Line Number
X:	UTM Easting NAD83 Zone 11, (Centre of the ZTEM loop) (meters)
Y:	UTM Northing NAD83 Zone 11 , (Centre of the ZTEM loop) (meters)
Longitude:	Longitude – WGS84 (Centre of the ZTEM loop) (Decimal degree)
Latitude	Latitude – WGS84 (Centre of the ZTEM loop) (Decimal degree)
Z:	Elevation- WGS84 (Centre of the ZTEM loop) (metres)
Radar:	Helicopter terrain clearance from radar altimeter (metres - AGL)
alt_B:	Calculated ZTEM Bird terrain clearance (metres)
DEM	Digital Elevation Model (meters)
Gtime	GPS Time (seconds)
basemag	Base station mag
Mag1	Measured Total Magnetic Intensity
Mag2	Measured Total Magnetic Intensity
Mag3:	Levelled Total Magnetic field data
xIp_030Hz:	Z/X In-Phase 30 Hz final corrected
xIp_045Hz:	Z/X In-Phase 45 Hz final corrected
xIp_090Hz:	Z/X In-Phase 90 Hz final corrected
xIp_180Hz:	Z/X In-Phase 180 Hz final corrected
xIp_360Hz:	Z/X In-Phase 360 Hz final corrected
xIp_720Hz[3]:	Z/X In-Phase 720 Hz final corrected
xQd_030Hz:	Z/X Quadrature 30 Hz final corrected
xQd_045Hz:	Z/X Quadrature 45 Hz final corrected
xQd_090Hz:	Z/X Quadrature 90 Hz final corrected
xQd_180Hz:	Z/X Quadrature 180 Hz final corrected
xQd_360Hz:	Z/X Quadrature 360 Hz final corrected
xQd_720Hz[3]:	Z/X Quadrature 720 Hz final corrected
yIp_030Hz:	Z/Y In-Phase 30 Hz final corrected
yIp_045Hz:	Z/Y In-Phase 45 Hz final corrected
yIp_090Hz:	Z/Y In-Phase 90 Hz final corrected
yIp_180Hz:	Z/Y In-Phase 180 Hz final corrected
yIp_360Hz:	Z/Y In-Phase 360 Hz final corrected
yIp_720Hz3:	Z/Y In-Phase 720 Hz final corrected
yQd_030Hz:	Z/Y Quadrature 30 Hz final corrected
yQd_045Hz:	Z/Y Quadrature 45 Hz final corrected
yQd_090Hz:	Z/Y Quadrature 90 Hz final corrected
yQd_180Hz:	Z/Y Quadrature 180 Hz final corrected
yQd_360Hz:	Z/Y Quadrature 360 Hz final corrected
yQd_720Hz[3]:	Z/Y Quadrature 720 Hz final corrected
PLM:	Power Line Monitor (60Hz)

[3] 720Hz for Barren Hills Block was not provided due to lack of signal.

- Grids in Geosoft GRD format, as follows:

MAG: Total Magnetic Intensity
DEM: Digital Elevation Model
XIP_30Hz_PR: Z/X In-Phase Component Phase Rotated grid at 30 Hz
XIP_45Hz_PR: Z/X In-Phase Component Phase Rotated grid at 45 Hz
XIP_90Hz_PR: Z/X In-Phase Component Phase Rotated grid at 90 Hz
XIP_180Hz_PR: Z/X In-Phase Component Phase Rotated grid at 180 Hz
XIP_360Hz_PR: Z/X In-Phase Component Phase Rotated grid at 360 Hz
XIP_720Hz_PR[4]: Z/X In-Phase Component Phase Rotated grid at 720 Hz
XQd_30Hz_PR: Z/X Quadrature component Phase Rotated grid at 30 Hz
XQd_45Hz_PR: Z/X Quadrature component Phase Rotated grid at 45 Hz
XQd_90Hz_PR: Z/X Quadrature component Phase Rotated grid at 90 Hz
XQd_180Hz_PR: Z/X Quadrature component Phase Rotated grid at 180 Hz
XQd_360Hz_PR: Z/X Quadrature component Phase Rotated grid at 360 Hz
XQd_720Hz_PR[4] Z/X Quadrature component Phase Rotated grid at 720 Hz
YIP_30Hz_PR: Z/Y In-Phase Component Phase Rotated grid at 30 Hz
YIP_45Hz_PR: Z/Y In-Phase Component Phase Rotated grid at 45 Hz
YIP_90Hz_PR: Z/Y In-Phase Component Phase Rotated grid at 90 Hz
YIP_180Hz_PR: Z/Y In-Phase Component Phase Rotated grid at 180 Hz
YIP_360Hz_PR: Z/Y In-Phase Component Phase Rotated grid at 360 Hz
YIP_720Hz_PR[4] Z/Y In-Phase Component Phase Rotated grid at 720 Hz
YQd_30Hz_PR: Z/Y Quadrature component Phase Rotated grid at 30 Hz
YQd_45Hz_PR: Z/Y Quadrature component Phase Rotated grid at 45 Hz
YQd_90Hz_PR: Z/Y Quadrature component Phase Rotated grid at 90 Hz
YQd_180Hz_PR: Z/Y Quadrature component Phase Rotated grid at 180 Hz
YQd_360Hz_PR: Z/Y Quadrature component Phase Rotated grid at 360 Hz
YQd_720Hz_PR[4]Z/Y Quadrature component Phase Rotated grid at 720 Hz
IP_30Hz_DT: Total Divergence grid from In-phase components at 30 Hz
IP_45Hz_DT: Total Divergence grid from In-phase components at 45 Hz
IP_90Hz_DT: Total Divergence grid from In-phase components at 90 Hz
IP_180Hz_DT: Total Divergence grid from In-phase components at 180 Hz
IP_360Hz_DT: Total Divergence grid from In-phase components at 360 Hz
IP_720Hz_DT[4] Total Divergence grid from In-phase components at 720 Hz
QD_30Hz_DT: Total Divergence grid from Quadrature components at 30 Hz
QD_45Hz_DT: Total Divergence grid from Quadrature components at 45 Hz
QD_90Hz_DT: Total Divergence grid from Quadrature components at 90 Hz
QD_180Hz_DT: Total Divergence grid from Quadrature components at 180 Hz
QD_360Hz_DT: Total Divergence grid from Quadrature components at 360 Hz
QD_720Hz_DT[4] Total Divergence grid from Quadrature components at 720 Hz

The Final DVD has 3 folders one for each block which contains the above grids.

[4] 720Hz g for Barren Hills and Alum Blocks were not provided due to lack of signal.

A Geosoft .GRD file has a .GI metadata file associated with it, containing grid projection information. A grid cell size of 100 metres was used.

- Maps at 1:20,000 scale in Geosoft MAP format, as follows:

  9136_20K_TMI_bb: Total Magnetic Intensity (TMI)
  9136_20K_DEM_bb: Digital Elevation model (DEM)
  9136_20K_3D_IP_DT_bb:3D View of In-Phase DT Grids versus Skin Depth
  9136_20K_30Hz_XIP_PR_bb: 30 Hz Z/X Component In-Phase Phase Rotated
  9136_20K_90Hz_XIP_PR_bb: 90 Hz Z/X Component In-Phase Phase Rotated
  9136_20K_360Hz_XIP_PR_bb: 360 Hz Z/X Component In-Phase Phase Rotated
  9136_20K_30Hz_IP_DT_bb: 30Hz In-Phase Total Divergence Grid
  9136_20K_45Hz_IP_DT_bb: 45Hz In-Phase Total Divergence Grid
  9136_20K_90Hz_IP_DT_bb: 90Hz In-Phase Total Divergence Grid
  9136_20K_180Hz_IP_DT_bb: 180Hz In-Phase Total Divergence Grid
  9136_20K_360Hz_IP_DT_bb: 360Hz In-Phase Total Divergence Grid
  9136_20K_30Hz_QD_DT_bb: 30Hz Quadrature Total Divergence Grid
  9136_20K_45Hz_QD_DT_bb: 45Hz Quadrature Total Divergence Grid
  9136_20K_90Hz_QD_DT_bb: 90Hz Quadrature Total Divergence Grid
  9136_20K_180Hz_QD_DT_bb: 180Hz Quadrature Total Divergence Grid
  9136_20K_360Hz_QD_DT_bb: 360Hz Quadrature Total Divergence Grid
  9136_20K_XIP_profiles_XIP_PR_bb: Z/X (In-line) In-Phase Profiles over 90Hz Phase Rotated In-Phase Grid
  9136_20K_XQD_profiles_XQD_PR_bb:Z/X (In-line) Quadrature Profiles over a 90Hz Phase Rotated Quadrature Grid.
  9136_20K_YIP_profiles_YIP_PR_bb: Z/Y (Cross-line) In-Phase Profiles over 90Hz Phase Rotated In-Phase Grid
  9136_20K_YQD_profiles_YQD_PR_bb:Z/Y (Cross-line) Quadrature Profiles over a 90Hz Phase Rotated Quadrature Grid.
  Where bb represents the block name (ie: 9136_20K_TMI_Alum.map)

- 2D Resistivity Inversion maps for all lines.

  Maps are also presented in PDF format.

  The topographic data base was derived from 1:100,000 USGS (United States Geological Survey) DLG (Digital Line Graph) Dataset downloaded from Geocommunity (http://www.gecomm.com)

- A Google Earth file *"9136_SierraGeothermal.kml"* is included, showing the flight path of each block. Free versions of Google Earth software from: http://earth.google.com/download-earth.html

6. CONCLUSIONS AND RECOMMENDATIONS

6.1 Conclusions

A helicopter-borne ZTEM and aeromagnetic geophysical survey has been completed over the Alum, Barren Hills and Silver Peak & Pearl Blocks located near the towns of Tonopah and Yerington, Nevada.

The total area coverage is 301.4 km^2. Total survey line coverage is 622 line kilometres. The principal sensors included a Z-Axis Tipper electromagnetic (ZTEM) system and a caesium magnetometer. Results have been presented as stacked profiles and contour colour images at a scale of 1:20,000. The survey results are supported by 2D inversions (Appendix G) that were performed.

Both the In-phase and Quadrature components of the airborne AFMAG Tipper fields (Z/X and Z/Y) were extracted from the data collected, then processed and presented together. Accordingly, maps of the profiles and 90 Hz Phase Rotated grids, as well as DT (Total Divergence) and TPR (Total Phase Rotated) grids were also created, which helped contribute to a clearer presentation of our data.

6.2 Recommendations

Based on the geophysical results obtained, a number of interesting structures were identified across the property. The magnetic results may also contain worthwhile information in support of exploration targets of interest. We therefore recommend a more detailed interpretation of the available geophysical, in conjunction with the geology, based on structure and possibly using inversion and modelling techniques prior to ground follow up and drill testing.

Respectfully submitted[6],

Wendy Acorn
Geotech Ltd.

Jean Legault, P. Geo, P. Eng
Geotech Ltd.

Biljana Milicevic
Geotech Ltd.

Gord Smith
Geotech Ltd.

January 2010

[6] Final data processing of the EM and magnetic data were carried out by Biljana Milicevic, from the office of Geotech Ltd. in Aurora, Ontario, under the supervision of Gord Smith, Manager of Data Processing and Jean Legault, P. Geo, P. Eng, Chief Geophysicists (Interpretation)

7. REFERENCES AND SELECTED BIBLIOGRAPHY

Anav, A., Cantarano, S., Cerruli-Irelli, P., and Pallotino, G.V.(1976). A correlation method for measurement of variable magnetic fields: *Inst. Elect. and Electron. Eng. Trans., Geosc. Elect.* GE14, 106-114.

De Lugao, P.P.,and Wannamaker, P.E.(1996). Calculating the two-dimensional magnetotelluric Jacodian in finite elements using reciprocity: Geophys. J. Int., **127**, 806-810

Karous, M.R., and S. E. Hjelt (1983). Linear filtering of VLF dip-angle measurements: *Geophysical Prospecting*, **31**, 782-794.

Kuzmin, P., Lo, B. and Morrison, E. (2005). Final Report on Modeling, interpretation methods and field trials of an existing prototype AFMAG system, Miscellaneous Data Release 167, Ontario Geological Survey, 2005.

Labson, V. F., Becker A., Morrison, H. F., and Conti, U. (1985). Geophysical exploration with audiofrequency natural magnetic fields. *Geophysics*, **50**, 656-664.

Legault, J.M., Kumar, H., Milicevic, B., and Hulbert, L. (2009), ZTEM airborne tipper AFMAG test survey over a magmatic copper-nickel target at Axis Lake in northern Saskatchewan, SEG Expanded Abstracts, **28**, 1272-1276

Legault, J.M., Kumar, H., Milicevic, B., and Wannamaker, P.,(2009), ZTEM tipper AFMAG and 2D inversion results over an unconformity uranium target in northern Saskatchewan, SEG Expanded Abstracts, **28**, 1277-1281.

Lo, B., Legault, J.M., Kuzmin, P. and Combrick, M. (2009). ZTEM (Airborne AFMAG) tests over unconformity uranium deposits, Extended abstract submitted to 20th ASEG International Conference and Exhibition, Adelaide, AU, 4pp.

Lo, B., and Zang, M., (2008), Numerical modeling of Z-TEM (airborne AFMAG) responses to guide exploration strategies, SEG Expanded Abstracts, **27**, 1098-1101.

Milicevic, B. (2007). Report on a helicopter borne Z-axis, Tipper electromagnetic (ZTEM) and magnetic survey at Safford, Giant Hills, Baldy Mountains and Sierrita South Areas, Arizona, USA., Geotech internal survey report (job A226), 33pp.

Murakami, Y. 1985, Short Note: Two representations of the magnetotelluric sounding survey, Geophysics, **50**, 161-164.

Pedersen, L.B., Qian, W., Dynesius, L. and Zhang, P. (1994). An airborne sensor VLF system. From concept to realization. *Geophysical Prospecting*, **42**, i.8, 863-883

Peterson, L.B. (1998). Tensor VLF measurements: first experiences, *Exploration Geophysics*, **29**, 52-57.

Strangway, D. W., Swift Jr., C. M., and Holmer, R. C. (1973). The Application of Audio-Frequency Magnetotellurics (AMT) to Mineral Exploration. *Geophysics*, **38**, 1159-1175.

Tarantola, A.,(1987) Inverse problem theory: Elsevier, New York, 613 pp.

Vozoff, K.(1972). The magnetotelluric method in the exploration of sedimentary basins. *Geophysics*, **37**, 98-141.

Vozoff, K. (1991). The magnetotelluric method. In: Electromagnetic Methods in Applied Geophysics - Volume 2 Applications, edited by Nabighian, M.N., Society of Exploration Geophysicists, Tulsa., 641-711.

Ward, S. H. (1959). AFMAG - Airborne and Ground. *Geophysics*, **24**, 761-787.

Ward, S. H, O'Brien, D.P., Parry, J.R. and McKnight, B.K. (1968). AFMAG Interpretation. *Geophysics*, **33**, 621-644.

Wannamaker, P.E., Stodt, J.A., and Rijo, L., (1987). A stable finite element solution for two-dimentional magnetotelluric modeling: Geophy. J. Roy. Astr. Soc.,**88**, 277-296.

Zhang, P. and King, A. (1998). Using magnetotellurics for mineral exploration, Extended Abstracts from 1998 Meeting of Society of Exploration Geophysics

APPENDIX A

SURVEY BLOCK LOCATION MAP

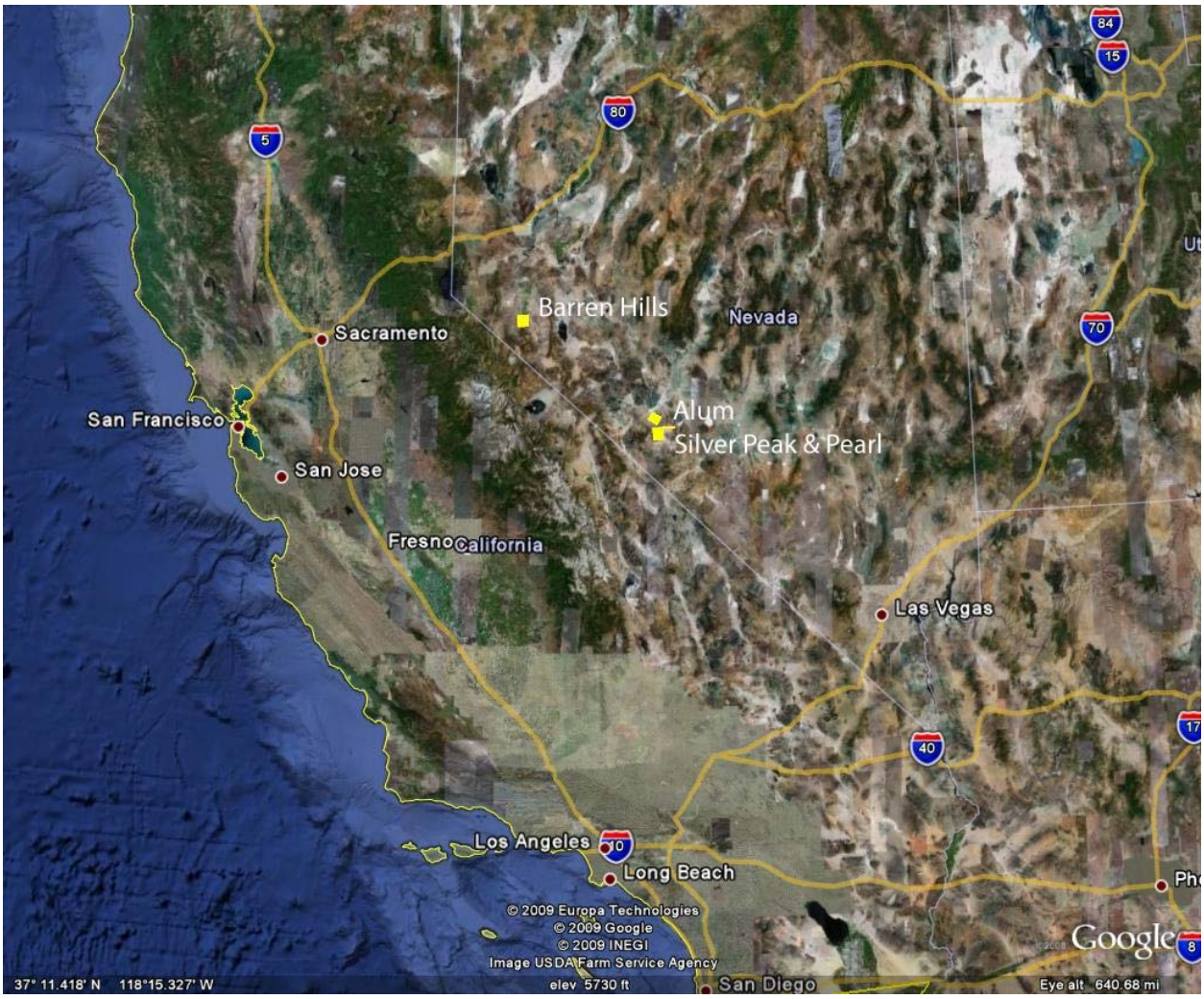

Survey Overview Location Map

APPENDIX B

SURVEY BLOCK COORDINATES

(WGS 84, UTM Zone 11 North)

Silver Peak & Pearl

X	Y
448493.5	4175534
438493.5	4175534
438493.5	4186554
448493.5	4186554
448493.5	4187034
459493.4	4187034
459493.4	4186504
448493.5	4186504

Barren Hills

X	Y
448493.5	4175534
438493.5	4175534
438493.5	4186554
448493.5	4186554
448493.5	4187034
459493.4	4187034
459493.4	4186504
448493.5	4186504

Alum

X	Y
433977.9	4195459
438038.7	4201765
446551.1	4196517
442490.3	4190211

APPENDIX C

GEOPHYSICAL MAPS[1]

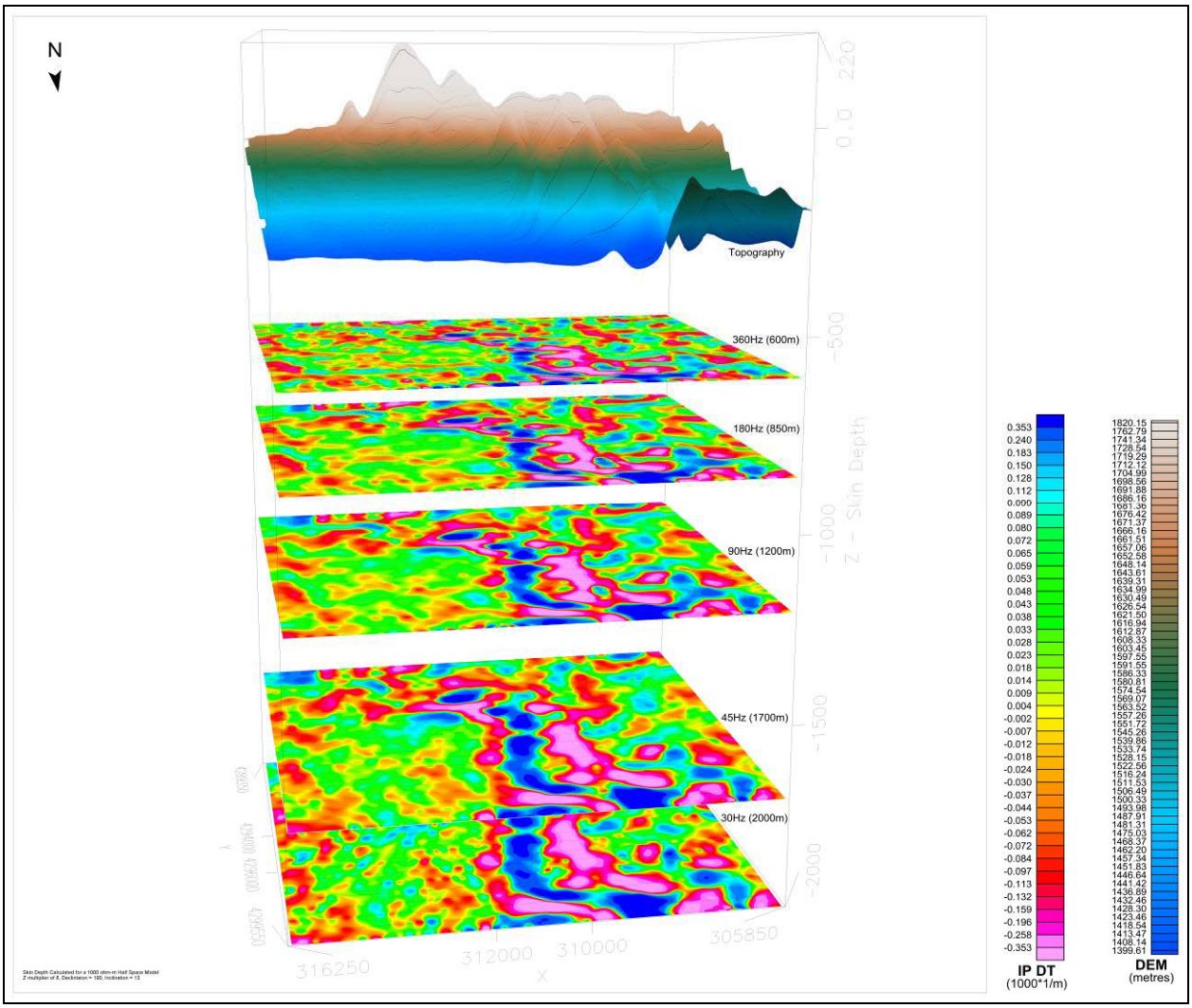

Barren Block - 3D View of In-Phase, Total Divergence (DT) grids versus Skin Depth (30 Hz - 360 Hz)

[1] Full size geophysical maps are also available in PDF format on the final DVD

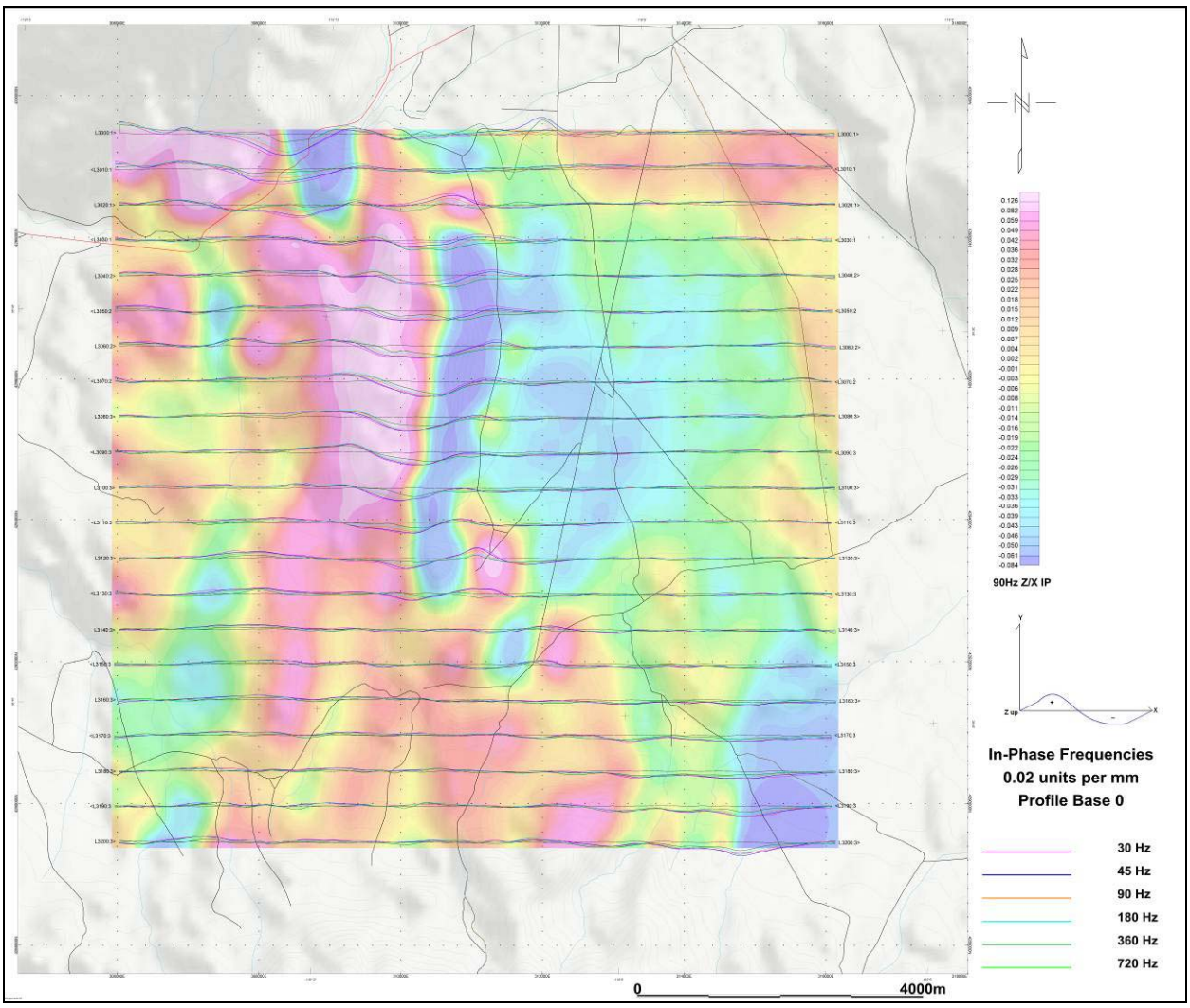

Barren Block – Z/X (In-line) In-Phase Profiles over 90 Hz Phase Rotated Z/X In-Phase Grid

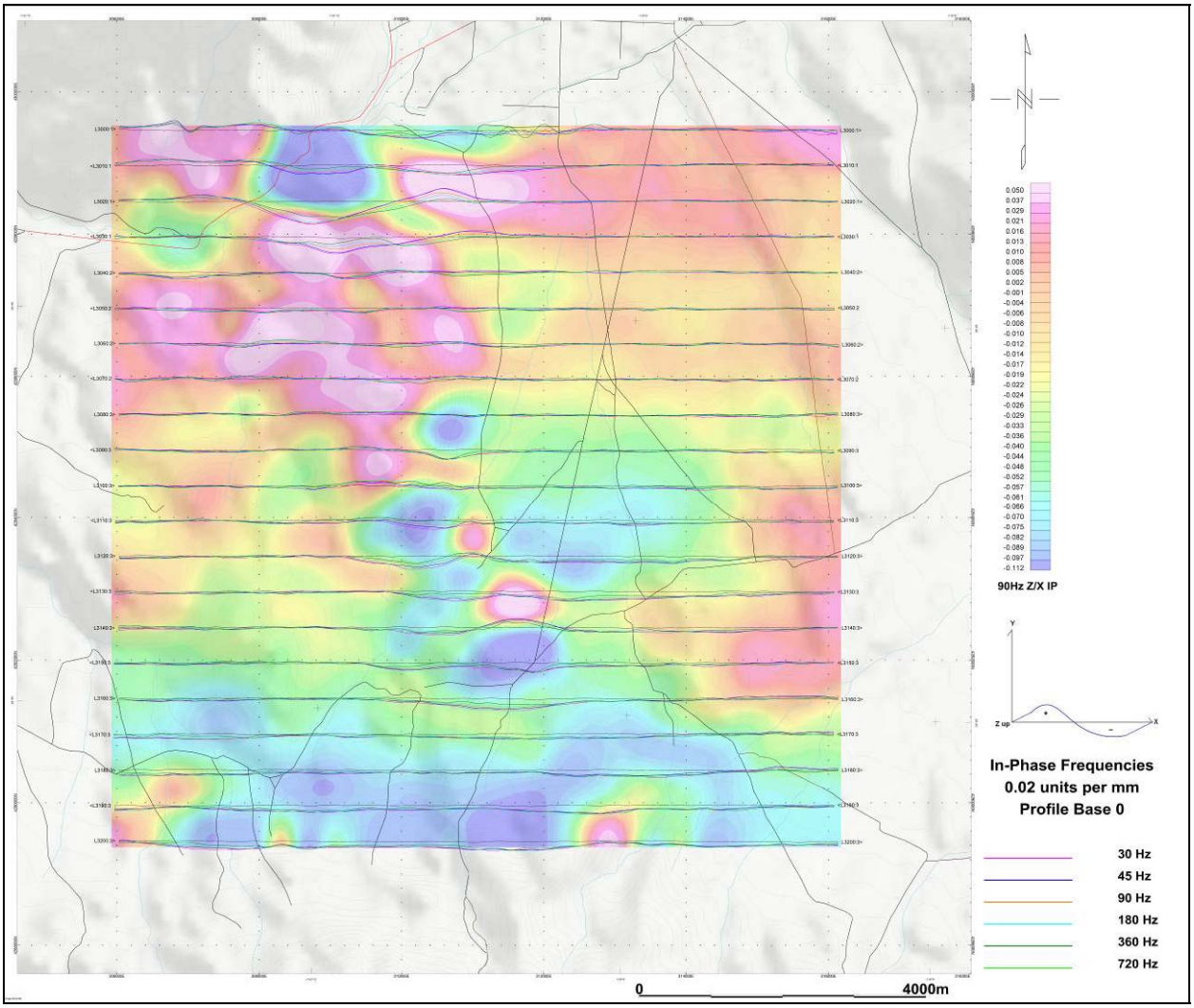

Barren Block – Z/Y (Cross-line) In-Phase Profiles over 90 Hz Phase Rotated Z/Y In-Phase Grid

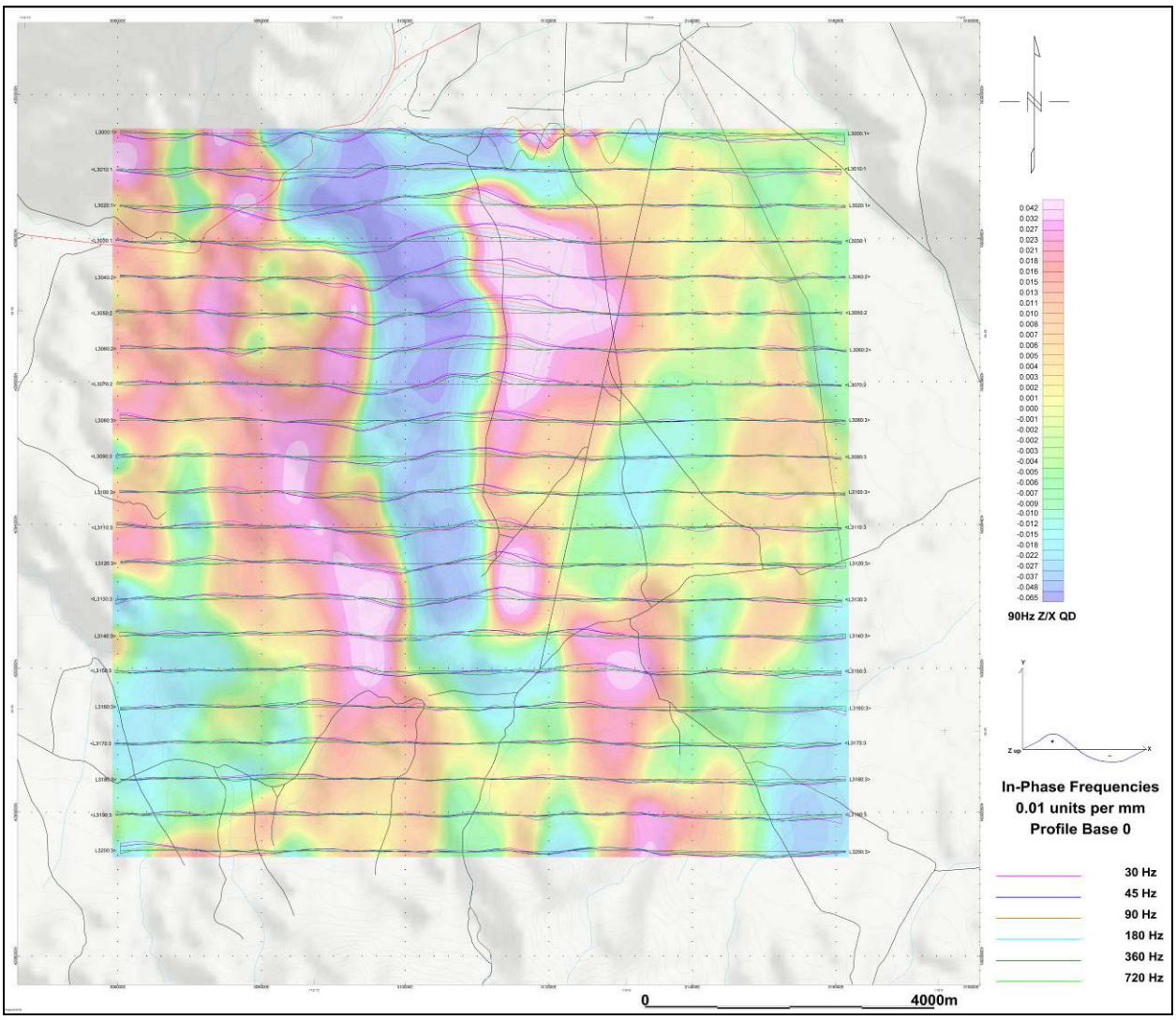

Barren Block – Z/X (In-line) Quadrature Profiles over 90 Hz Phase Rotated Z/X Quadrature Grid

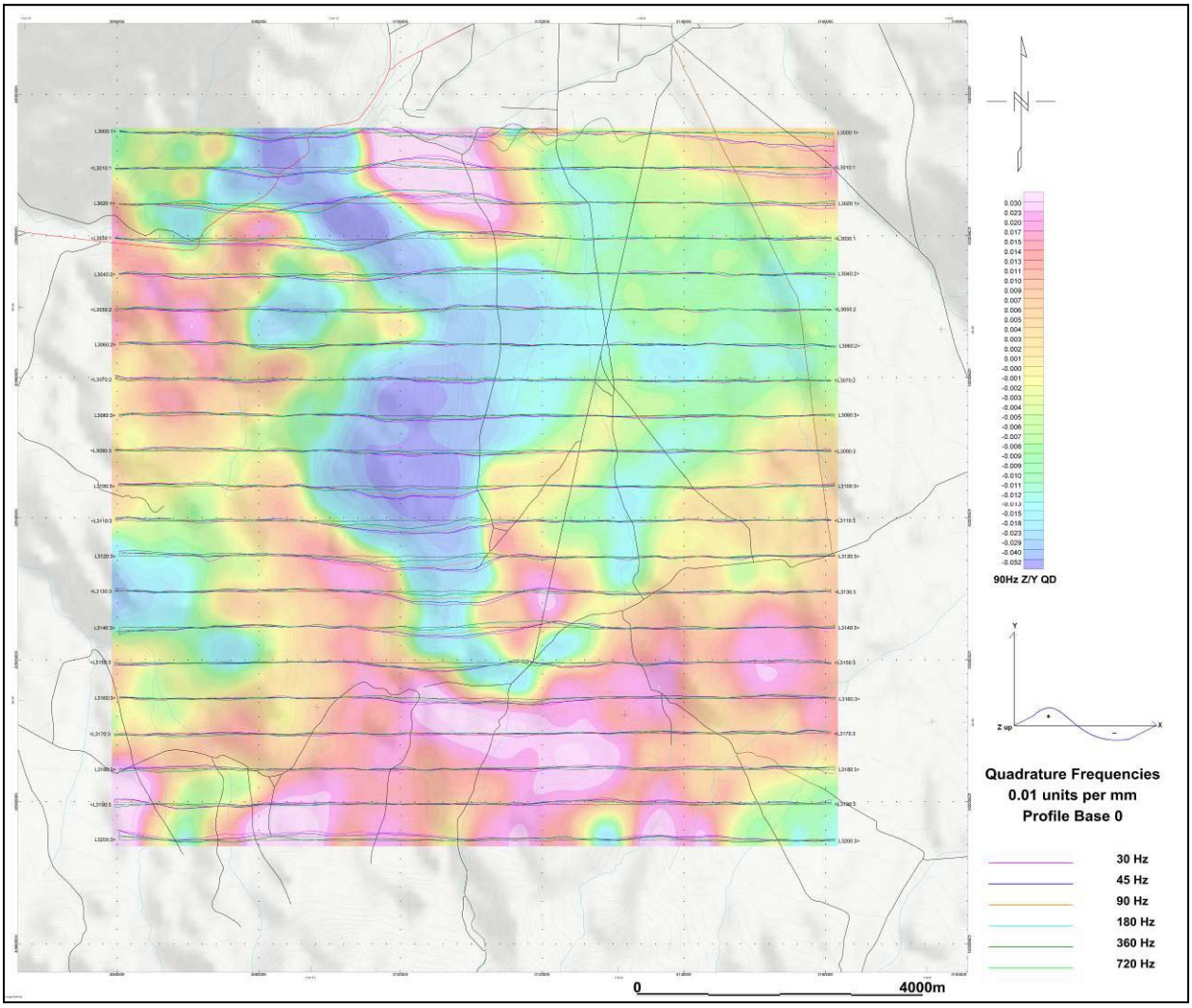

Barren Block – Z/Y (Cross-line) Quadrature Profiles over 90 Hz Phase Rotated Z/Y Quadrature Grid

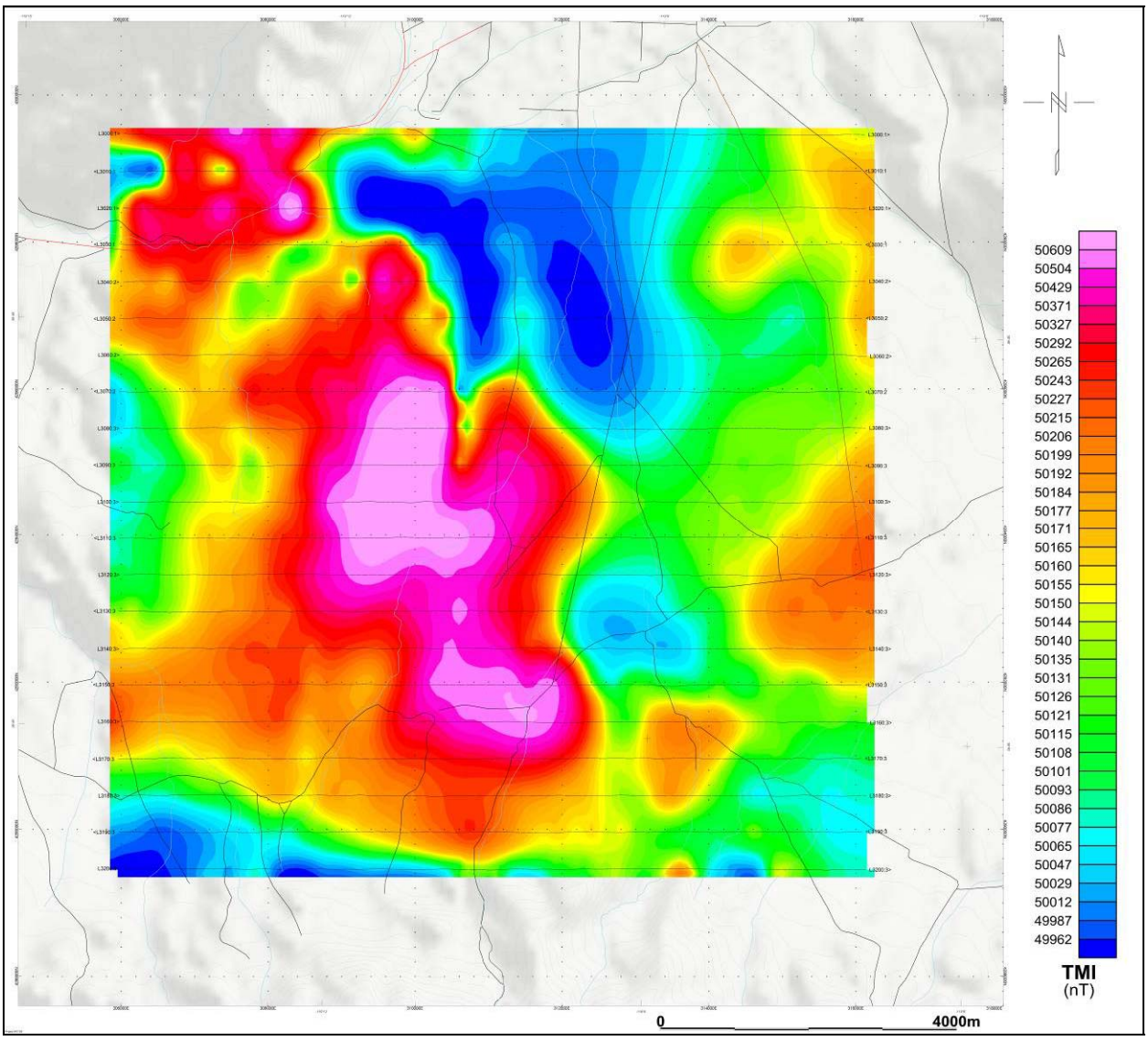

Barren Block – Total Magnetic Intensity (TMI) Grid

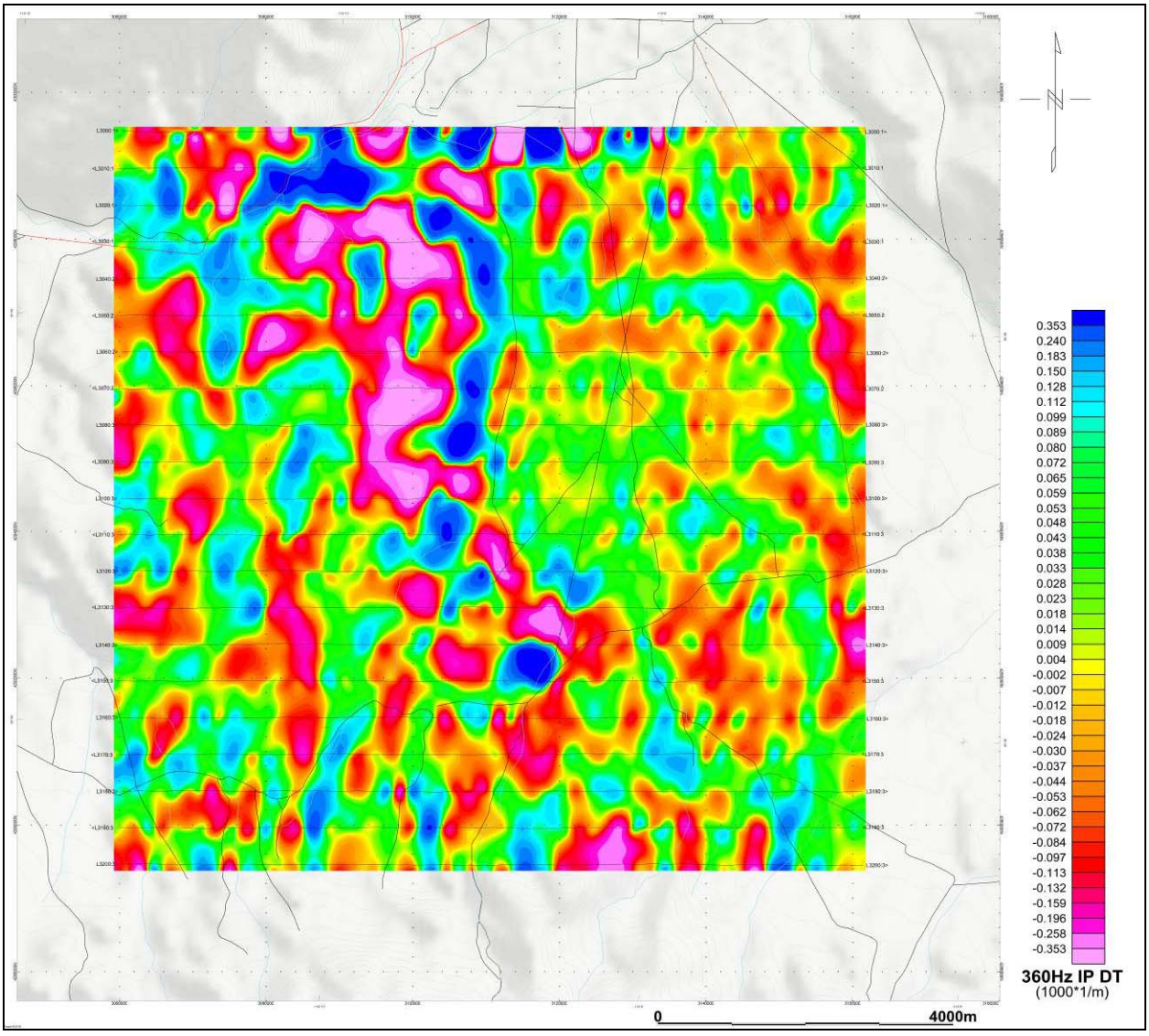

Barren Block – High Frequency (360Hz) In-Phase Total Divergence (DT)

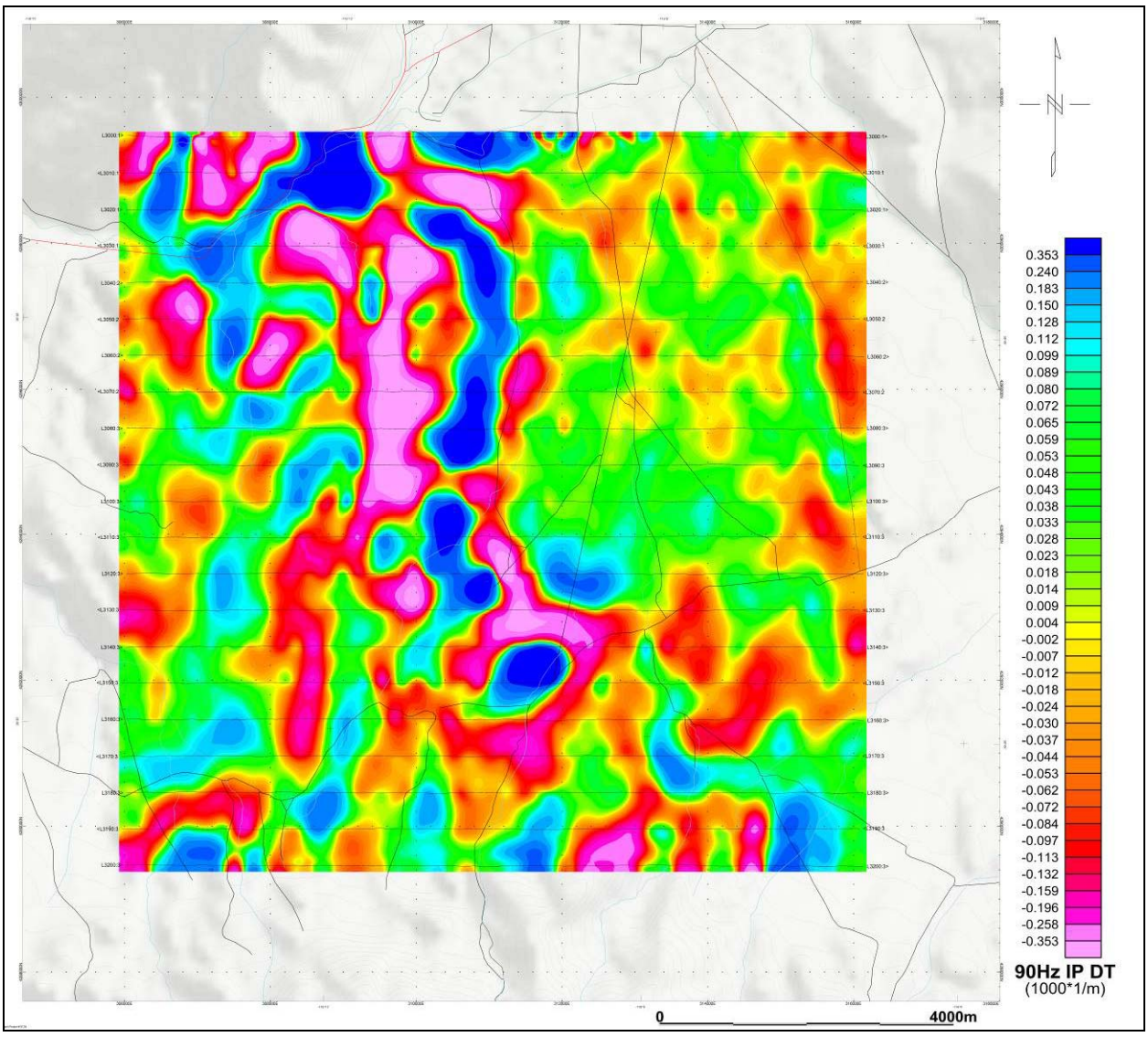

Barren Block – Mid Frequency (90Hz) In-Phase Total Divergence (DT)

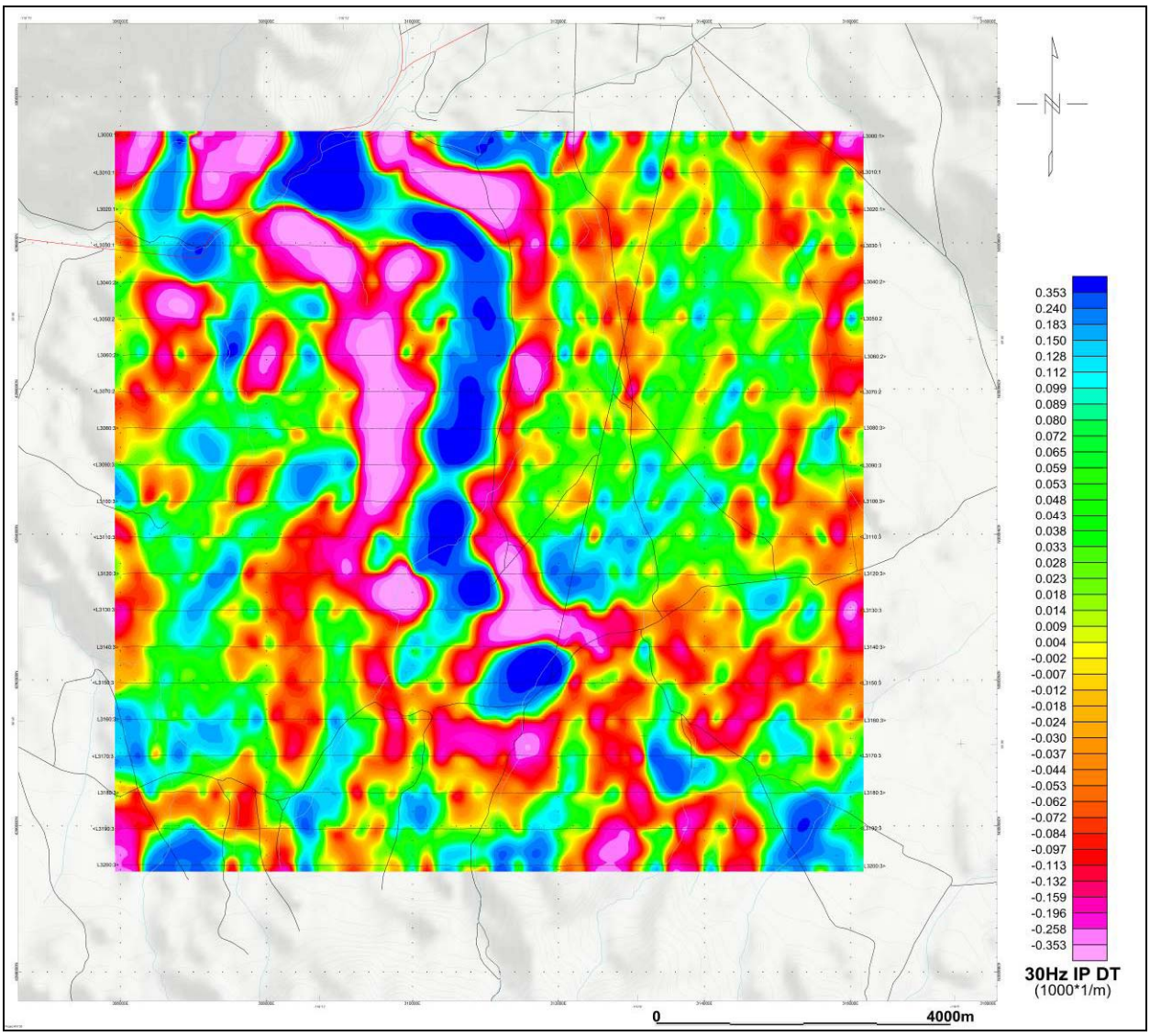

Barren Block – Low Frequency (30Hz) In-Phase Total Divergence (DT)

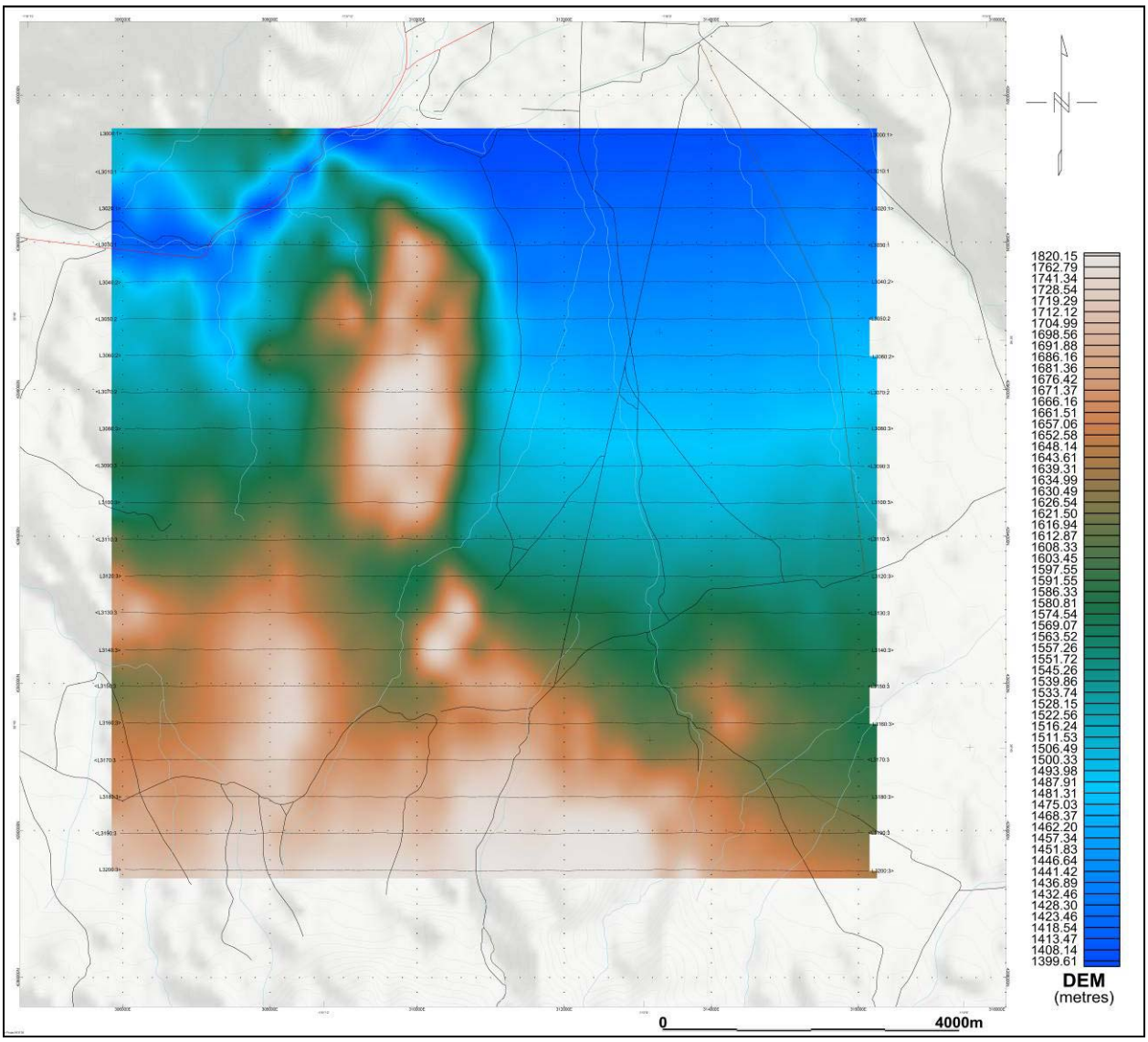

Barren Block –Digital Elevation Model (DEM) Grid

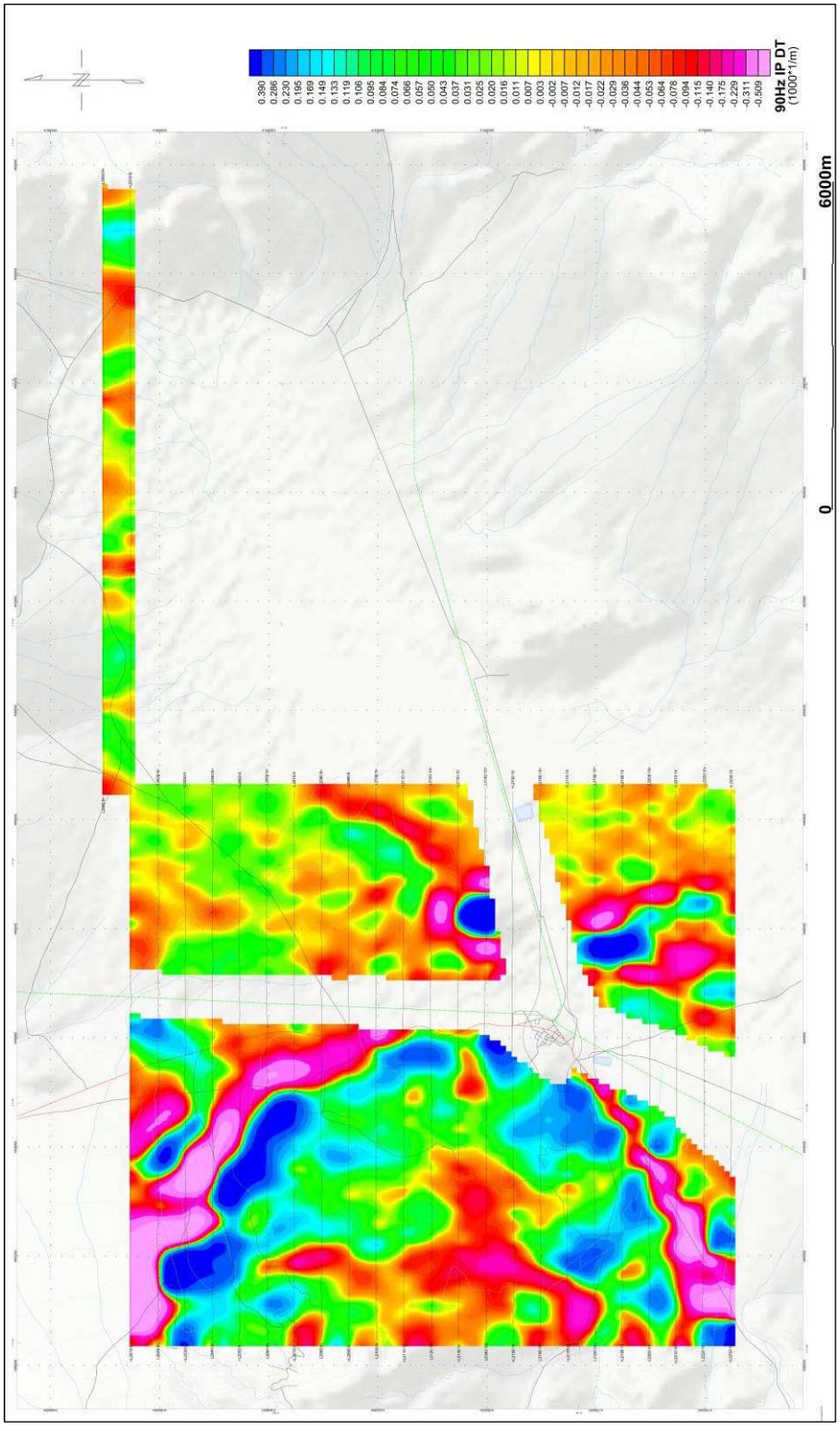

Silver Peak and Pearl Block –90Hz In-Phase Total Divergence (DT)

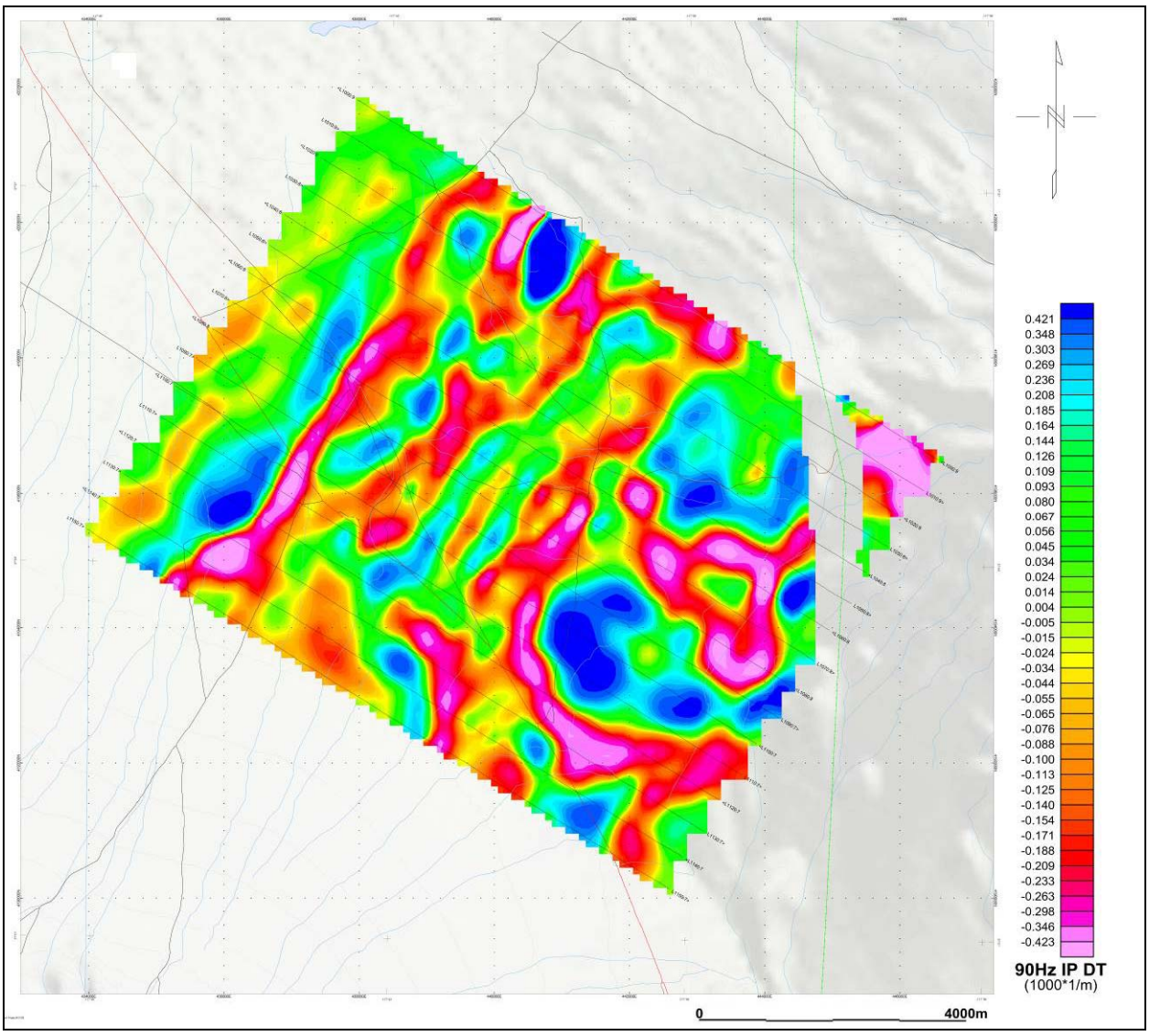

Alum Block –90Hz In-Phase Total Divergence (DT)

APPENDIX D

ZTEM THEORETICAL CONSIDERATIONS

A brief section on the theory behind the AFMAG technique is provided for completeness and a more comprehensive development of the theory can be found in standard texts. The natural EM field is normally horizontally polarized. Subsurface lateral variations of conductivity generate a vertical component, which is linearly related to the horizontal field. Although the fields look like random signals, they may be treated as the sum of sinusoids. At each frequency the field can be expressed as a complex number with magnitude and argument equal to the amplitude and phase of the sinusoid. The relation between the field components can then be expressed by a linear complex equation with two complex coefficients at any one frequency. These coefficients are dependent upon the subsurface and not upon the horizontal field present at any particular time and are appropriate parameters to measure (Vozoff, 1972).

$$\mathbf{Hz(f) = Tx(f)\ Hx(f) + Ty(f)\ Hy(f),} \qquad \mathbf{(1)}$$

Where

Hx(f), Hy(f) and Hz(f) are x, y and z components of the field,

Tx(f) and Ty(f) are the "tipper" coefficients.

In the case of a horizontally homogeneous environment, Tx and Ty are equal to zero because Hz =0. They show certain anomalies only by the presence of changes in subsurface conductivity in the horizontal direction. The real parts of the coefficients correspond to tangents of tilt angles measured with a controlled source. The complex tensor [Tx, Ty] known as the "tipper" defines the vertical response to horizontal fields in the x and y directions respectively.

Tx and Ty are two unknown coefficients in one equation, and we therefore must combine two or more sets of measurements to solve them. To reduce effects of noise, multiple sets of measurements can be made, and the coefficients, which minimize the squared error in predicting the measured Z from X and Y, can be found. This leads to next formulas for estimating the coefficients.

$$\mathbf{Tx = ([HzHx^*]\ [HyHy^*] - [HzHy^*]\ [HyHx^*]) / ([HxHx^*]\ [HyHy^*] - [HxHy^*]\ [HyHx^*]),} \qquad \mathbf{(2)}$$

and

$$\mathbf{Ty = ([HzHy^*]\ [HxHx^*] - [HzHx^*]\ [HxHy^*]) / ([HxHx^*]\ [HyHy^*] - [HxHy^*]\ [HyHx^*]\ .} \qquad \mathbf{(3)}$$

Where

[HxHy*] (For example) denotes a sum of the product of Hx with the complex conjugate of Hy.

In practical processing algorithms, all numbers Hx, Hy and Hz can be obtained by applying the same digital band-pass filters to three incoming parallel data signals. FFT algorithms are also applicable. All sums like [HxHy*] can be calculated on the basis of a discrete time interval in the range from 0.1 to 1 sec or on a sliding time base.

Using platform attitude data in the EM data processing can be done at different stages of the signal processing. The most obvious idea is to transform parallel data from local coordinates of the platform into absolute geographical coordinates before the main signal processing procedure. Unfortunately, the proper algorithms of attitude data obtained, often require some post-processing algorithms such as using post-calculated accelerations based on GPS data etc. That is why it is preferable to treat x-y-z coordinates in formulas above in the local coordinate system of the platform and to recalculate resulting local tilt angles into a geographical or global coordinate system later, during the data post processing.

In weak field conditions where the level of the signal is comparable with input noise levels in preamplifiers, the bias in the estimated values of Tx and Ty caused by noise in the horizontal signals become substantial and can not be reduced by any averaging. This bias can be removed by the use of separate reference signals containing noise uncorrelated with noise in signals Hx and Hy. (Anav et al., 1976).

$$Tx = ([HzRx^*]\,[HyRy^*] - [HzRy^*]\,[HyRx^*]) / ([HxRx^*]\,[HyRy^*] - [HxRy^*]\,[HyRx^*]), \quad (4)$$

and

$$Ty = ([HzRy^*]\,[HxRx^*] - [HzRx^*]\,[HxRy^*]) / ([HxRx^*]\,[HyRy^*] - [HxRy^*]\,[HyRx^*]). \quad (5)$$

Where:

Rx is the reference field x component,
Ry is the reference field y component.

An additional two electromagnetic sensors, providing these reference signals can be placed at some distance away from the main x, y and z sensors. Currently, though, no additional remote-reference processing are applied to ZTEM data.

Numerical Modelling

In order to understand the airborne AFMAG responses to conductors for a variety of geological environments, EMIGMA^{TM} modelling code from PetRos EiKon (Toronto, ON) was obtained to conduct the formulated model studies.

Below are some of the modelling results from their study.

Modelling assumption:

The assumptions for the modelling are that:

3 components of the magnetic field are measured and they are processed according to:

$$Hz(f) = Tx(f)\,Hx(f) + Ty(f)\,Hy(f)$$

The vector (Tx,Ty) is usually referred to as the 'tipper' vector and is determined in the frequency domain through processing. This is normally done by determining transfer functions from an extended time series.

For the modelling exercise, the 3 components of the magnetic vector (Hx,Hy,Hz) are modelled twice for 2 orthogonal polarizations of a plane wave source field and then the tipper is calculated from a matrix calculation using the results of the 2 source polarizations' models. For the 2D forward modelling results, the tipper vectors are shown as a function of frequency

Basic Model Response

For the initial models, we assume a thin plate-like model . The model is perpendicular to the flight direction. Initially, we will assume very long strike directions. From this quasi-2D model, there are 2 basic responses. The so-called TE response and the so-called TM response.

For the initial models, we will assume the strike is in the y (North) directions and the flight is in the x (East) direction Sensor heights are 30m above ground.

TE Mode: For the TE response, the electric field excitation flows along strike (current channelling) and the horizontal H field (Hx) flows perpendicular to strike thus causing induction through Faraday's law. The Hz response is generated both from channelling and induction.

TM Mode: For this response, the electric field excitation flows perpendicular to strike generating quasi-static charges on faces and the horizontal H field (Hx) flows parallel to strike. Since, the XZ face is very small for this model, little current is induced. The charges on the faces have a small dipole moment due to the thinness of the model.

For the rest of the models unless otherwise noted, the parameters used are:

Strike Length: 1km
Depth Extent: 1km
Conductance: 100S
Depth to Top: 10m
Background: Thin-overburden (10m), Resistive Basement (1000 Ohm-m)

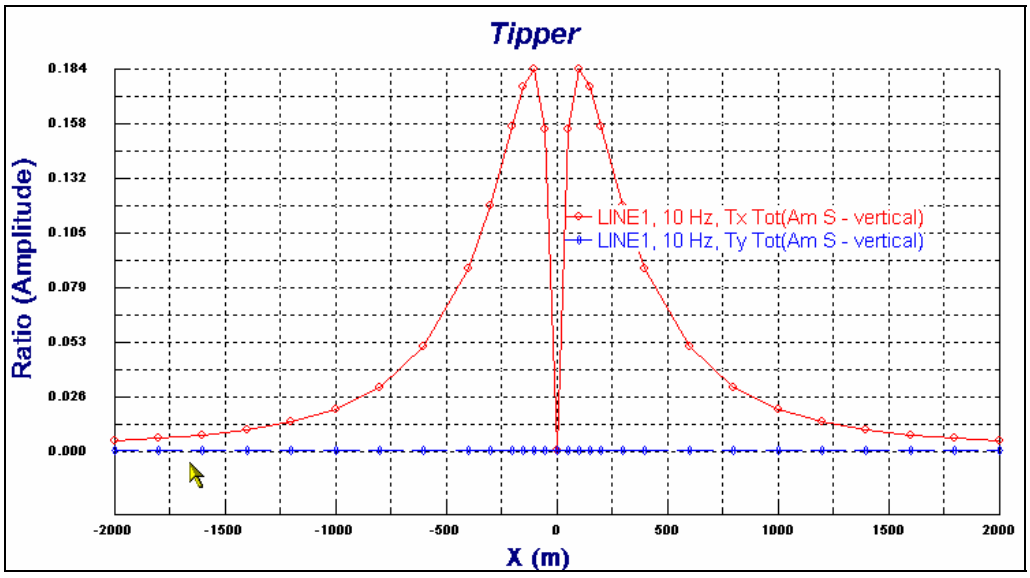

Figure D-1 – Calculated Tipper components at 10 Hz for above model parameters.

Figure D1 shows the Tipper (Tx,Ty) Amplitudes at 10Hz using a10Ωm overburden. Note small Ty (ie quasi-TM response)

Amplitude Response

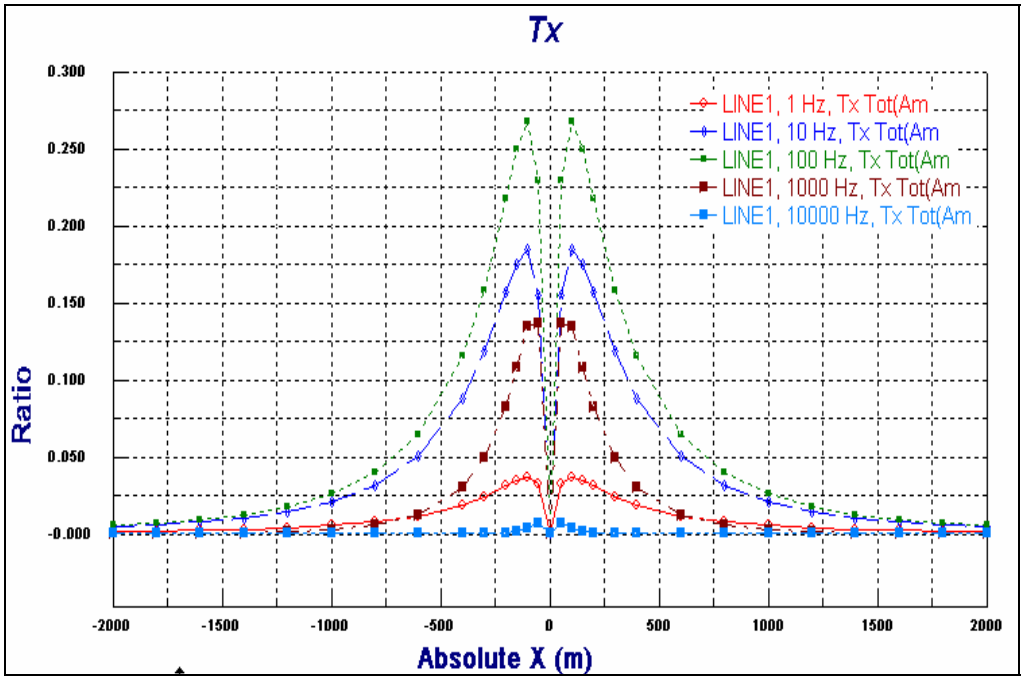

Figure D-2 – Calculated Tx component of the Tipper at various frequencies

The (Tx) response amplitude at 1,10,100,1000,10000 Hx. Peak amplitude at 100Hz

Inphase and Quadrature Response

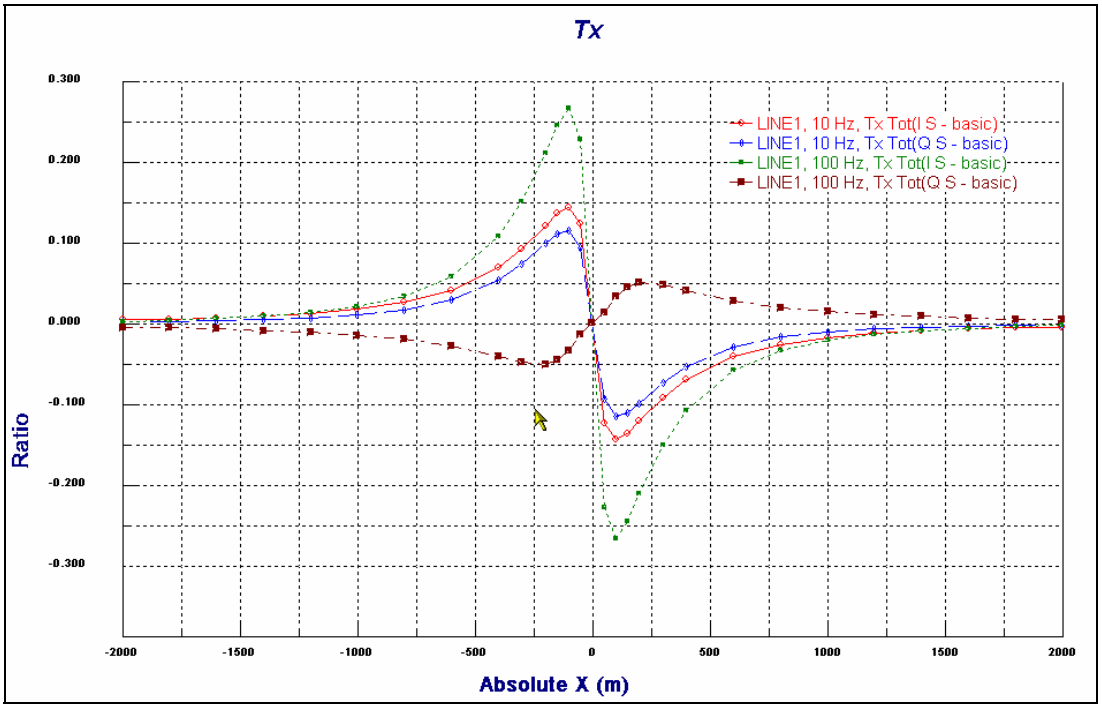

Figure D-3 – Calculated In-phase and Quadrature of the Tx component at various frequencies

Figure D-3 shows the In-phase and Quadrature response at 10 and 100Hz. Note the crossovers in the In-phase and Quadrature, and the phase reversal in the Quadrature responses from low to high frequencies.

Bo Lo, P.Eng, B.Sc. (Geophysics), Consultant
Geotech Ltd.
September, 2007

AFMAG Source Fields and ZTEM method[1]

AFMAG uses naturally occurring audio frequency magnetic fields as the source of the primary field signal, and therefore requires no transmitter (Ward, 1959). The primary fields resemble those from VLF except that they are lower frequency (tens & hundreds of Hz versus tens of kHz) and are usually not as strongly directionally polarized (Labson et al., 1985). These EM fields used in AFMAG are derived from world wide atmospheric thunderstorm activity, have the unique characteristic of being uniform, planar and horizontal, and also propagate vertically into the earth – to great depth, up to several km, as determined by the magnetotelluric (MT) skin depth (Vozoff, 1972), which is directly proportional to the ratio of the bedrock resistivity to the frequency (Figure D4).

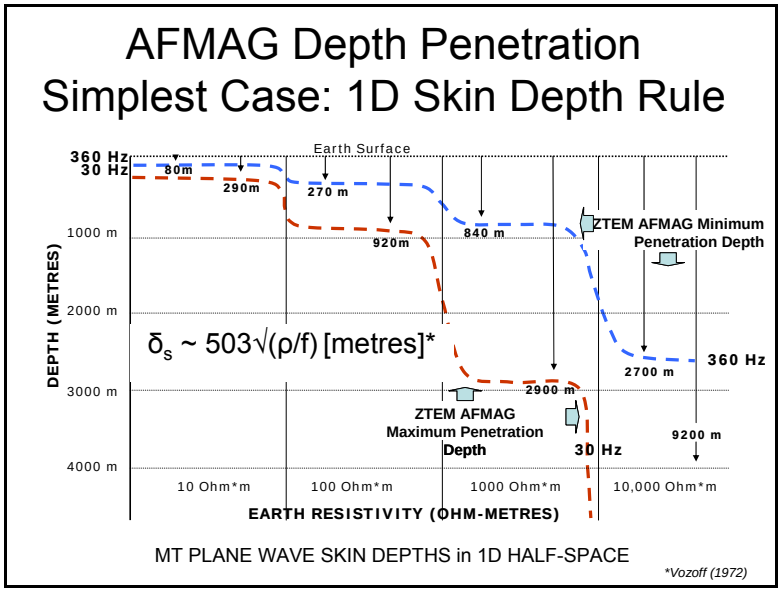

Figure D4: MT Skin Depth Penetrations for ZTEM in 30-360Hz and 10-1000 ohm resistivity

At the frequencies used for ZTEM, the penetration depths likely range between approx. 600m to 2km in this region (approx. 1k ohm-m avg. resistivity assumed), according to the following equation for the Bostick skin depth $\delta_B = 356 * \sqrt{(\rho / f)}$ metres (Murakami, 1985), which is considered appropriate as a rule of thumb equivalent depth estimate.

The other unique aspect of AFMAG fields is that they react to relative contrasts in the resistivity, and therefore do not depend on the absolute conductance, as measured using inductive EM systems, such as VTEM. Hence poorly, conductive targets, such as alteration zones and fault zones can be mapped, as well as higher conductance features, like graphitic units. Conversely, resistive targets can also be detected using AFMAG– provided they are of a sufficient size and contrast to produce a vertical field anomaly. Indeed resistors produce reversed anomalies relative to conductive features. Hence AFMAG can be effective as an

[1] From: Legault, J.M., Kumar, H., and Milicevic, B. (2009): ZTEM tipper AFMAG and 2D inversion results over an unconformity uranium target in northern Saskatchewan, Expanded Abstract submitted to Society of Exploration Geophysics SEG conference, Houston, Tx, Nov-2009, 5 pp.

all-round resistivity mapping tool, making it unique among airborne EM methods. A series of 2D synthetic models that illustrate these aspects have been created using the 2D forward MT modelling code of Wannamaker et al. (1987) and are presented in figures D5-D7.

The tipper from a single site contains information on the dimensionality of the subsurface (Pedersen, 1998), for example, in a horizontally stratified or 1D earth, $\boldsymbol{T}$=0 and as such H_Z is absent. For a 2D earth with the y-axis along strike, T_Y=0 and $H_Z = T_X * H_X$. In 3D earths, both T_X and T_Y will be non-zero. H_Z is therefore only present, as a secondary field, due to a lateral resistivity contrast, whereas the horizontal H_X and H_Y fields are a mixture of secondary and primary fields (Stodt et al., 1981). But, as an approximation, as in the telluric-magnetotelluric method (T-MT; Hermance and Thayer, 1975) used by distributed MT acquisition systems, the horizontal fields are assumed to be practically uniform, which is particularly useful for rapid reconnaissance mapping purposes. By measuring the vertical magnetic field H_X, using a mobile receiver and the orthogonal horizontal H_X and H_Y fields at a fixed base station reference site, ZTEM is a direct adaptation of this technique for airborne AFMAG surveying.

_____

Jean M. Legault, M.Sc.A., P.Eng., P.Geo.
Geotech Ltd.

References

Hermance, J.F., and Thayer, R.E., 1975, The telluric-magnetotelluric method, Geophysics, **37**, 349-364.

Labson, V. F., A. Becker, H. F. Morrison, and U. Conti, 1985, Geophysical exploration with audio-frequency natural magnetic fields: Geophysics, **50**, 656–664.

Murakami, Y., 1985, Short Note: Two representations of the magnetotelluric sounding survey, Geophysics, **50**, 161-164.

Pedersen, L.B., 1998, Tensor VLF measurements: Our first experiences, Exploration Geophysics, **29**, 52-57.

Stodt. J.A., Hohmann, G.W., and Ting, S.C., 1981, The telluric-magnetotelluric method in two- and three-dimensional environments, Geophysics, **46**, 1137-1147.

Vozoff, K., 1972, The magnetotelluric method in the exploration of sedimentary basins, Geophysics, **37**, 98–141.

Ward, S. H., 1959, AFMAG—Airborne and ground: Geophysics, **24**, 761–787.

Wannamaker, P.E., Stodt, J.A., and Rijo, L., 1987, A stable finite element solution for two-dimensional magnetotelluric modelling, Geophy. J. Roy. Astr. Soc., **88**, 227-296.

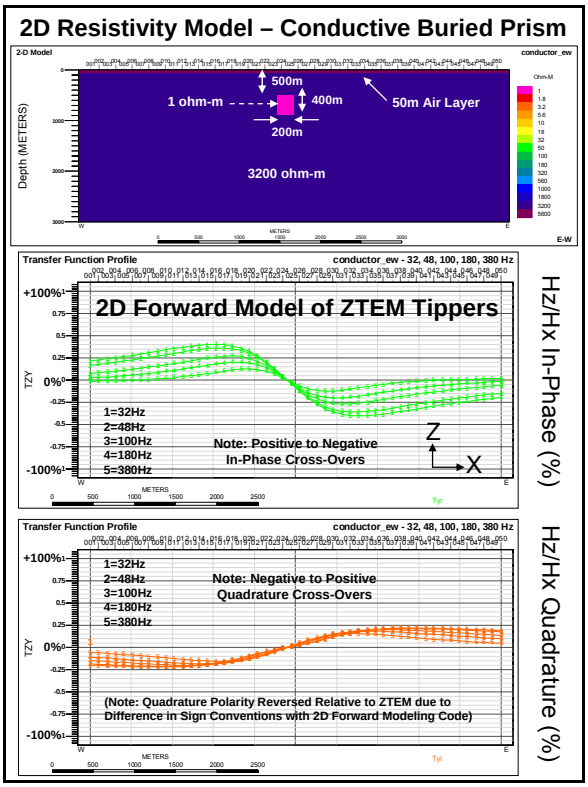

Figure D5: 2D synthetic forward model Tipper responses for conductive brick model.

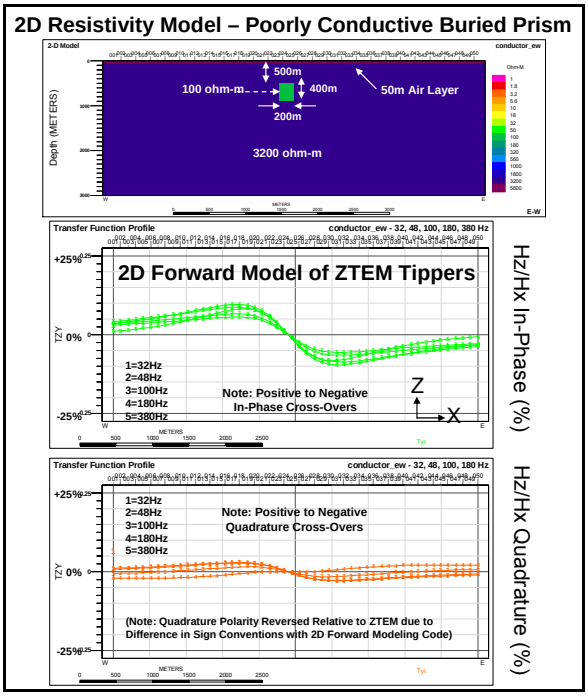

Figure D6: 2D synthetic forward model Tipper response for poorly conductive brick model.

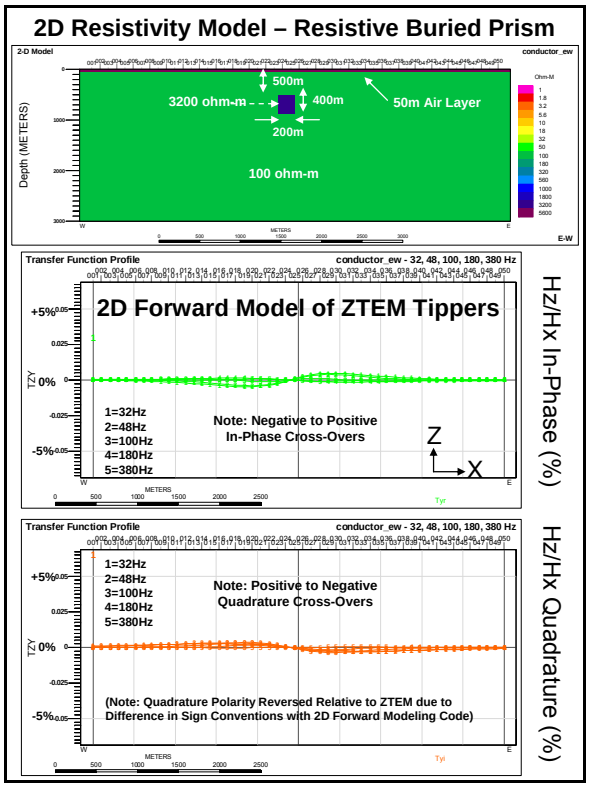

Figure D7: 2D synthetic forward model Tipper response for resistive brick model.

APPENDIX E

ZTEM (AIRBORNE AFMAG) TESTS OVER UNCONFORMITY URANIUM DEPOSITS[7]

Bob Lo [1], Jean Legault [2], Petr Kuzmin [3] [1] Formerly Geo Equipment Manufacturing Ltd., now Exploration Syndicate, Inc., bob.lo@expsyn.com, [2] Geotech Ltd., jean@geotech.ca, [3] Geo Equipment Manufacturing Ltd., petr@geotech.ca*

Key Words: ZTEM, AFMAG, electromagnetic, airborne, uranium, Athabasca.

INTRODUCTION

A series of demonstration tests were conducted using the ZTEM, airborne AFMAG system over deep targets in the Athabasca Basin of Saskatchewan, Canada. These tests were conducted in mid-2008 and were flown to test ZTEM's ability to detect large conductive targets at depth; deeper than conventional airborne EM methods. Data are presented over areas where the conductors are located 450-600 metres beneath the surface. As well, a case of ZTEM following the plunge of a conductor to over 800 metres depth is shown.

BACKGROUND

The ZTEM system is the latest implementation of an airborne AFMAG system first commercialized in late 2006. ZTEM uses a large, 8 metre diameter airborne air core coil, slung from a helicopter, to measure the vertical component of the AFMAG signal. Two 4 metre square coils are deployed on the ground to measure the horizontal field. The ZTEM system has flown successful demonstration surveys over porphyry copper deposits in the southwest USA (Zang et al., 2008).

ZTEM was tested in the Athabasca Basin in Canada in May of 2008 to determine its depth of investigation and to determine its suitability for mapping deep conductors in the crystalline basement. Over 30% of the world's U3O8 is mined in the Athabasca Basin from unconformity uranium deposits. Unconformity uranium deposits of the Athabasca Basin are often associated with conductors located in the crystalline basement. The search for economic uranium deposits is moving to areas of the basin which are deeper and beyond the detection limits of modern airborne instrumentation. This creates the requirement for a system which can detect conductivity past the detection limits of modern traditional EM systems. This was the motivation behind the field trials of the ZTEM system in the Athabasca Basin. Several areas where known deep conductors (450-600m+) were located were flown. Also, a test survey block in the northern part of the basin was able to trace a deep and plunging conductor to depths that no other airborne EM system has been able to achieve.

ATHABASCA BASIN GEOLOGY

The high-grade uranium deposits within the Athabasca Basin are associated with the unconformity between the essentially flat-lying Proterozoic Athabasca Group sandstones and the underlying Archean-Paleoproterozoic metamorphic and igneous basement rocks. The deposits occupy a range of positions from wholly basement-hosted to wholly sediment-hosted, at structurally favourable sites in the interface between the deeply weathered basement and overlying sediments of the Athabasca Basin (Ruzicka, 1997). The locations of These deposits are lithologically and structurally controlled by the sub-Athabasca unconformity and basement faults and fracture zones, which are localized in graphitic pelitic gneisses that may flank structurally competent Archean granitoid domes (Quirt, 1989).

In general, most of the known important deposits tend to occur within a few tens to a few hundred metres of the unconformity and within 500 m of the current ground surface. This may be more of a limitation of exploration techniques. There is no reason to believe that the distribution of the deposits is dependent on the modern day depth of

[7] Extended abstract submitted to 20TH ASEG International Geophysical Conference & Exhibition, Adelaide, AU, 22-26 Feb, 2009.

burial.
Empirically, the geophysical exploration for unconformity type uranium targets have been to search for large basement structures which post date the sandstone deposition of the basement (Matthews et. al, 1997). All the deposits located so far are associated with fault structures associated with a graphitic conductive basement. An alteration zone of clay silicification and enrichment around the deposits probably leads to magnetite destruction causing the magnetic low observed around the deposits. The clay alteration should give rise to a resistivity low signature about the deposits. The low conductivity of the clay alteration makes it a difficult target for airborne EM if it is buried at significant depth.

ZTEM INSTRUMENTATION AND PRESENTATION

ZTEM is an airborne AFMAG system introduced by Geotech Ltd. of Canada in early 2007 (Lo et al., 2008). In a ZTEM survey, a single vertical dipole air-core coil is flown over the survey area in a grid pattern similar to other airborne electromagnetic surveys. Two orthogonal, air-core, horizontal axis coils placed close to the survey site measures the horizontal EM fields for reference. A GPS array on the airborne coil monitors its attitude for post-flight corrections.

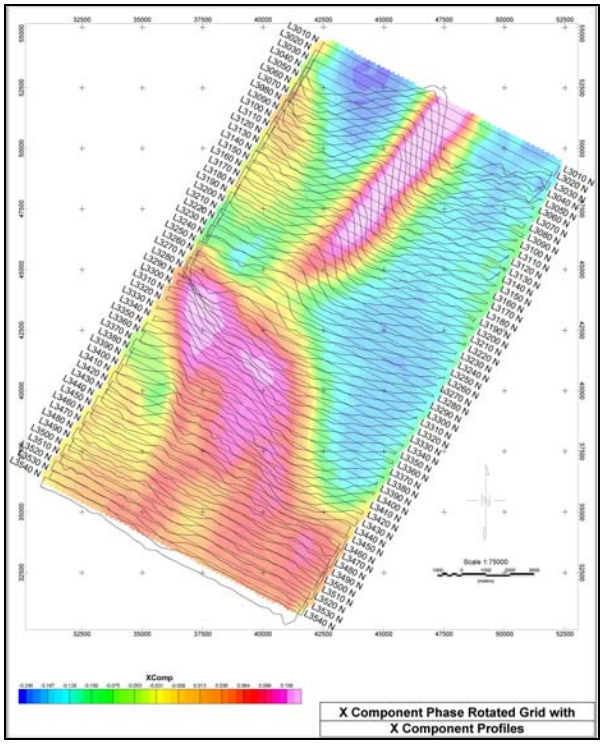

Figure 1 – Stacked profiles of the x-component Tipper over the gridded values of the phase rotated x-component data. Note that the cross-overs in the profiles are now peaks on the image.

As the source field is assumed to be far away, the excitation of the ground is more or less uniform. For large structures, the signal fall-off will be much slower than from a dipole source, such as those energized by traditional airborne systems. With the ZTEM system being less susceptible to terrain clearance, the planned ground clearance height is higher and the terrain drape is looser as compared to standard helicopter EM surveys.

The two Tippers obtained from the relationship between the vertical airborne coil and the two ground coils have a cross-over over a steeply dipping, plate-like body. The cross-overs can be made into local maxima via a 90 degree phase rotation which allows for easier interpretation of the gridded values. Figure 1 is an example of this transformation.

To present the data of both Tippers as one image, we calculate a parameter termed the DT which is the horizontal divergence of the two Tippers, much in the same manner as the "peaker" parameter in VLF (Pedersen, 1998). The DT is typically plotted with an inverted colour bar as it is negative over a steeply dipping thin body.

ZTEM RESULTS – NORTHERN ATHABASCA BASIN

Figure 2 shows gridded values from a number of ZTEM lines over an area where the sedimentary cover is approximately 450-600 metres thick. A number of traditional EM systems have also been flown over this block. While they were able to detect conductors, the resolution of the conductive features is not nearly as detailed as the information provided by ZTEM.

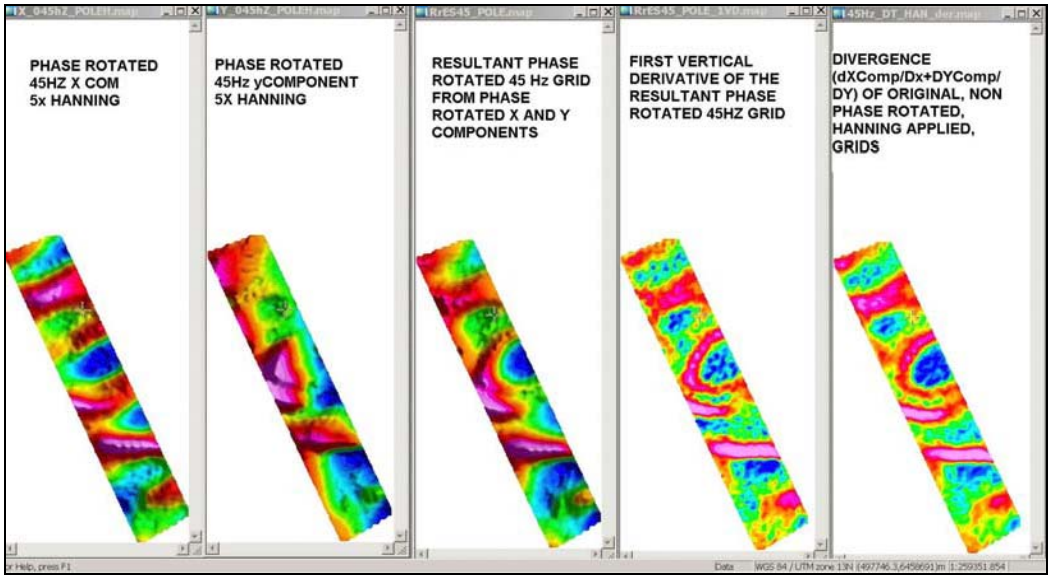

Figure 2 – ZTEM results over an area of 450-600 metre thick sedimentary cover.

Figure 3, from another area, shows the data from one of the larger blocks that was flown. It is a 3D composite image of the DT at various frequencies plotted at the equivalent skin depth assuming a 1,000 ohm-m average resistivity.

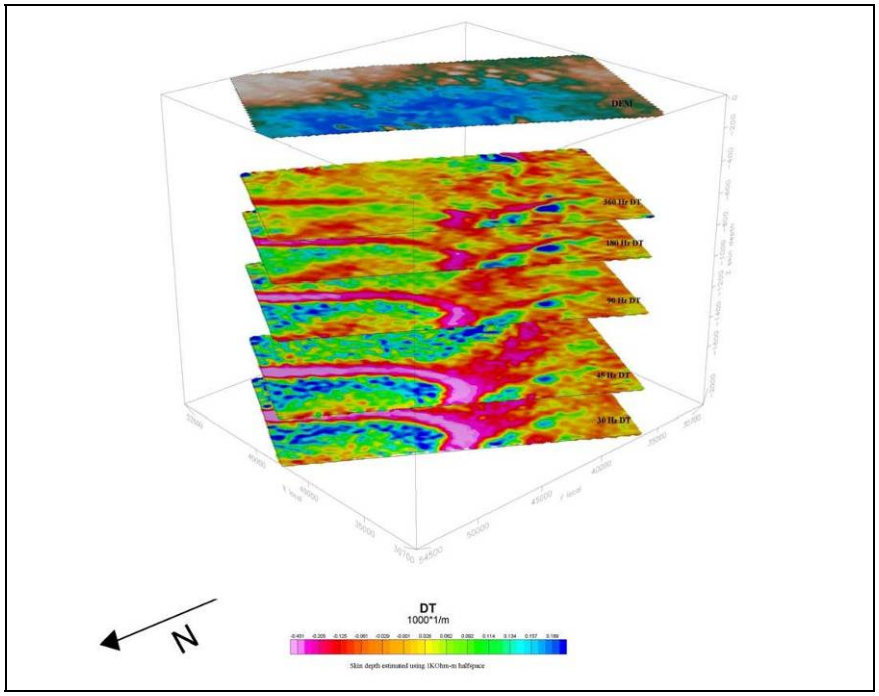

Figure 3 - Perspective view of DT's of different frequencies plotted at the skin depth (using a 1,000 ohm-m Earth.

The data in Figure 3 come from a survey over the north rim of the Athabasca Basin. The sandstone cover is about 500m on the left hand side of the image, and progressively getting deeper to the right. It is about 700m in the middle part of the image and over 800 metres thick on the right middle portion where exploration drilling is concentrated. Starting in the middle left and trending to the right of the image, there is a known graphitic shear.

In the uppermost (600m) "depth slice", Figure 3 shows a linear conductive feature that progressively weakens as one moves to the right until it is no longer seen. This is interpreted to be due to the graphitic shear conductor plunging deeper past the depth of investigation of the 360 Hz data. The lower frequencies penetrate more into the sedimentary cover that is deeper towards the right. DT's of decreasing frequency show the linear conductive feature extending more and more to the right. The feature also strengthens/sharpens into a synformal shape with lower frequencies. This fits with what the known geology of a plunging conductor at depth is doing.

At the nose of the fold, in the right third of the images, we also see another, broader anomalous zone that trends towards the back of the image. At this location, two radioactive springs are situated. These spring waters which are anomalously high in uranium and radon may reflect the upward migration of deep waters along faults, suggesting structural targets in areas where basinal waters may have tapped a radioactive source. This broad DT trend might be the plunge of the fold axis that is aligned away from the front of the image. An anomaly along this trend, at the highest frequency, that steadily grows with each decreasing frequency can be seen. This might represent an alteration zone in the sandstone that is detected at the shallowest depth. By about the 90Hz DT depth slice or so, we are possibly in the deeper basement and into a basement graphitic unit.

CONCLUSIONS

A number of successful ZTEM tests were conducted over the Athabasca Basin. The tests demonstrated that ZTEM can easily detect conductivity to 800 metres beneath relatively resistive sedimentary cover. Assuming a 1,000 ohm-metre

resistivity, the skin depth of the 30 Hz data is approximately 2,000 metres. The 30 Hz data presented have good signal to noise ratios indicating a deep depth of exploration. The observation that ZTEM may be detecting the clay alteration above the crystalline basement is a significant advantage for exploration of unconformity uranium deposits.

More demonstration surveys are planned in the Athabasca Basin later this year. And more target types for testing are also planned.

ACKNOWLEDGEMENTS

The authors thank Geotech Ltd. for allowing them to publish this work and for providing the support required to write this abstract and to present this paper.

REFERENCES

Labson, V. F., Becker A., Morrison, H. F., and Conti, U., 1985, Geophysical exploration with audiofrequency natural magnetic fields, Geophysics, Vol. 50, p. 656-664.

Lo, B., Zang, M., Kuzmin, P., 2008, Geotech's Z-TEM (Airborne AFMAG) Instrumentation, a paper presented at KEGS PDAC 2008 Symposium, Toronto.

Matthews, R., Koch, R. and Leppin, M., 1997, Advances in Integrated Exploration for Unconformity Uranium Deposits in Western Canada; in Proceeding of Exploration 97, edited by Arnis Gubins, Prospectors and Developers Association of Canada, Toronto.

McMullan, S.R., Matthews, R.B, and Robertshaw, P., 1990, Exploration geophysics for Athabasca Uranium Deposits, in: Proceedings of Exploration 87, Ontario Geological Survey.

Pedersen, L.B, Qian, W., Dynesius, L., Zhang, P., 1994, An airborne tensor VLF system. From concept to realization, Geophysical Prospecting, Vol. 42.

Ruzicka, V.R., 1997, Metallogenic features of the uranium-polymetallic mineralization of the Athabasca Basin, Alberta, and a comparison with other parts of the basin; in R.W. Macqueen, ed., Geological Survey of Canada, Bulletin 500, 31-79.

Wheatley, K., Murphy, J., Leppin, M., and Climie, J.A., 1996, Advances in the Genetic Model and Exploration Techniques for Unconformity-type Uranium Deposits in the Athabasca Basin; in Ashton, K.E., Harper, C.T., eds., MinExpo '96 Symposium – Advances in Saskatchewan Geology and Mineral Exploration: Saskatchewan Geological Society, Special Publication No 14, p. 126-136.

Quirt, D., 1989, Host rock alteration at Eagle Point South: Sask. Research Council, Publication no. R-855-1-E- 89, 95p.

Ward, S. H., 1959, AFMAG - Airborne and Ground: Geophysics, Vol. 24, p. 761-787.

Zang, M., Lo, B., 2008, The Application of Airborne Natural Field Electromagnetics (ZTEM): Some Examples from the Southwestern United States, a paper presented at the 2008 PDAC, Toronto

APPENDIX F

ZVERT2D INVERSION SUMMARY

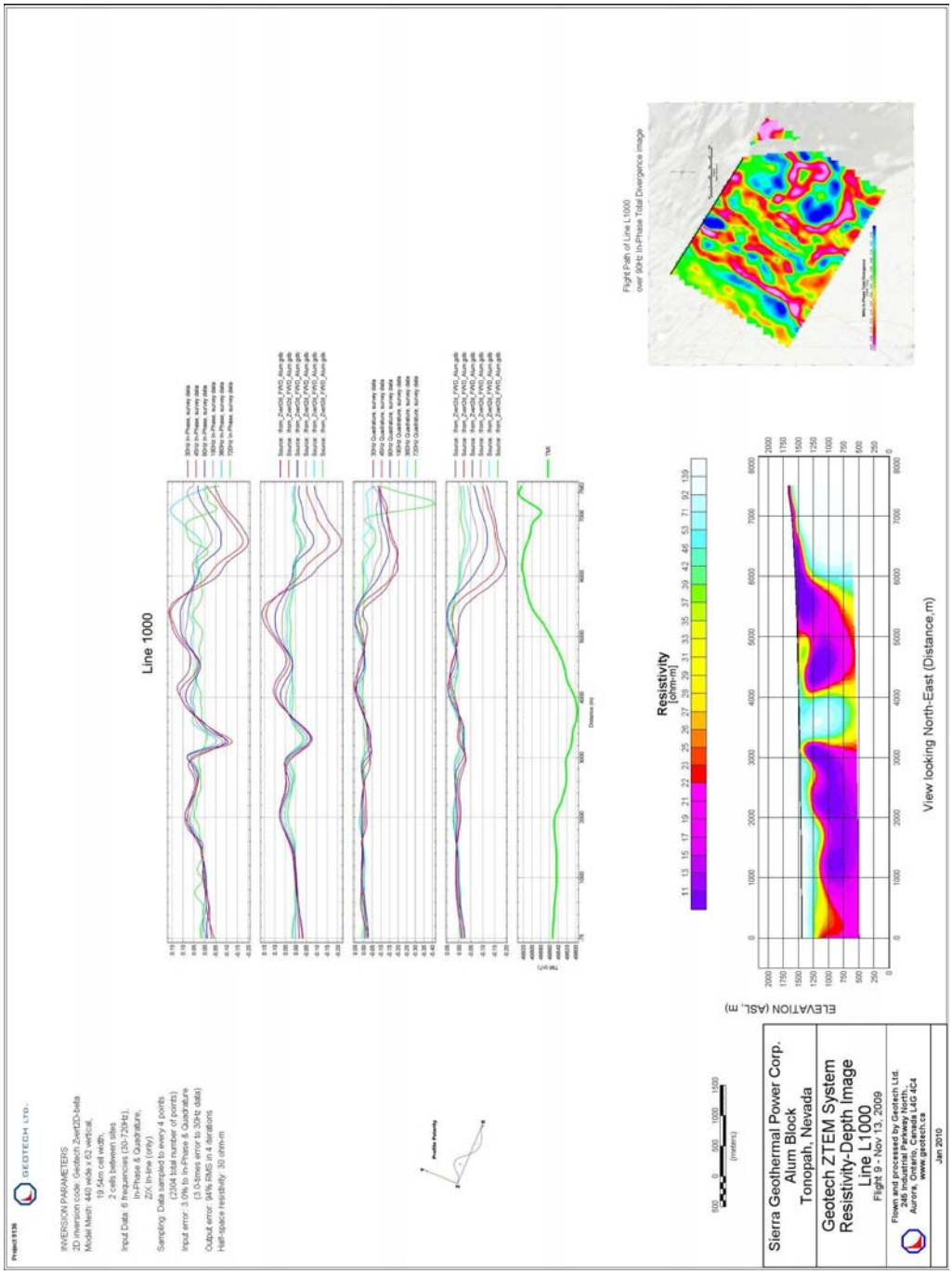

Alum Block Line 1000

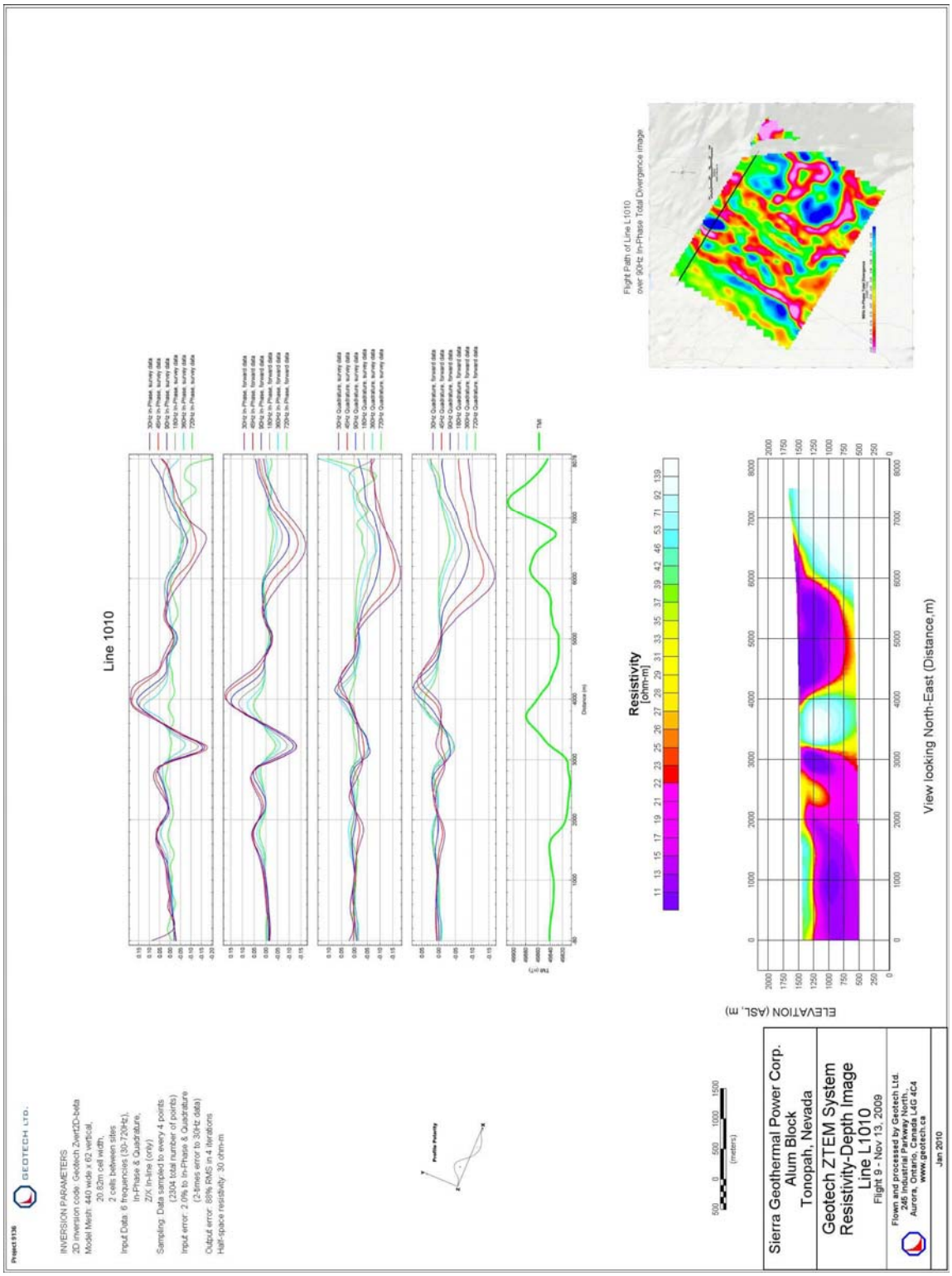

Alum Block Line 1010

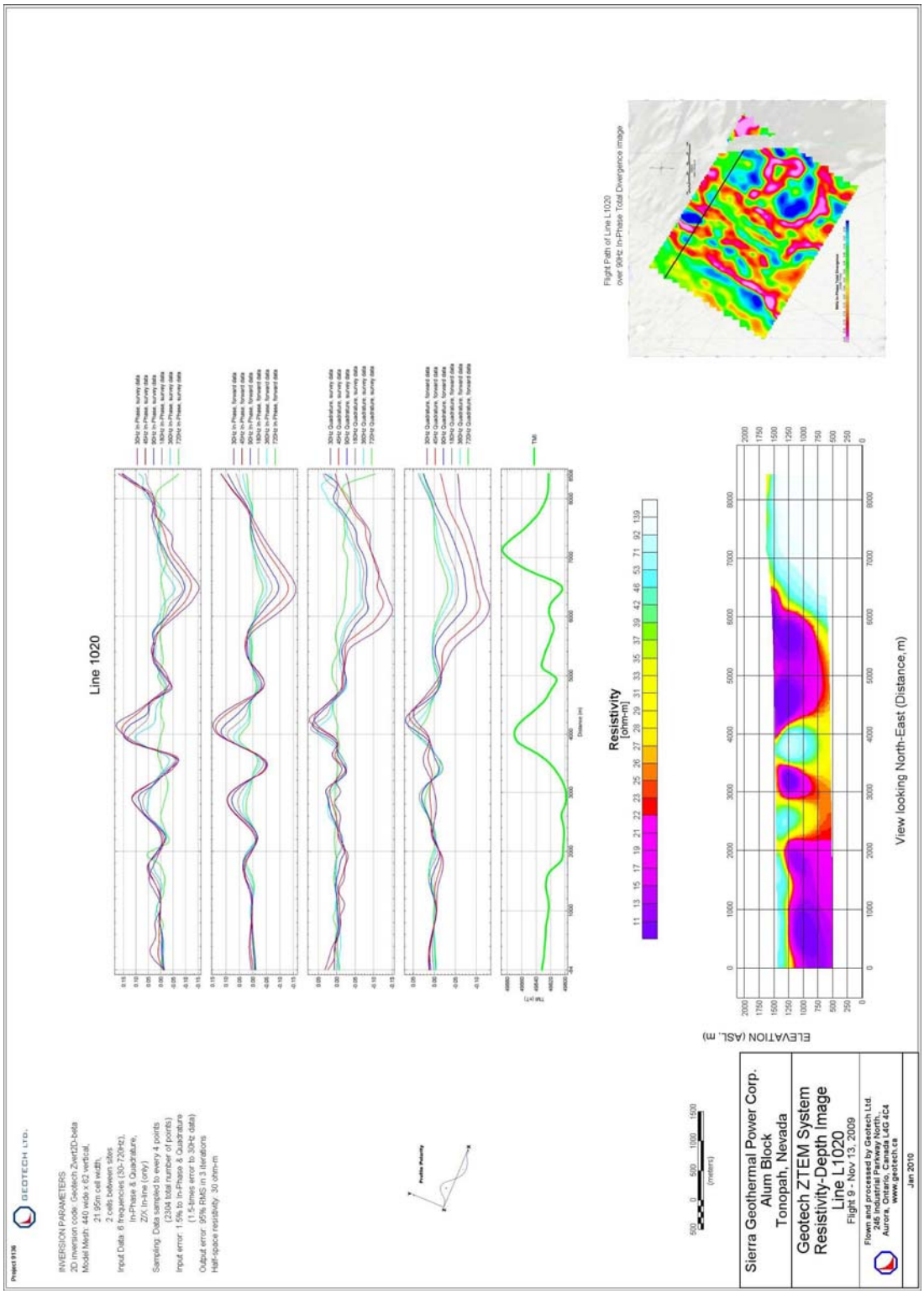

Alum Block Line 1020

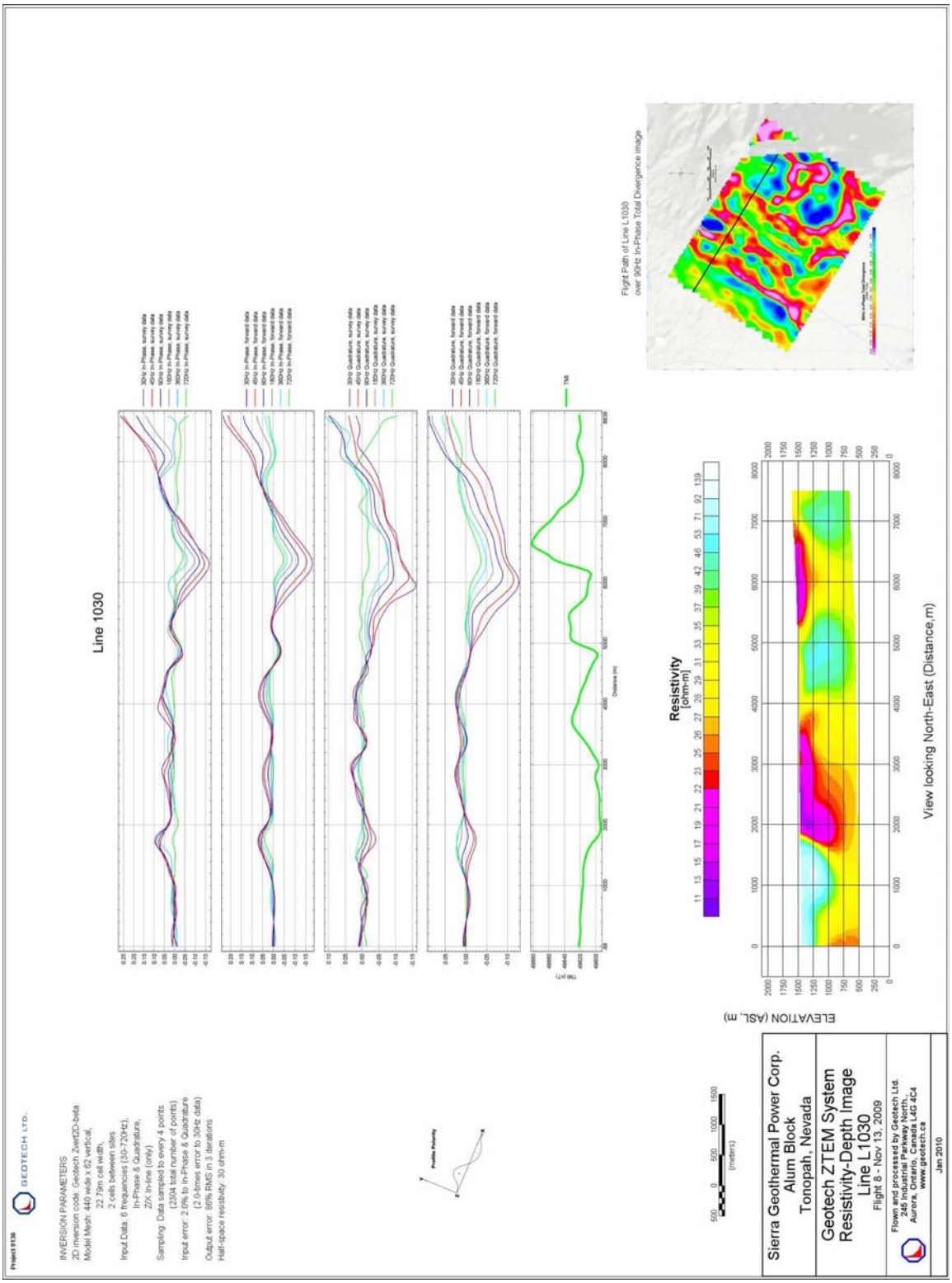

Alum Block Line 1030

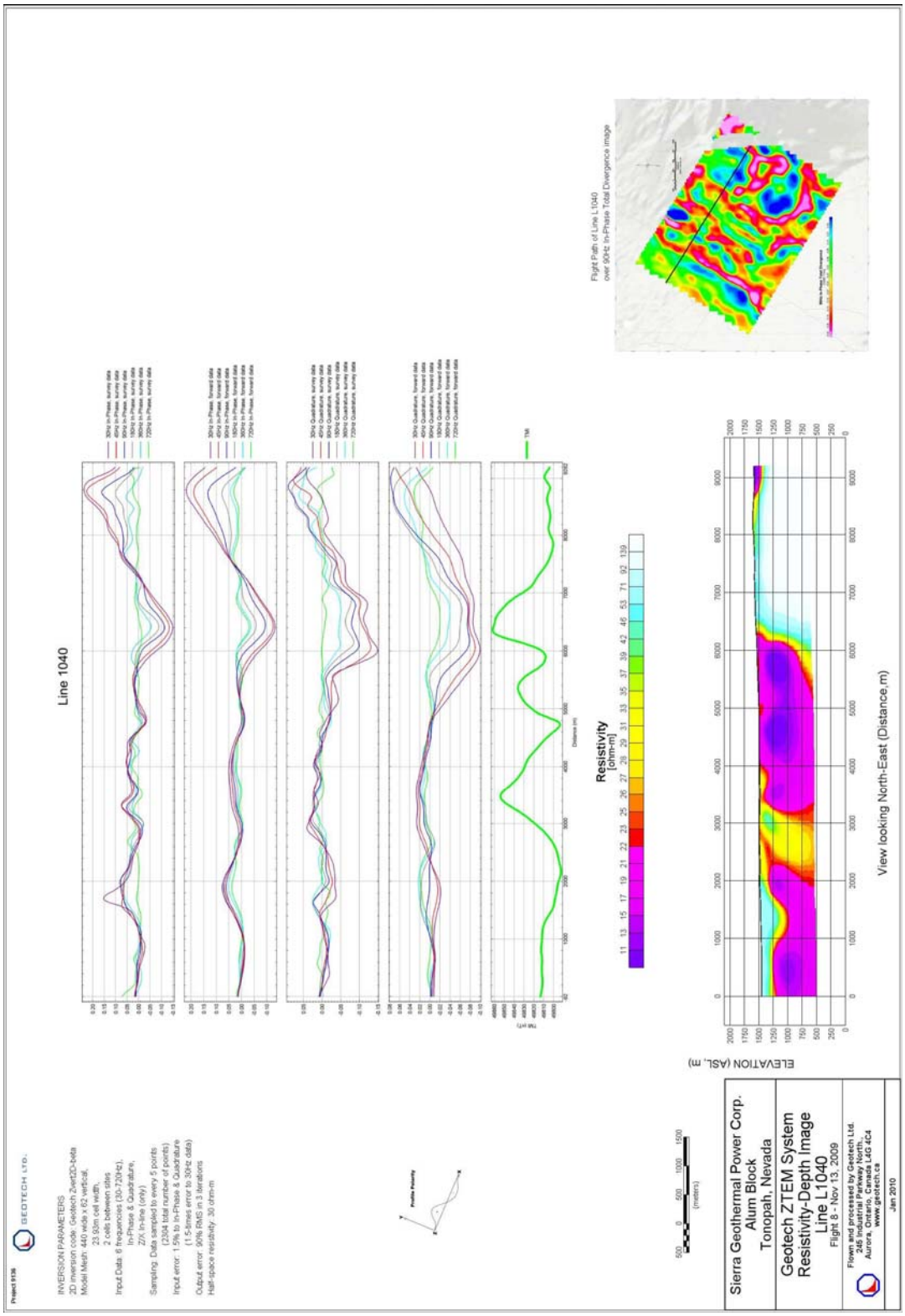

Alum Block Line 1040

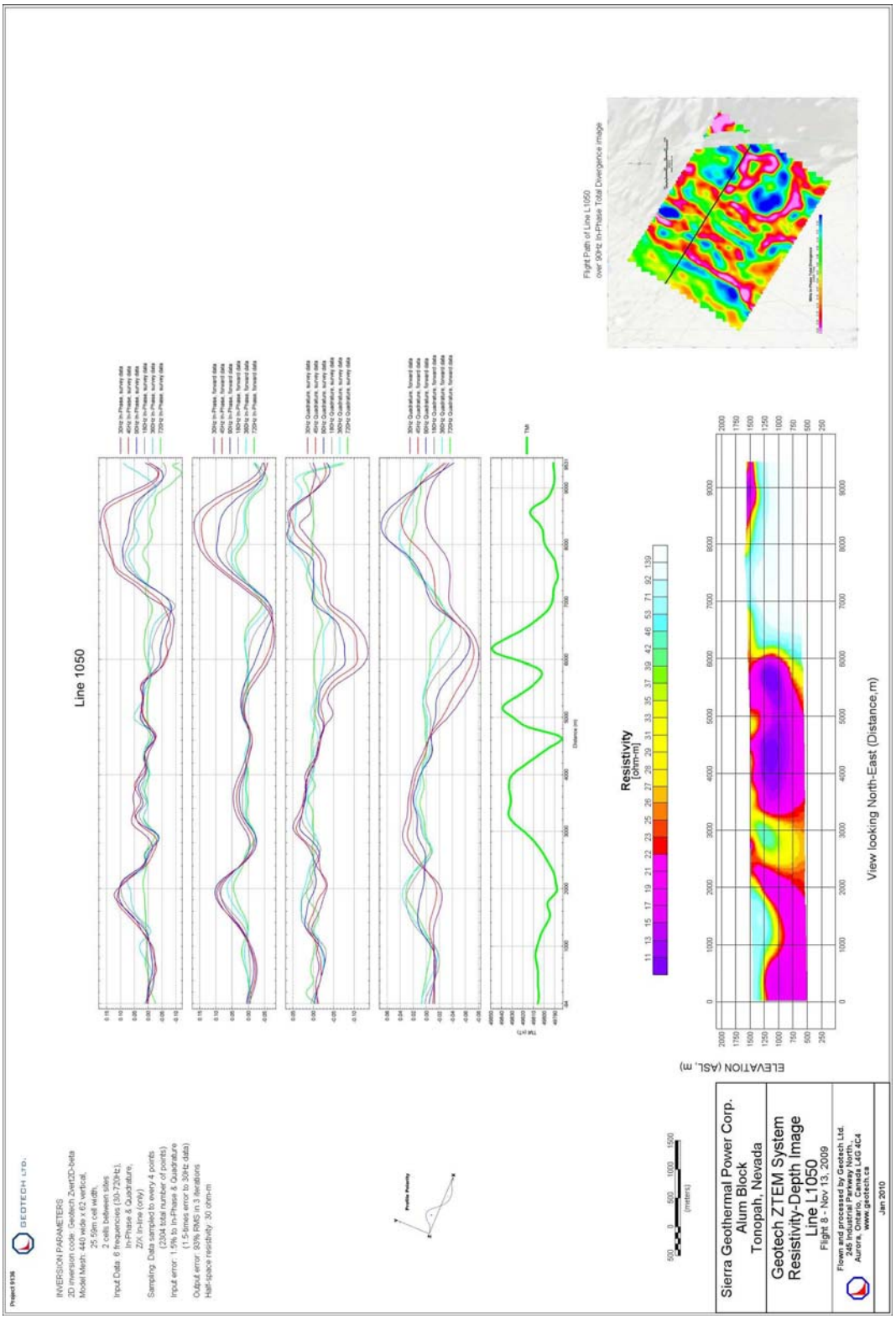

Alum Block Line 1050

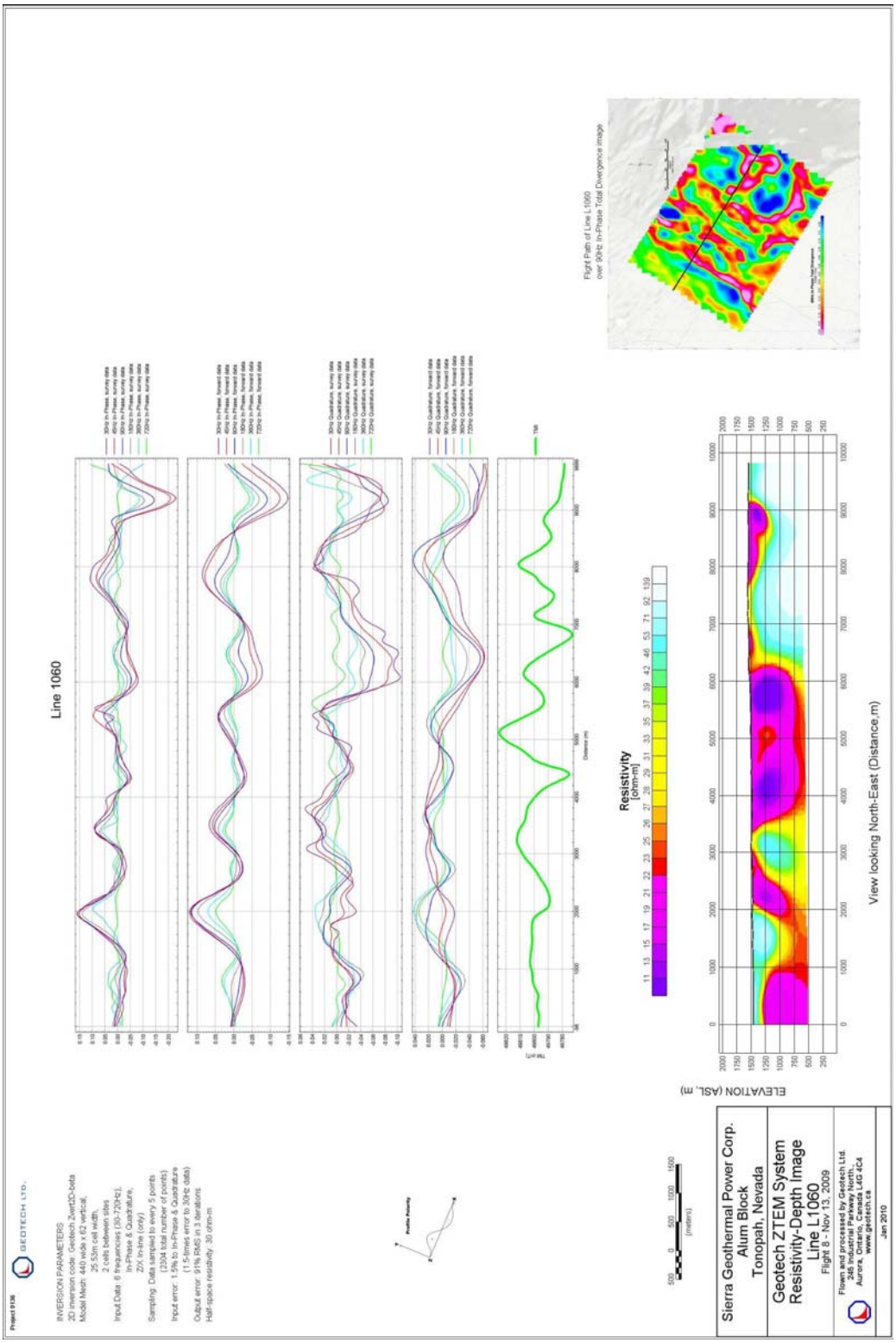

Alum Block Line 1060

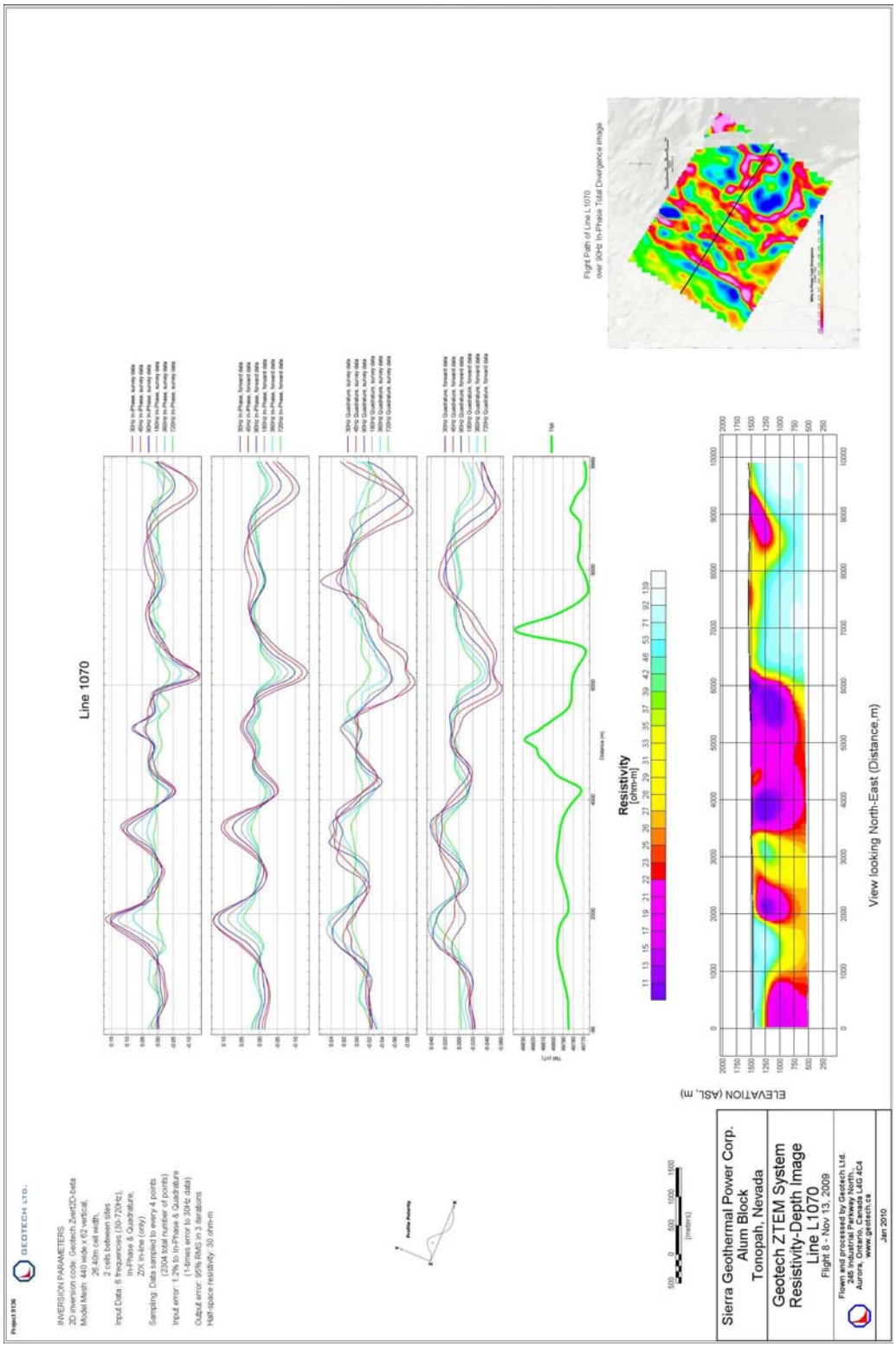

Alum Block Line 1070

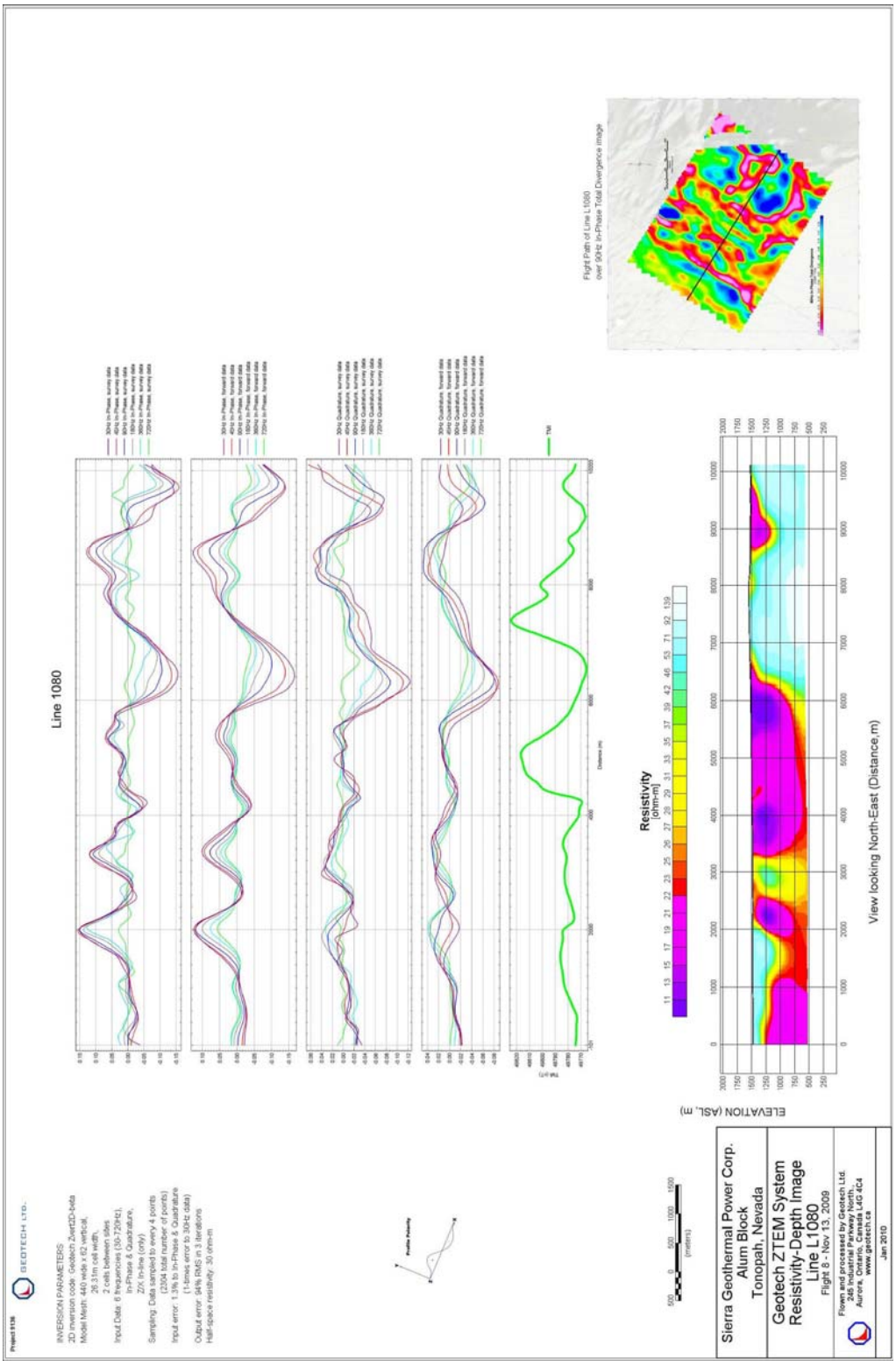

Alum Block Line 1080

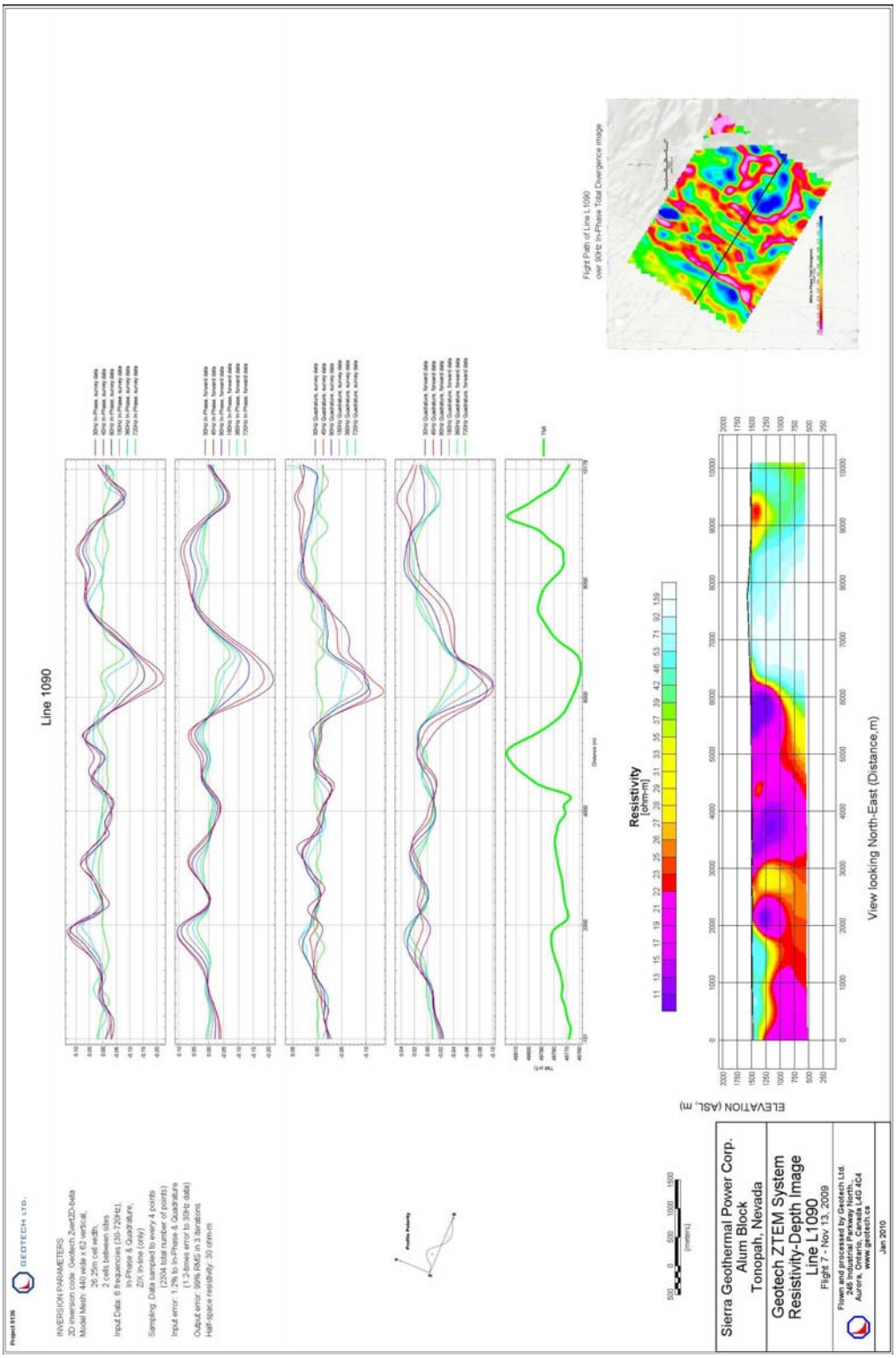

Alum Block Line 1090

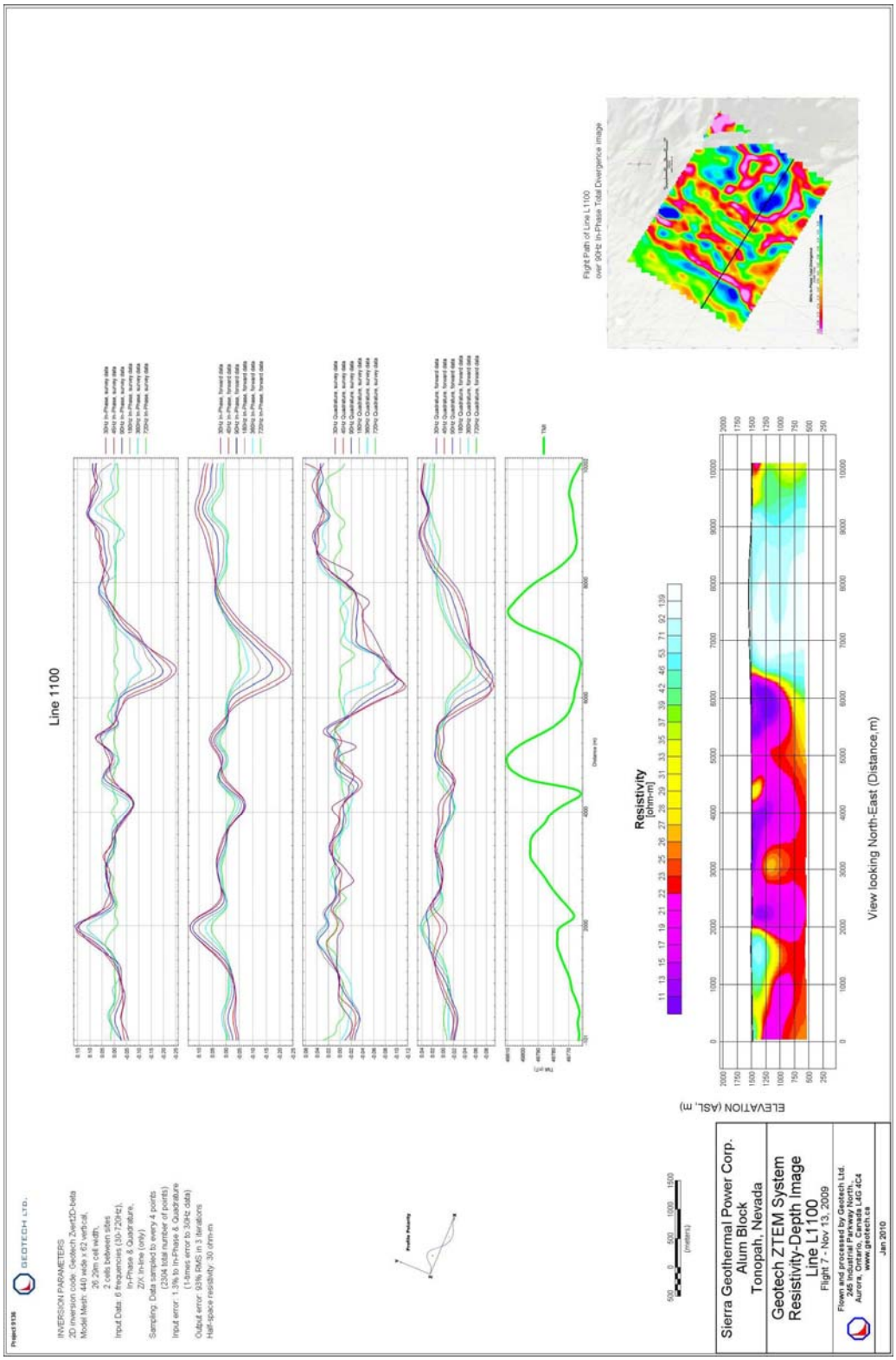

Alum Block Line 1100

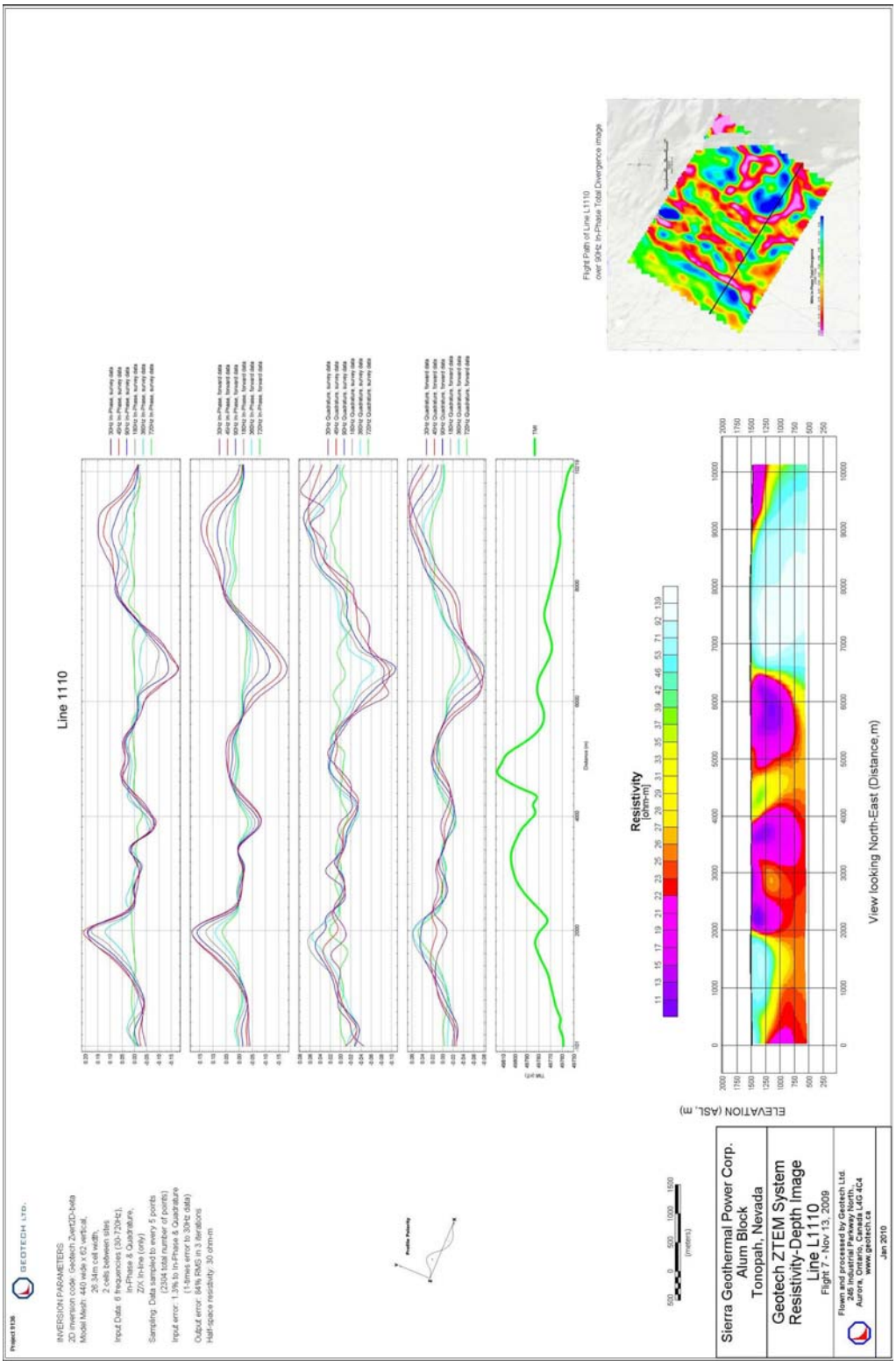

Alum Block Line 1110

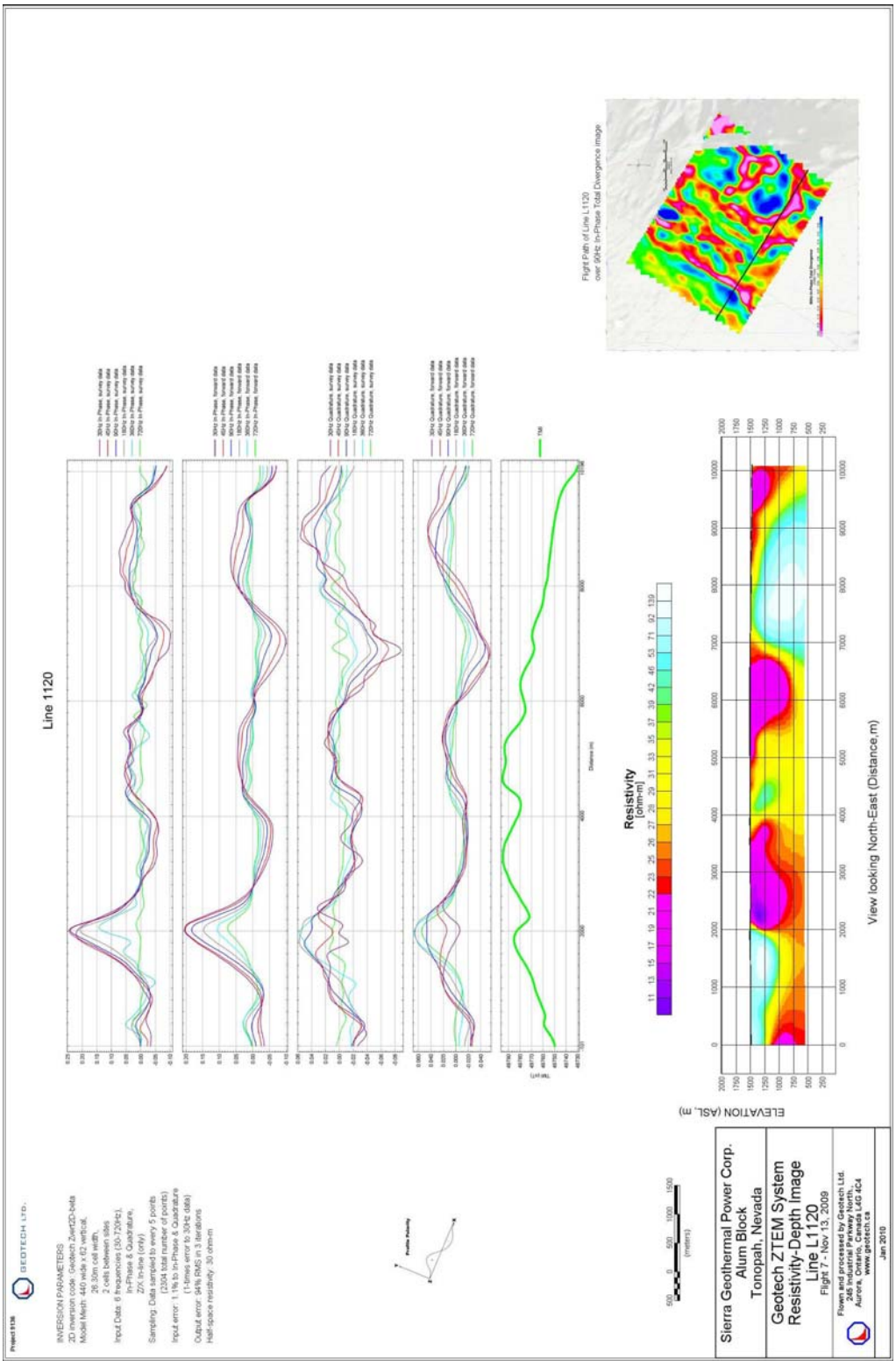

Alum Block Line 1120

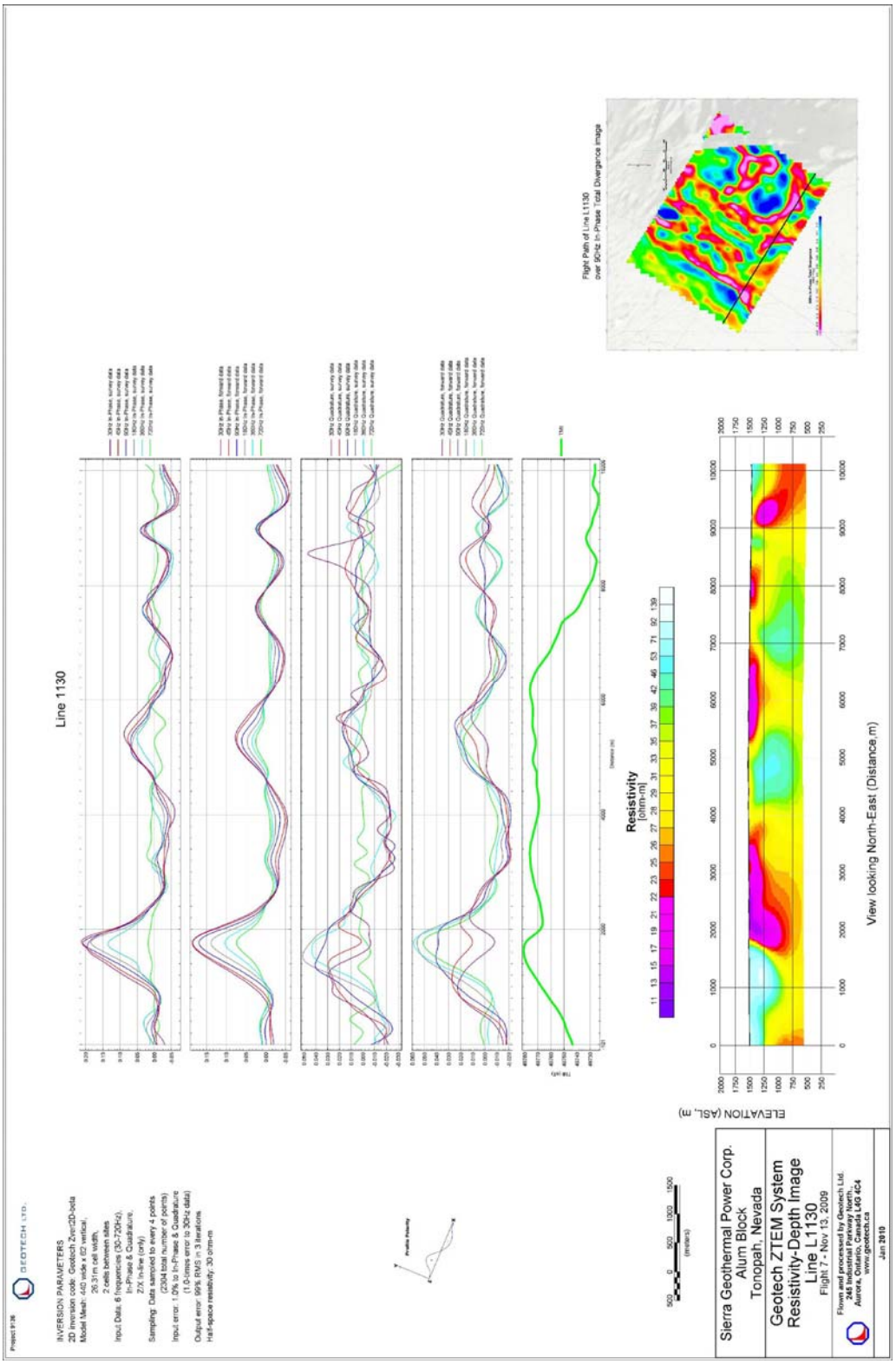

Alum Block Line 1130

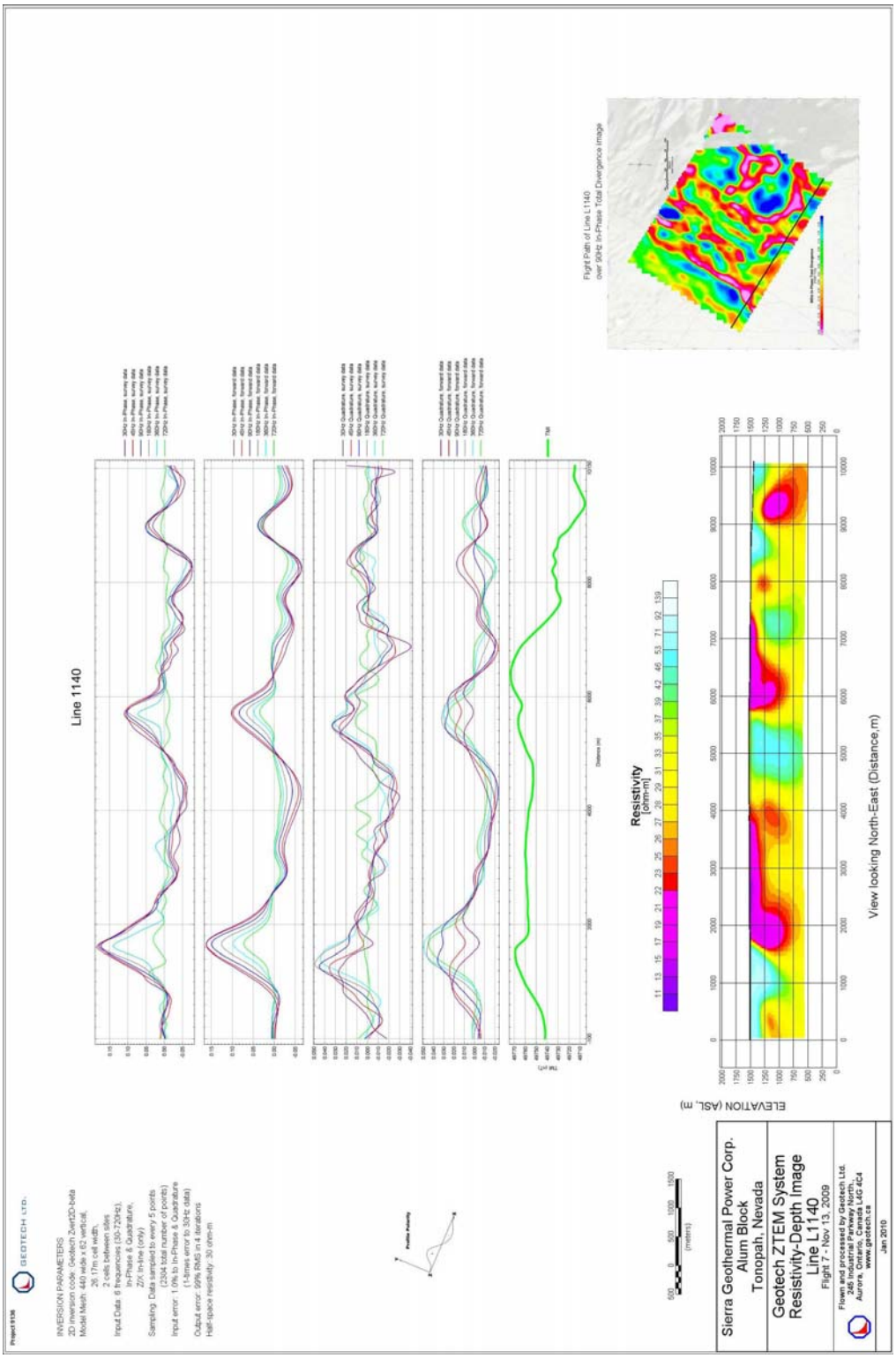

Alum Block Line 1140

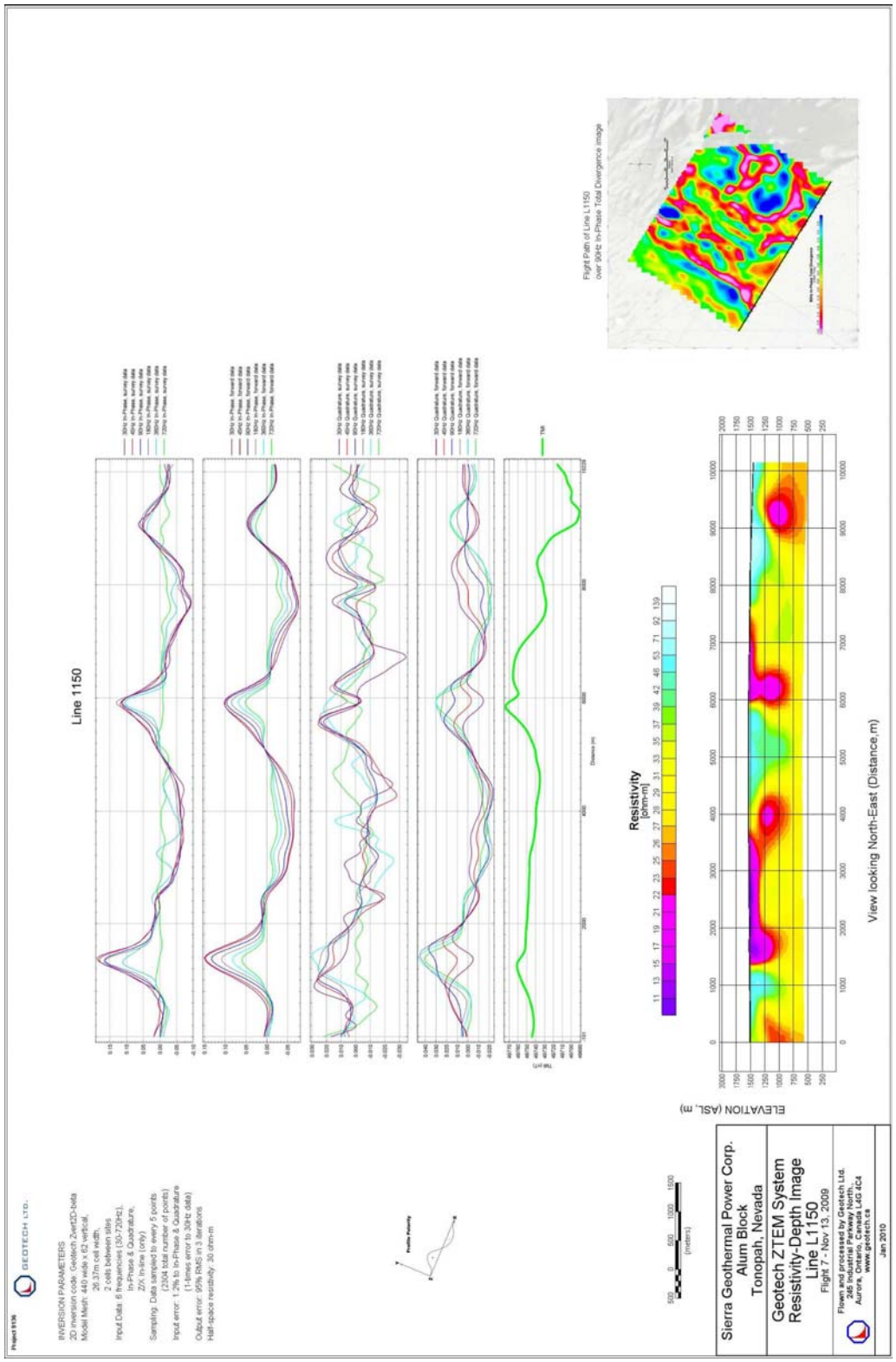

Alum Block Line 1150

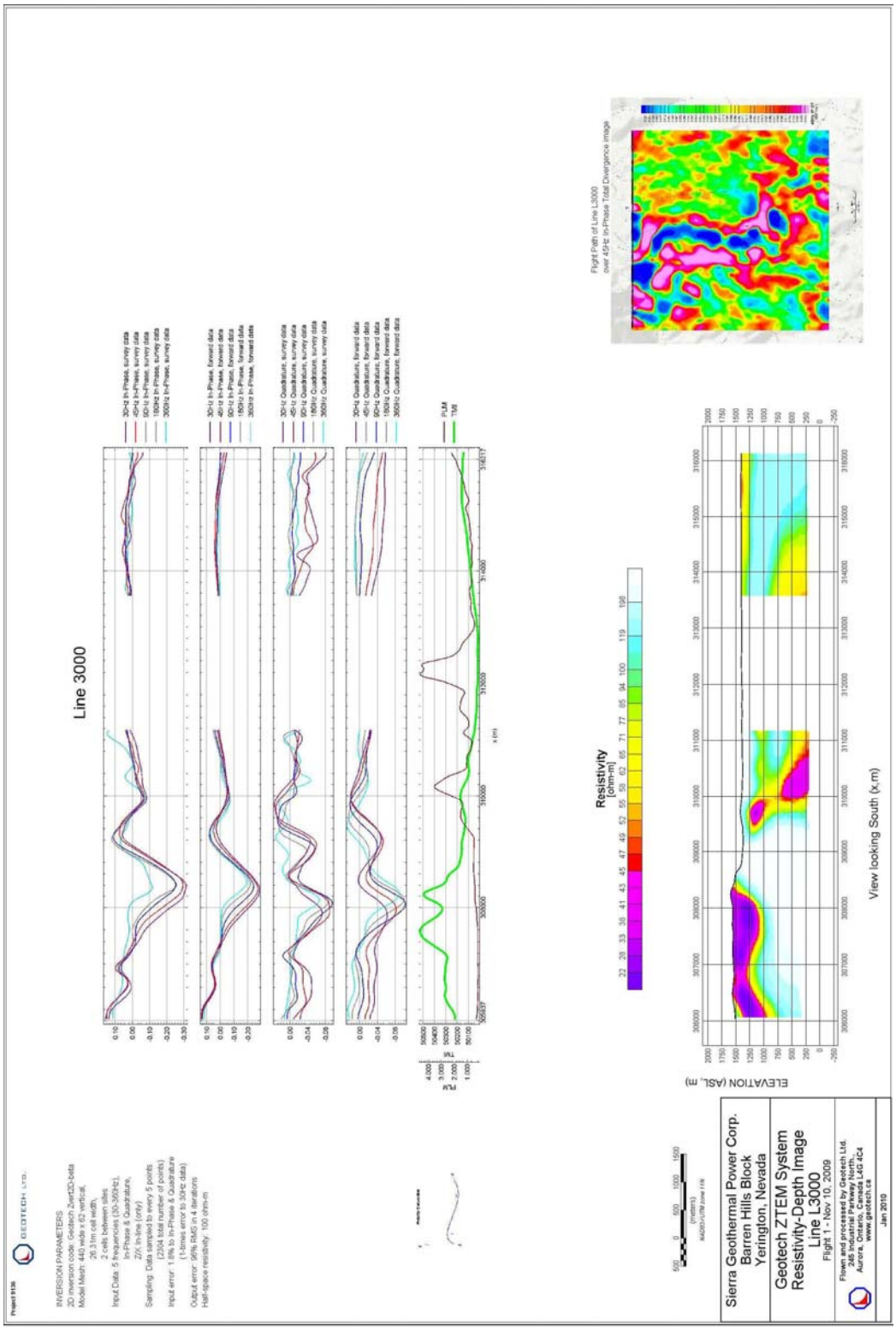

Barren Hills Block Line 3000

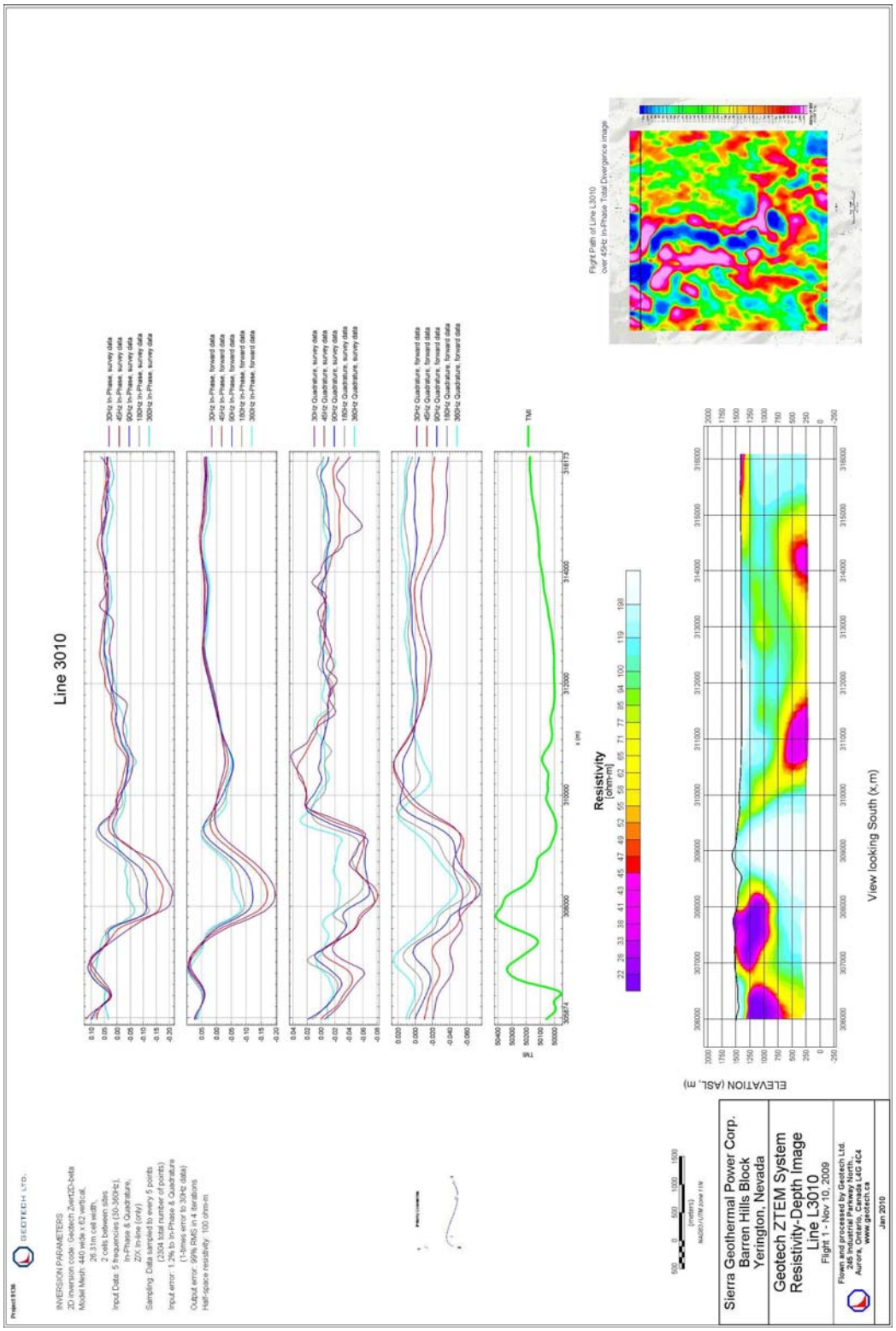

Barren Hills Block Line 3010

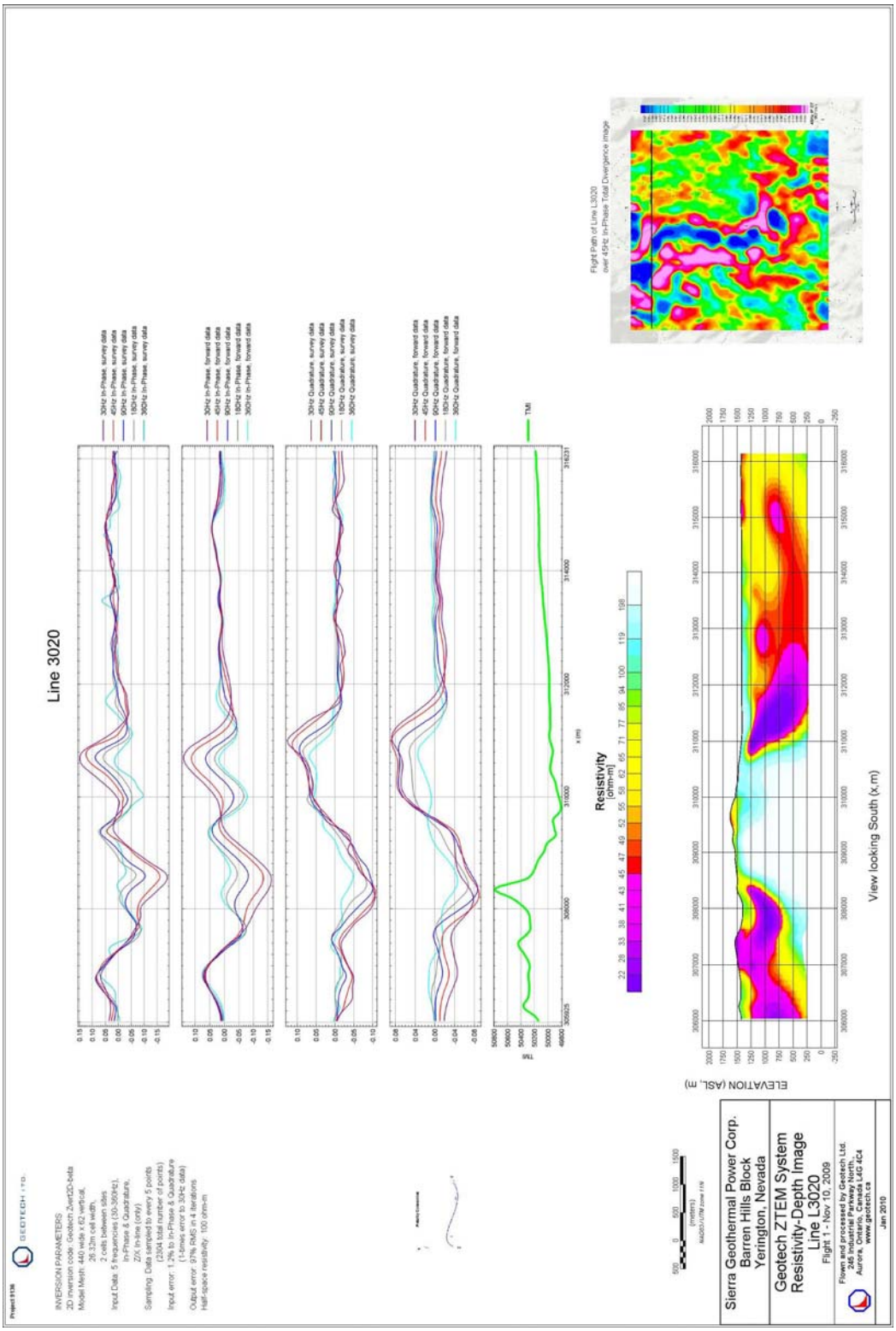

Barren Hills Block Line 3020

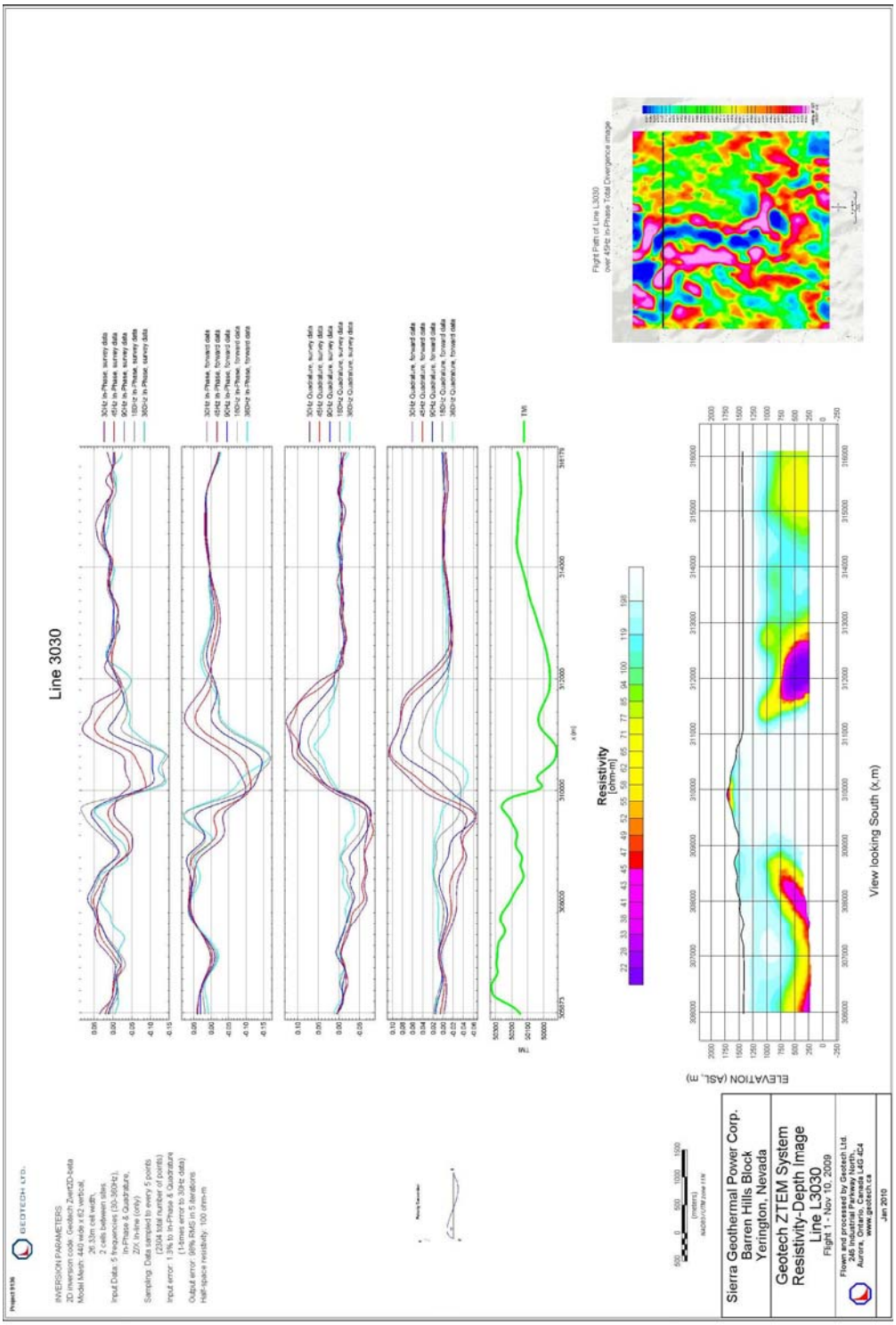

Barren Hills Block Line 3030

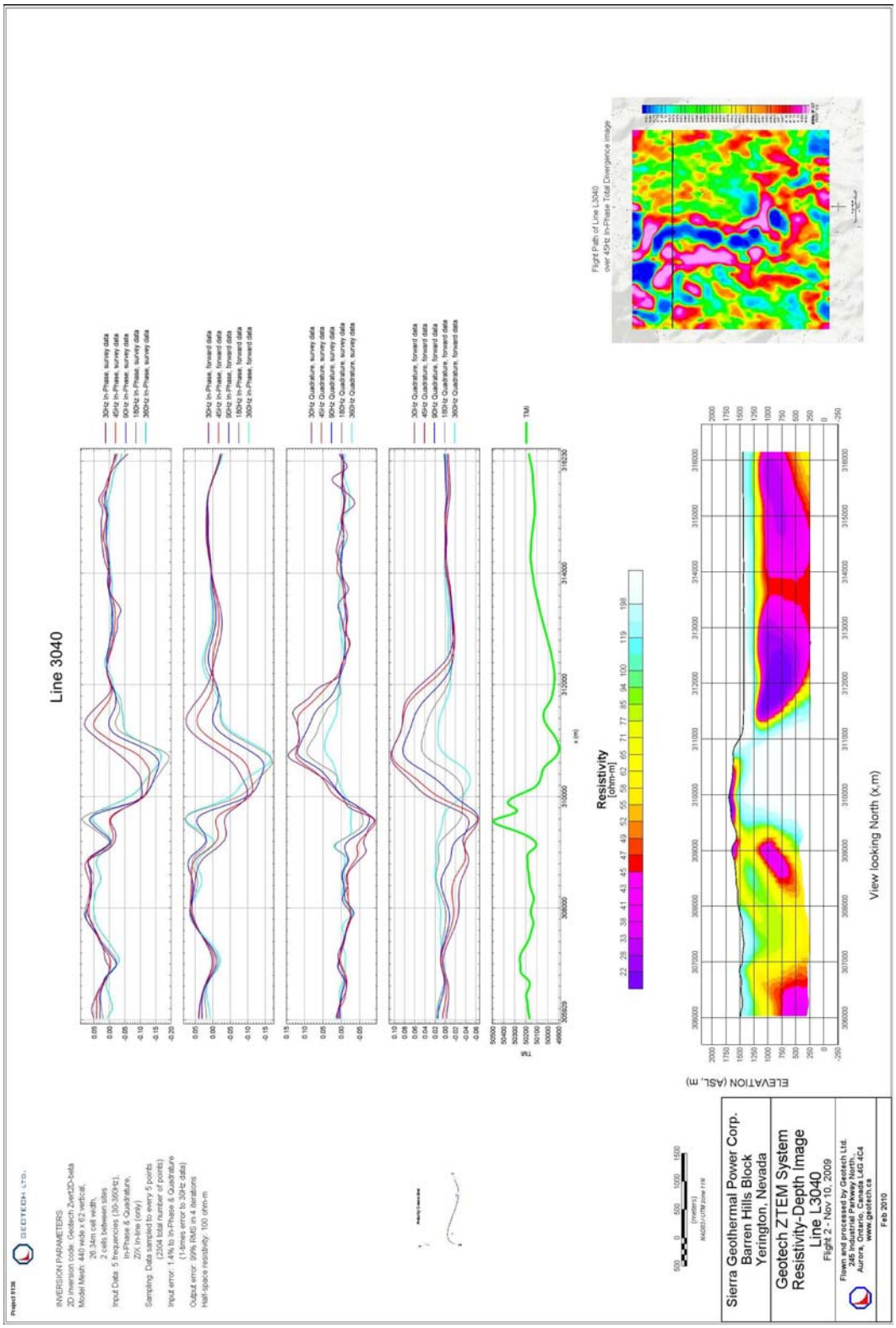

Barren Hills Block Line 3040

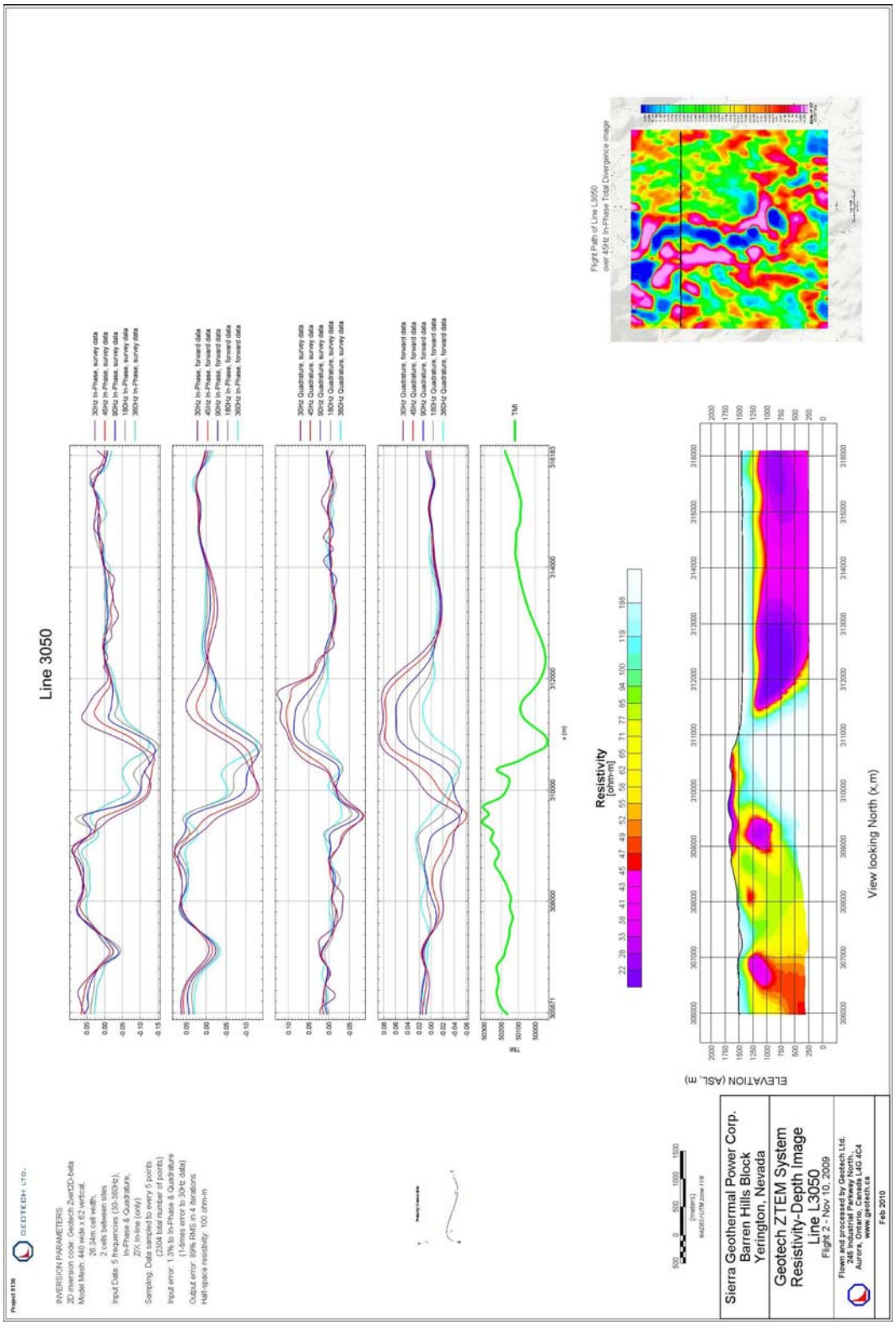

Barren Hills Block Line 3050

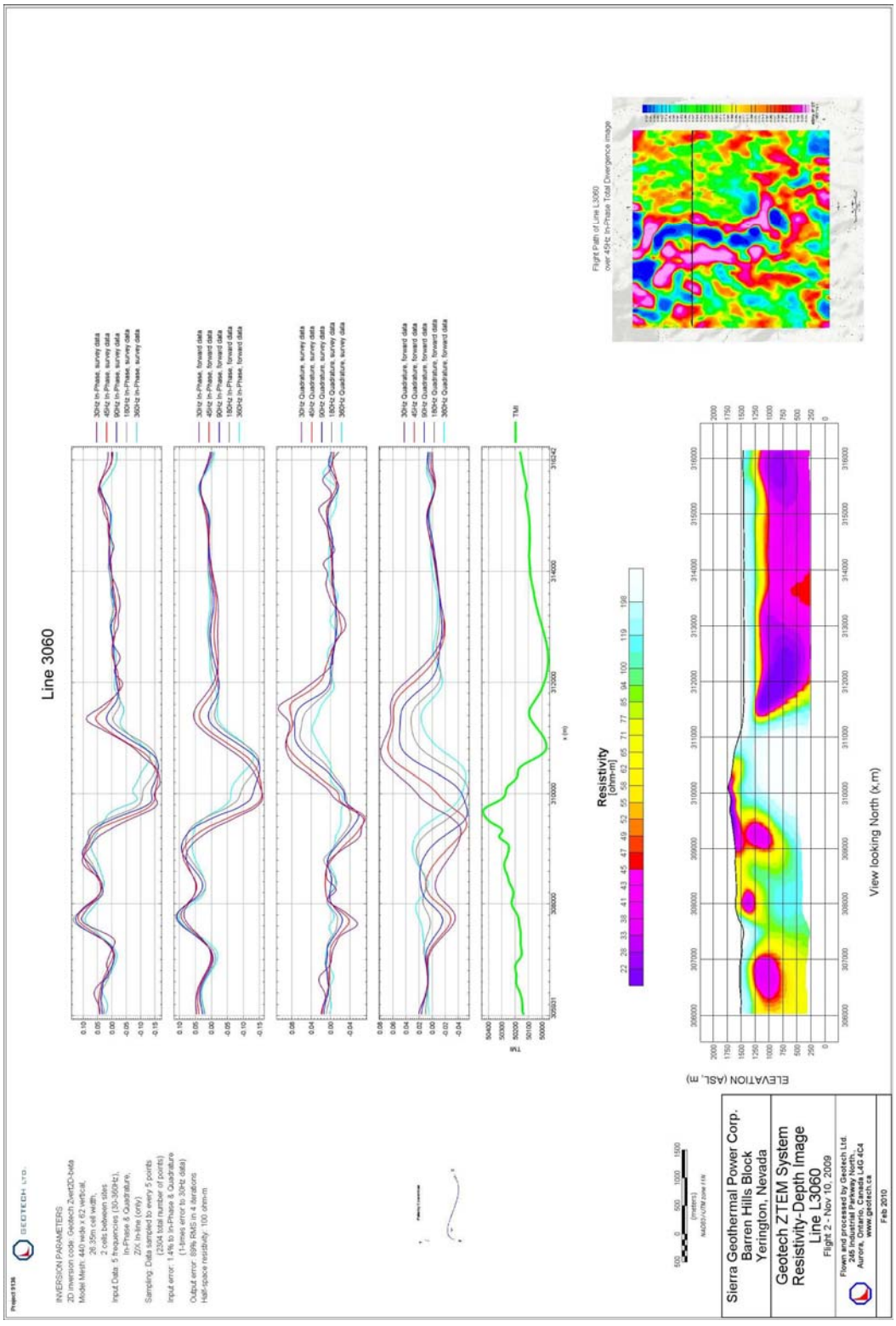

Barren Hills Block Line 3060

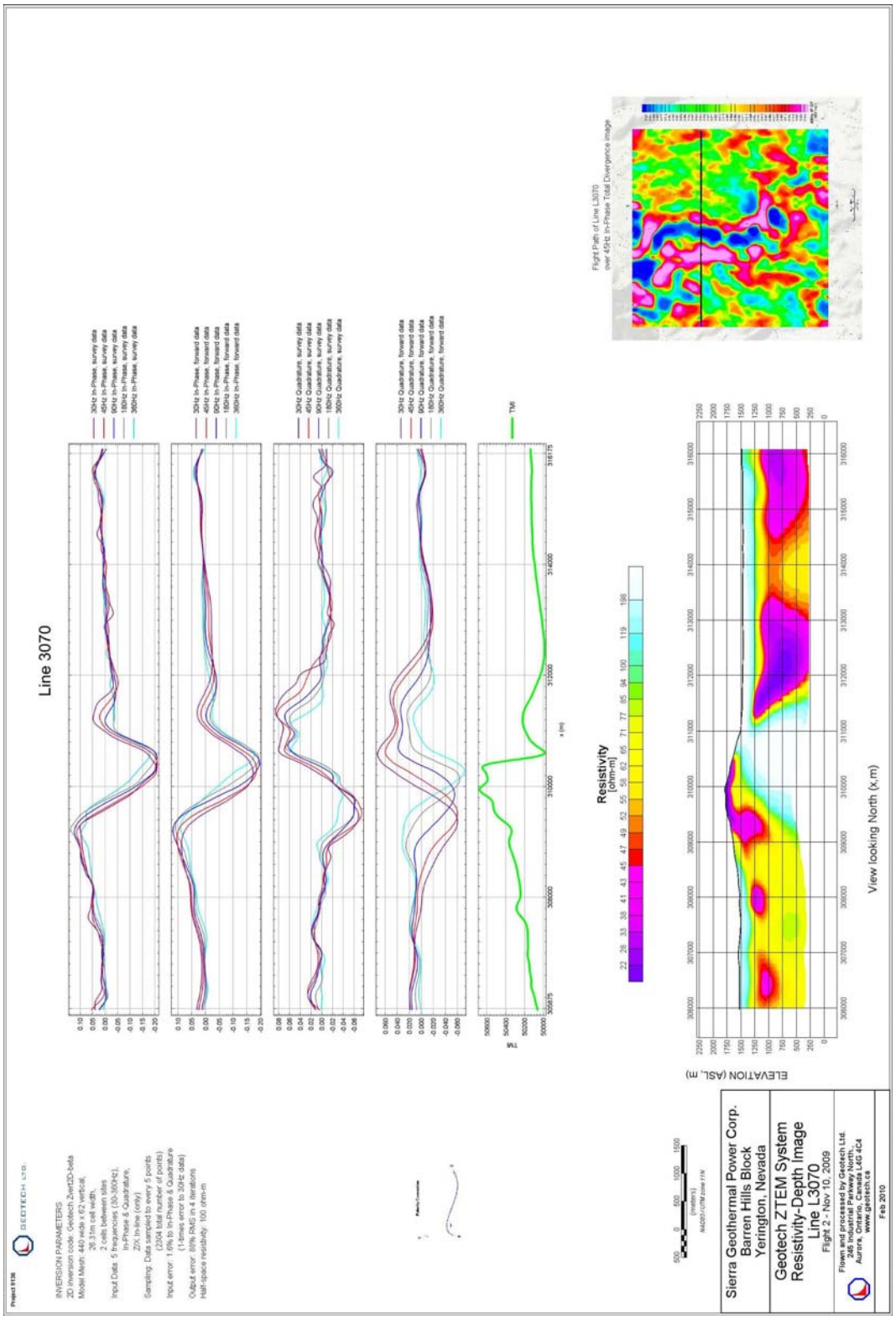

Barren Hills Block Line 3070

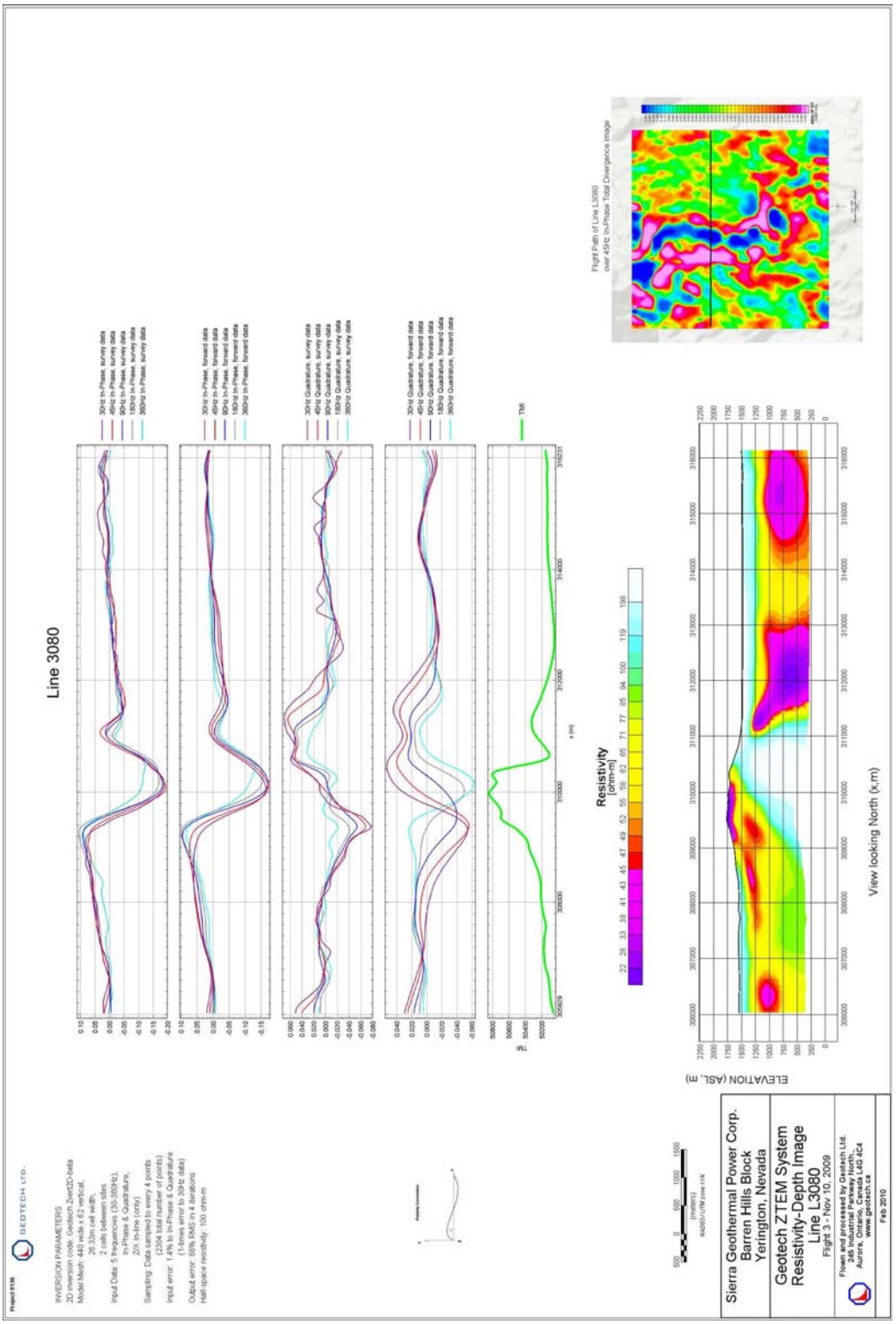

Barren Hills Block Line 3080

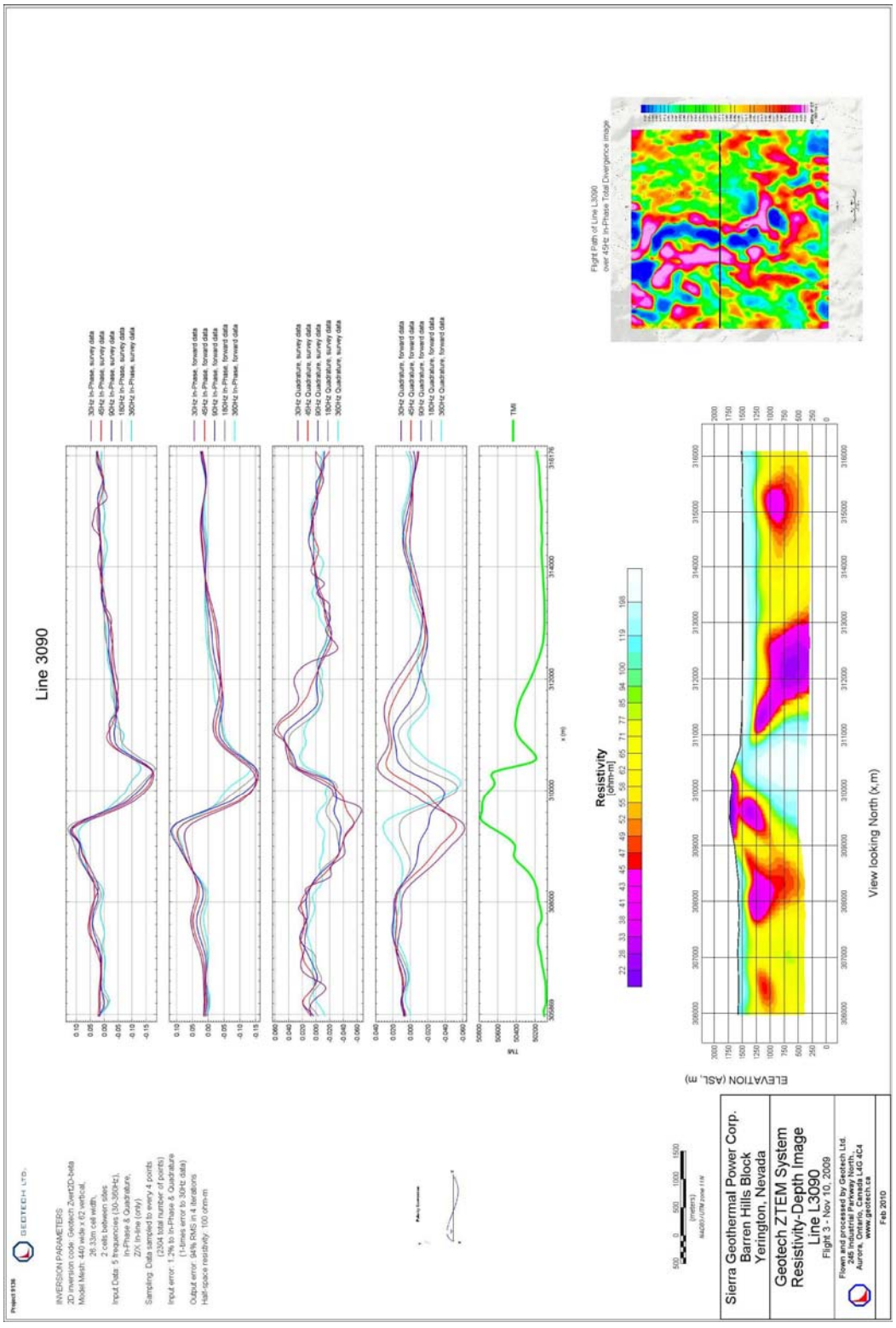

Barren Hills Block Line 3090

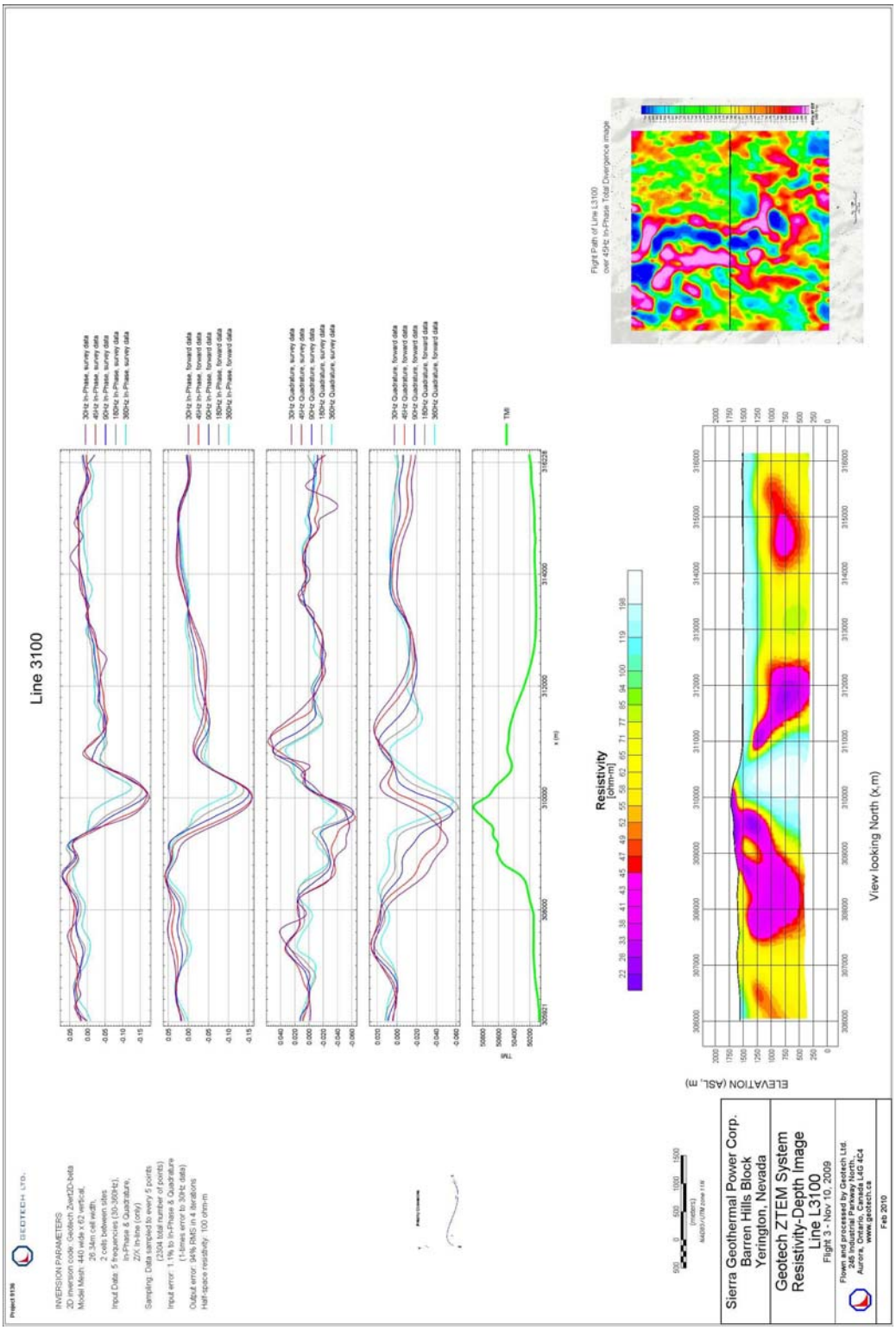

Barren Hills Block Line 3100

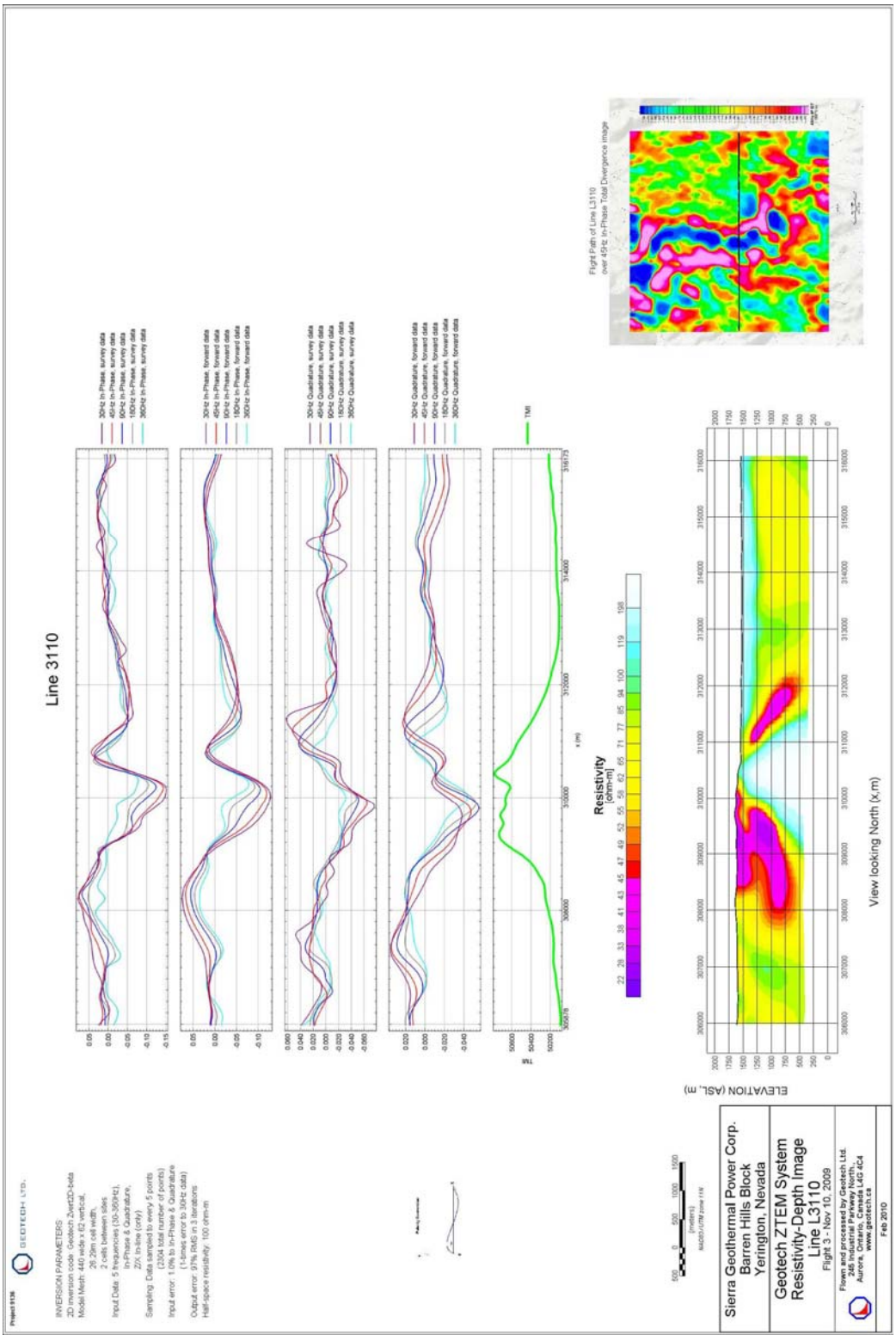

Barren Hills Block Line 3110

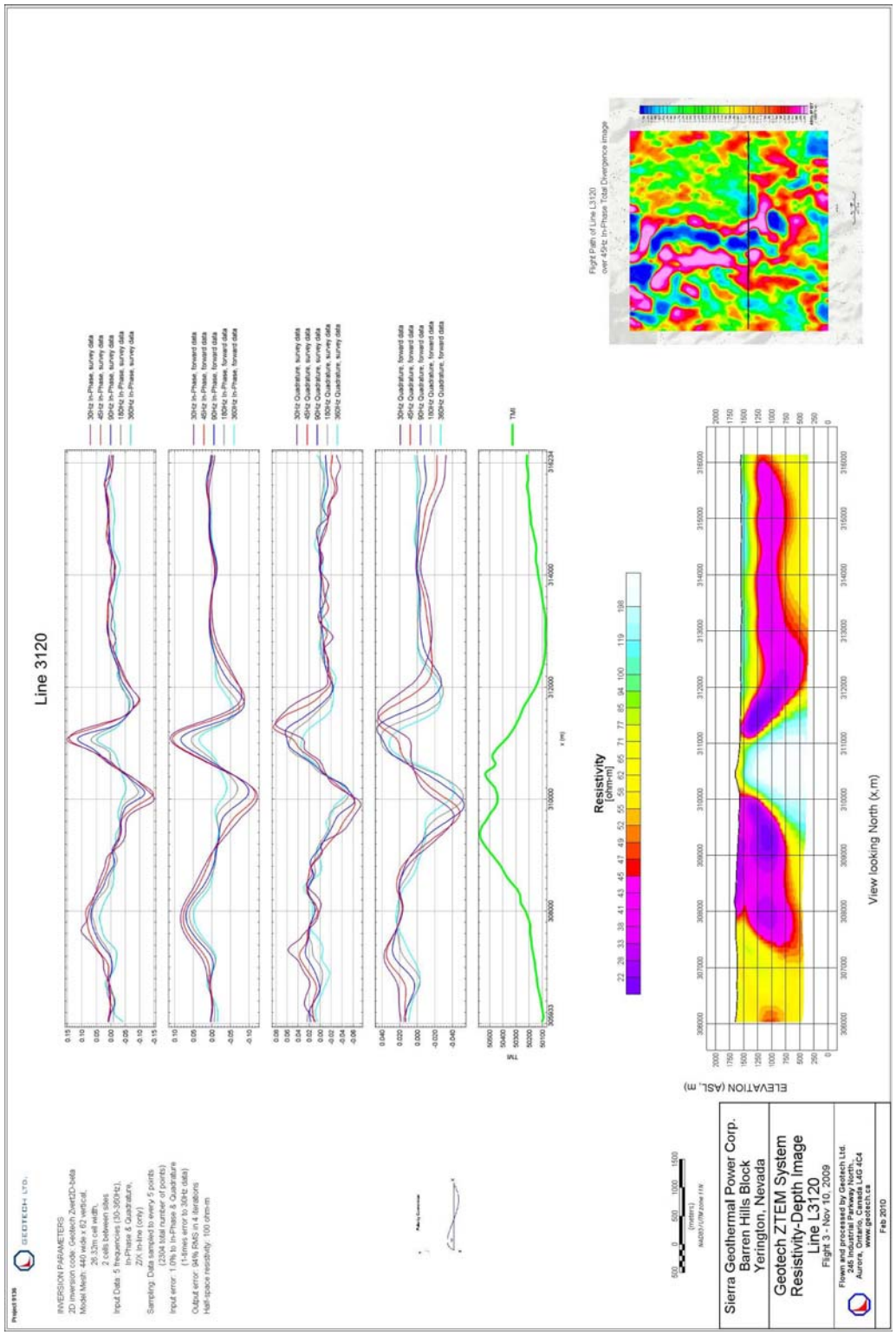

Barren Hills Block Line 3120

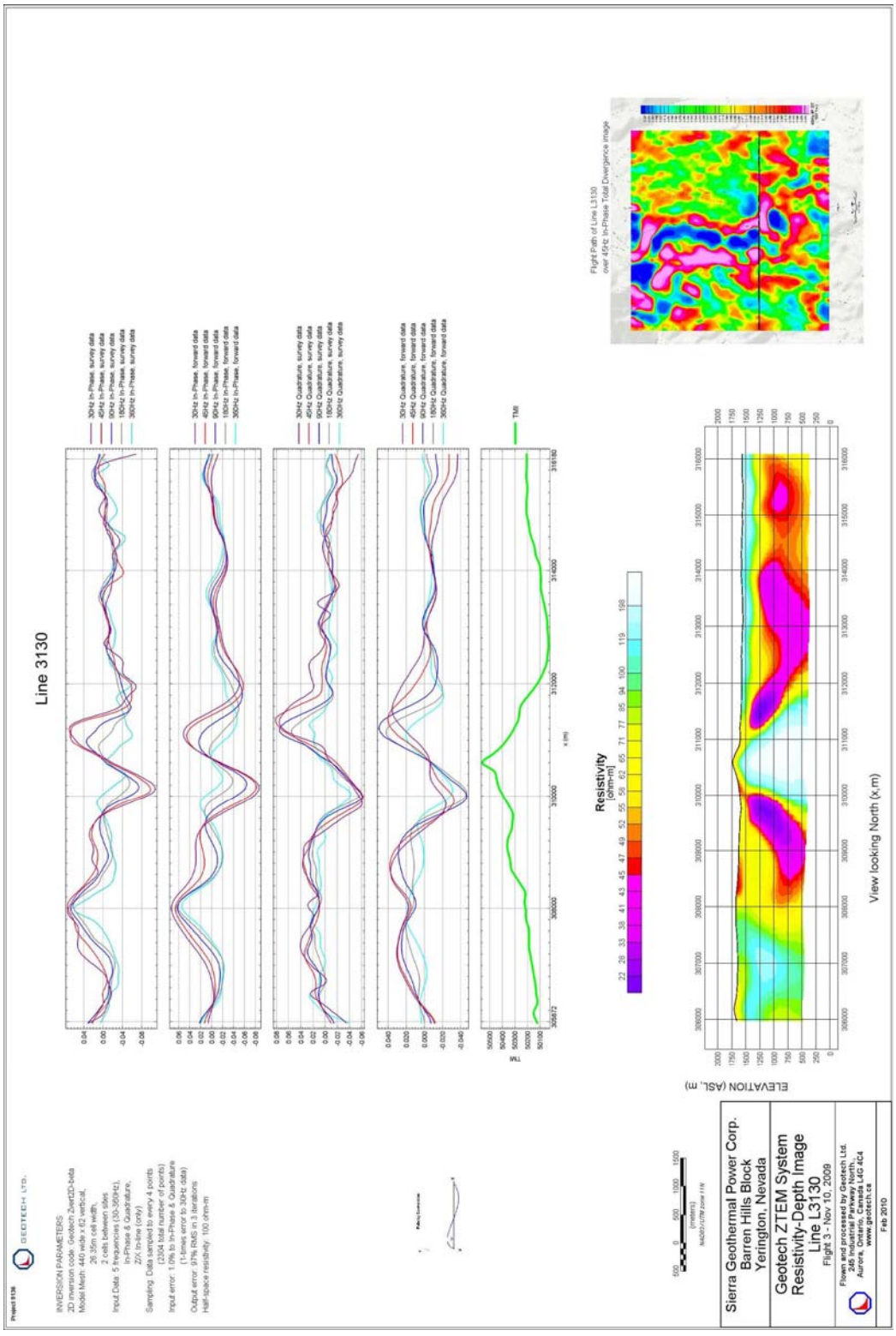

Barren Hills Block Line 3130

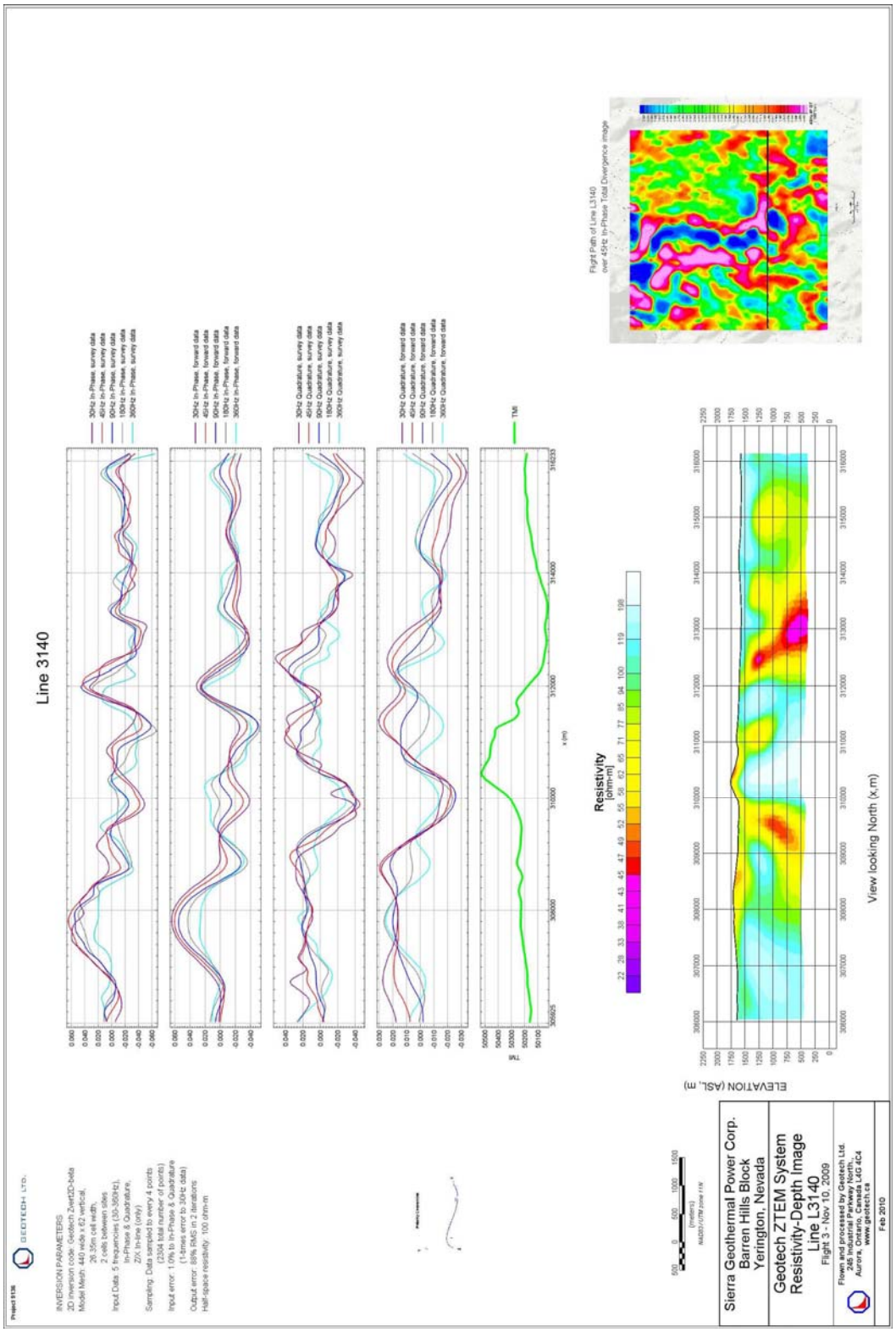

Barren Hills Block Line 3140

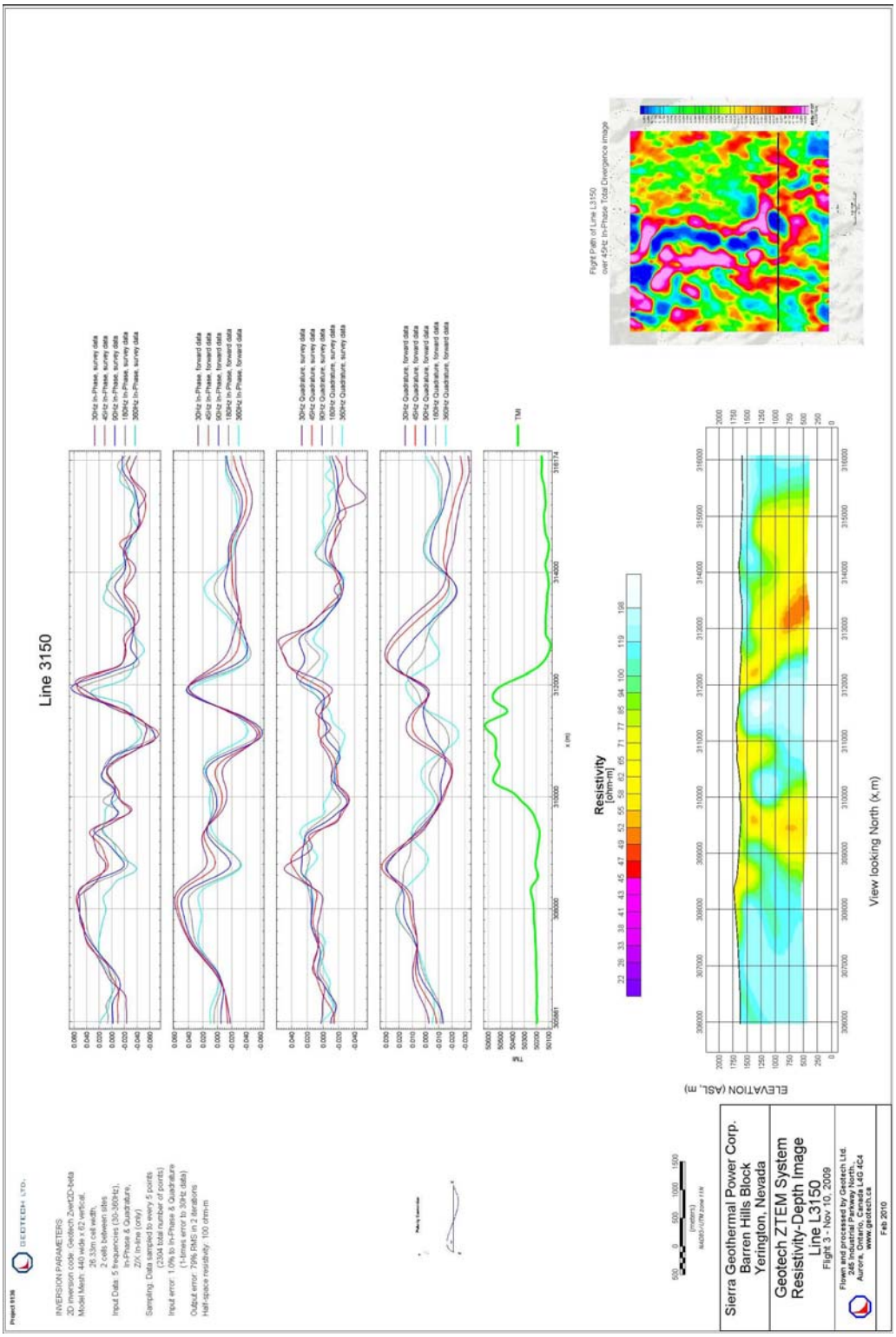

Barren Hills Block Line 3150

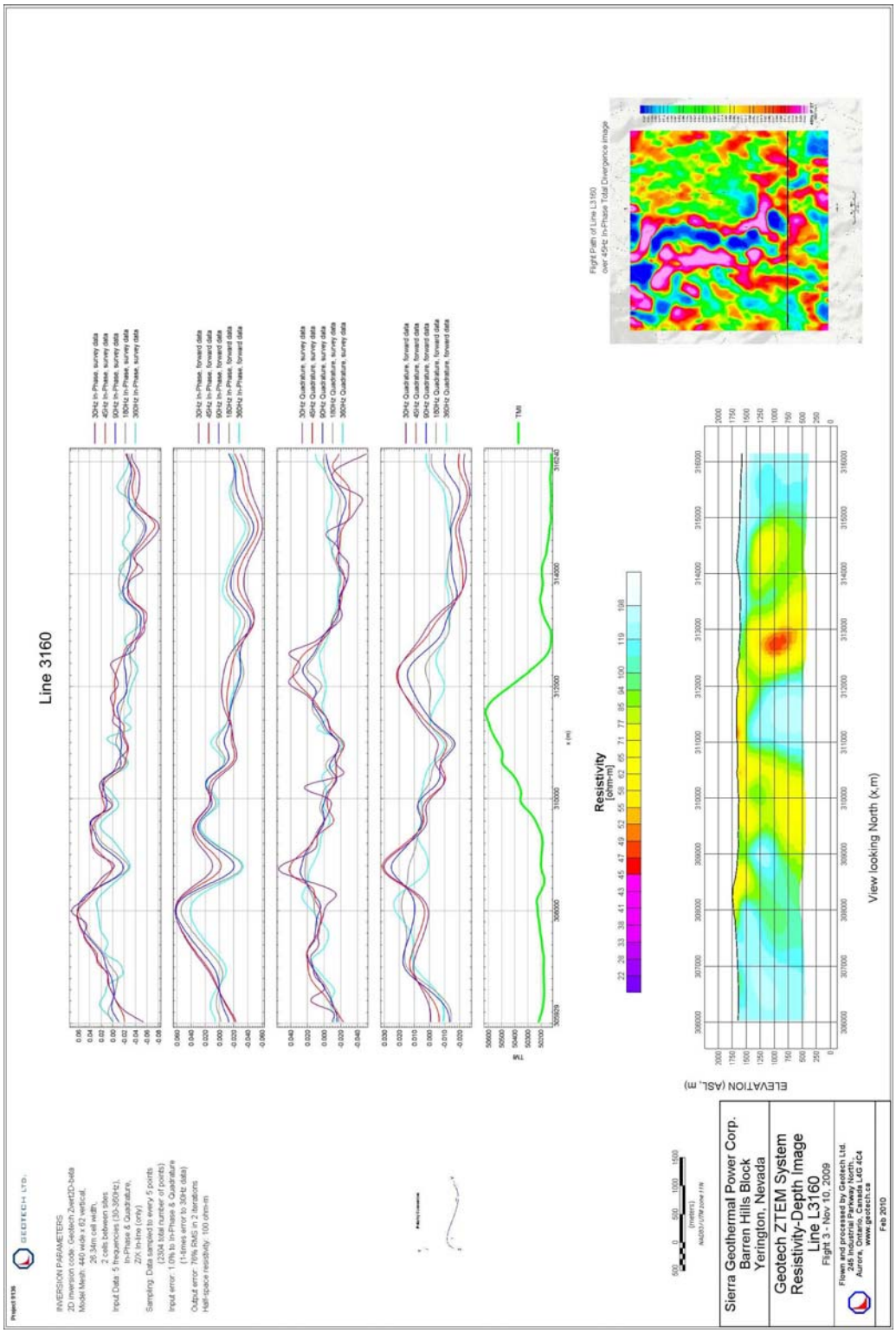

Barren Hills Block Line 3160

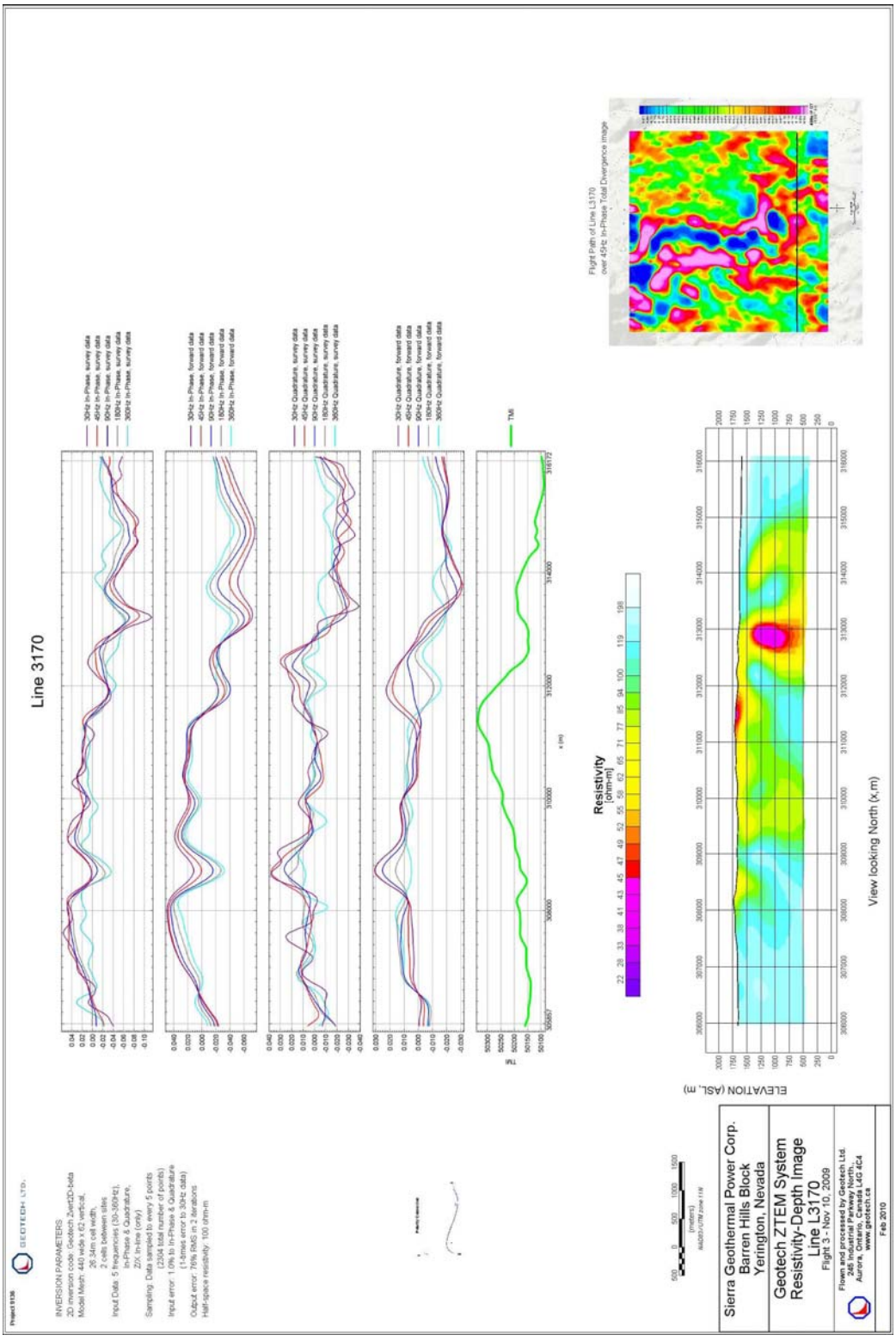

Barren Hills Block Line 3170

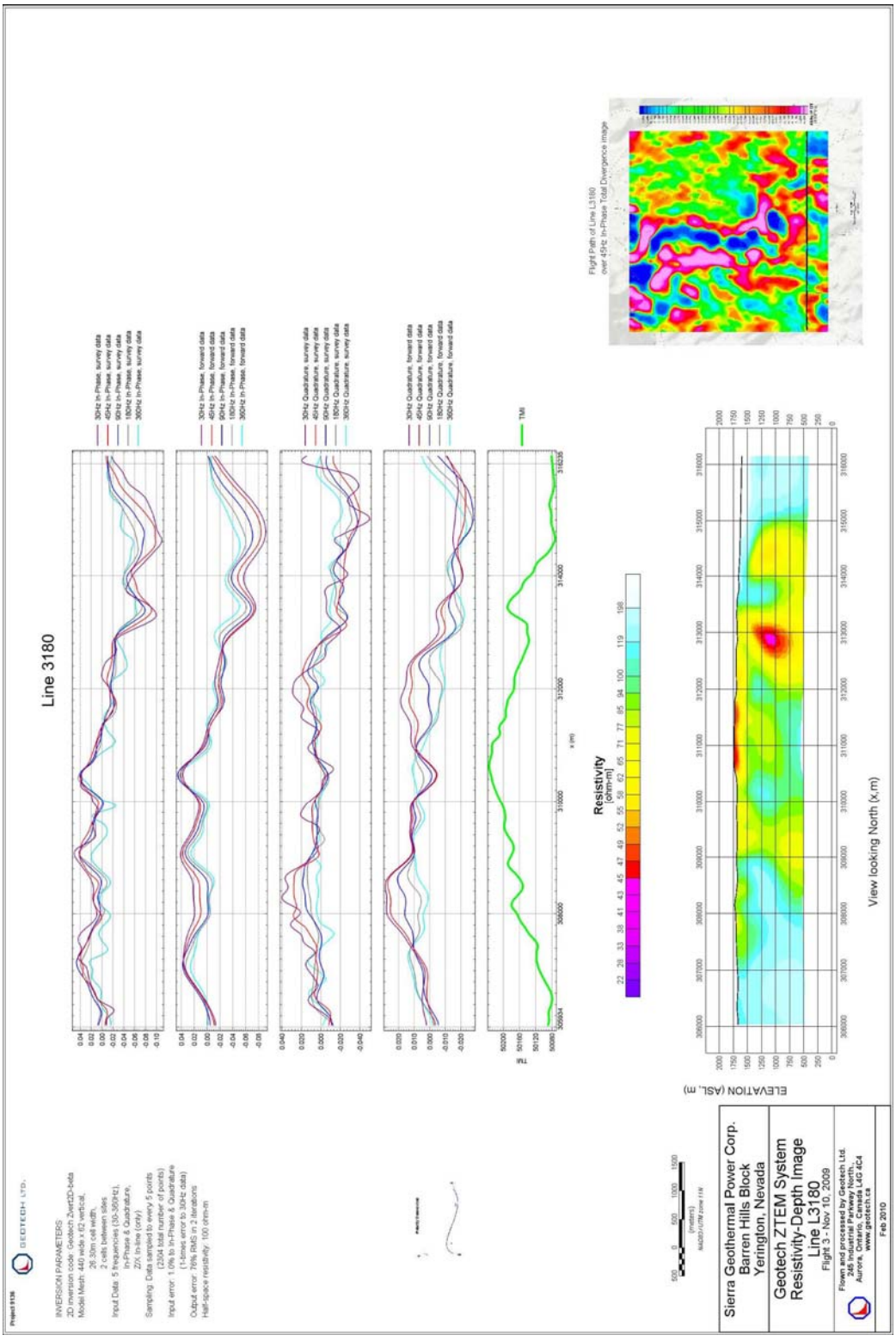

Barren Hills Block Line 3180

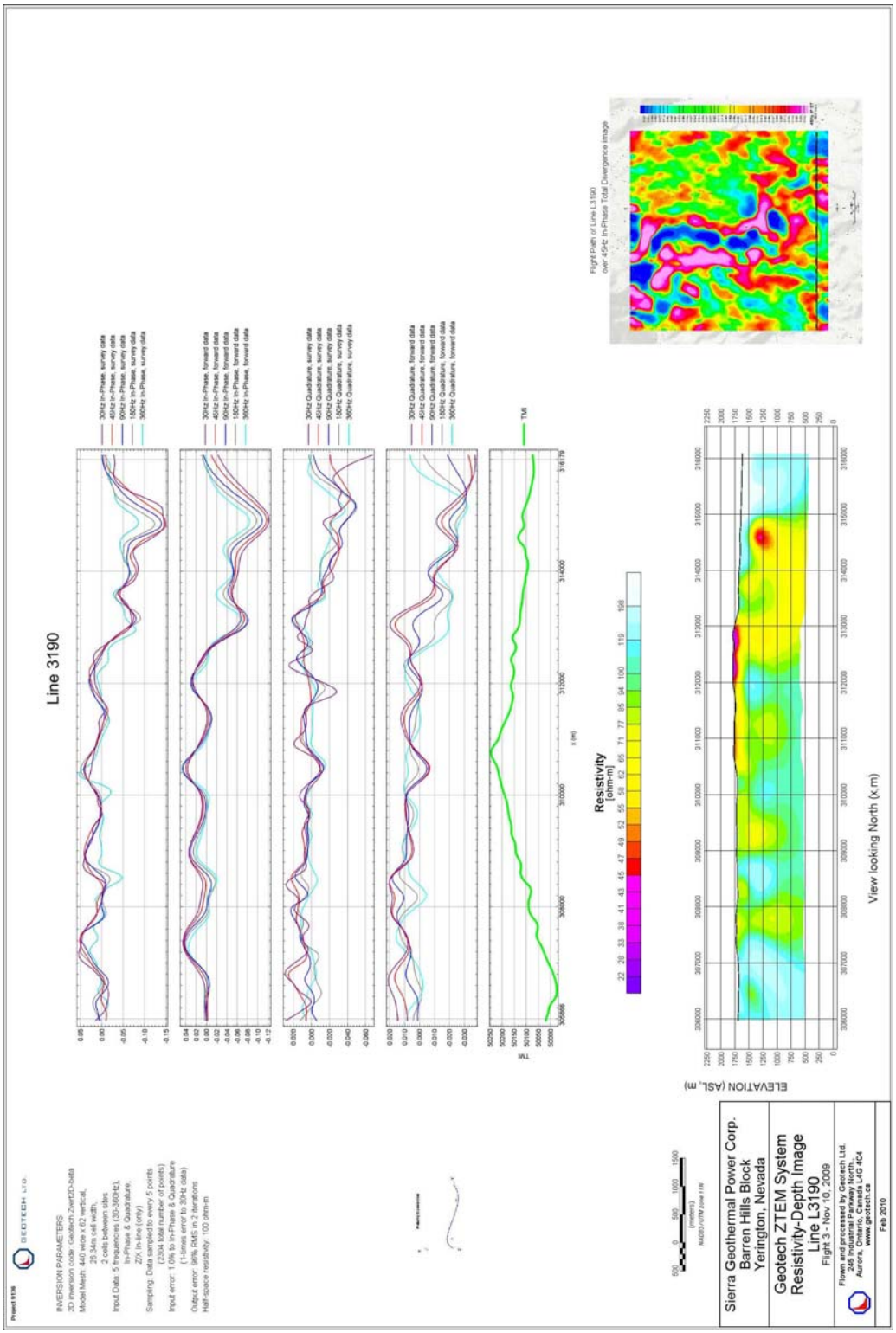

Barren Hills Block Line 3190

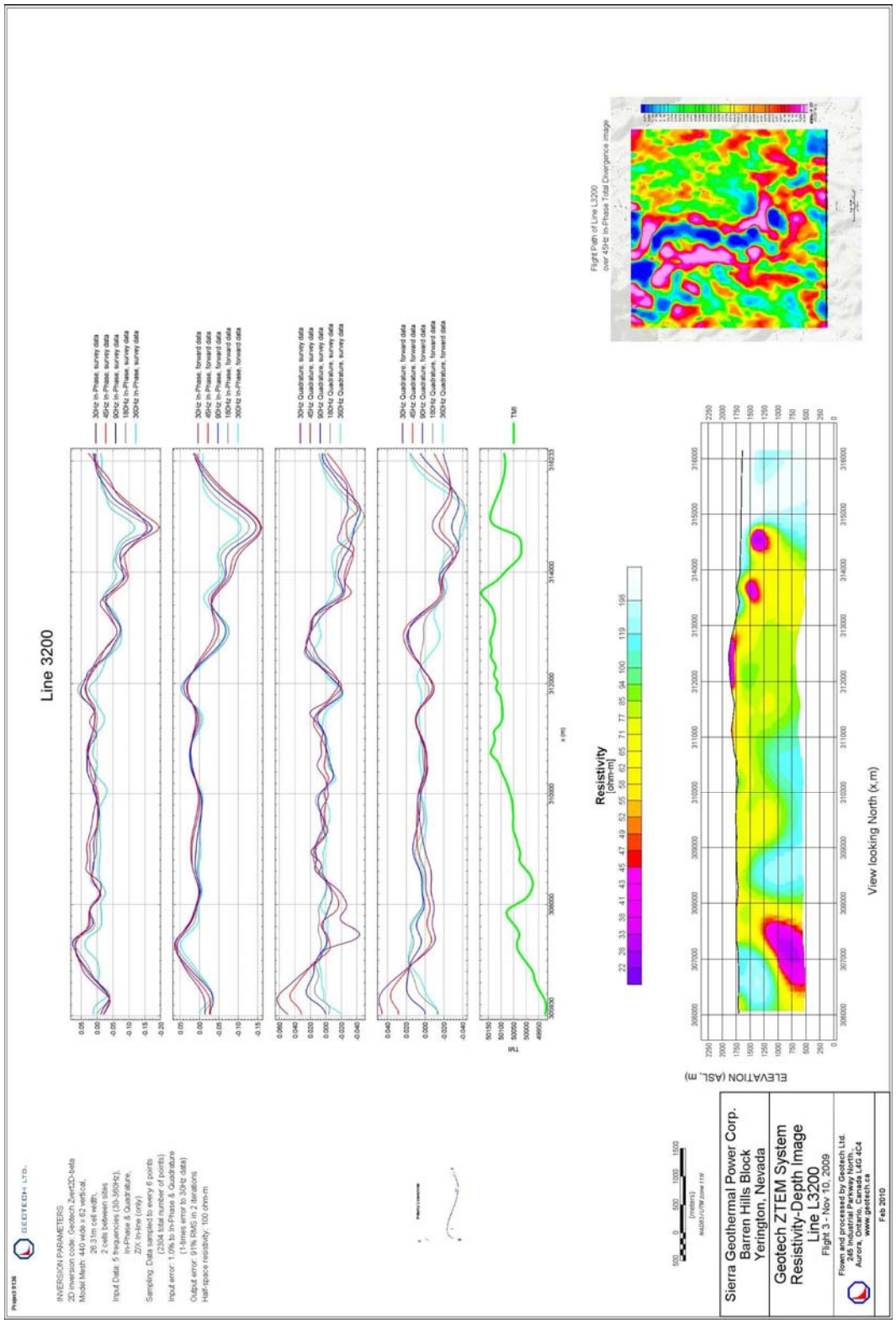

Barren Hills Block Line 3200

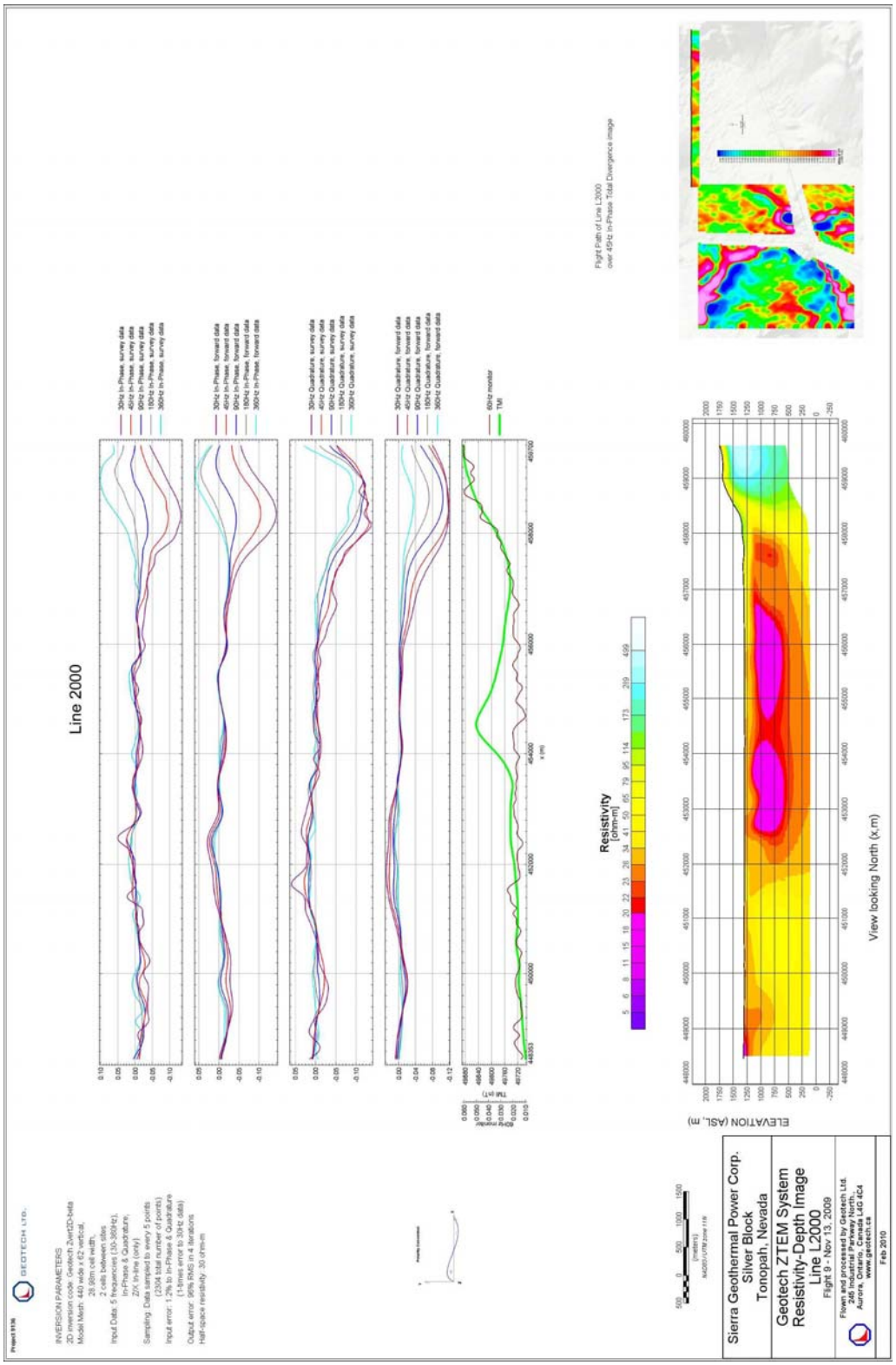

Silver Block Line 2000

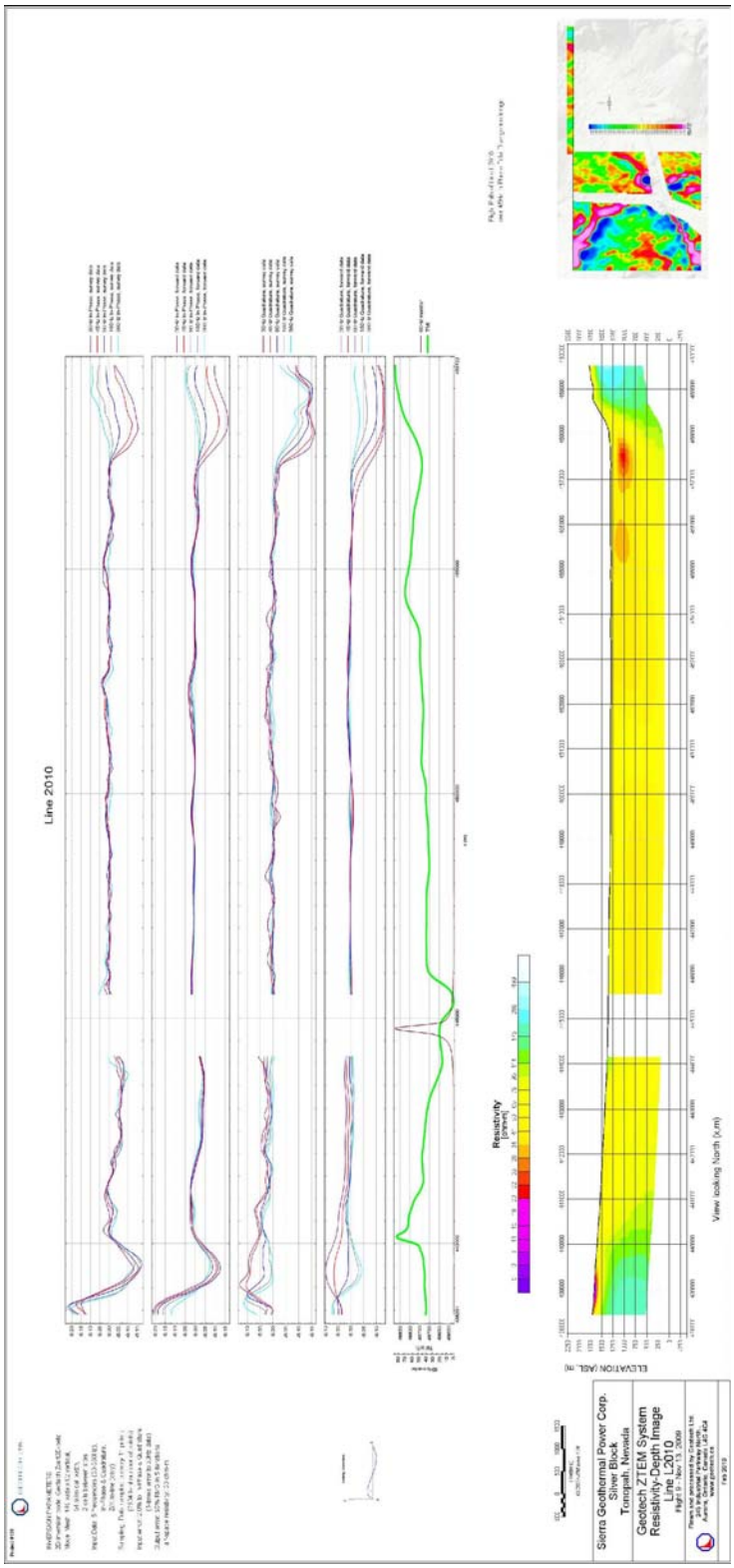

Silver Block Line 2010

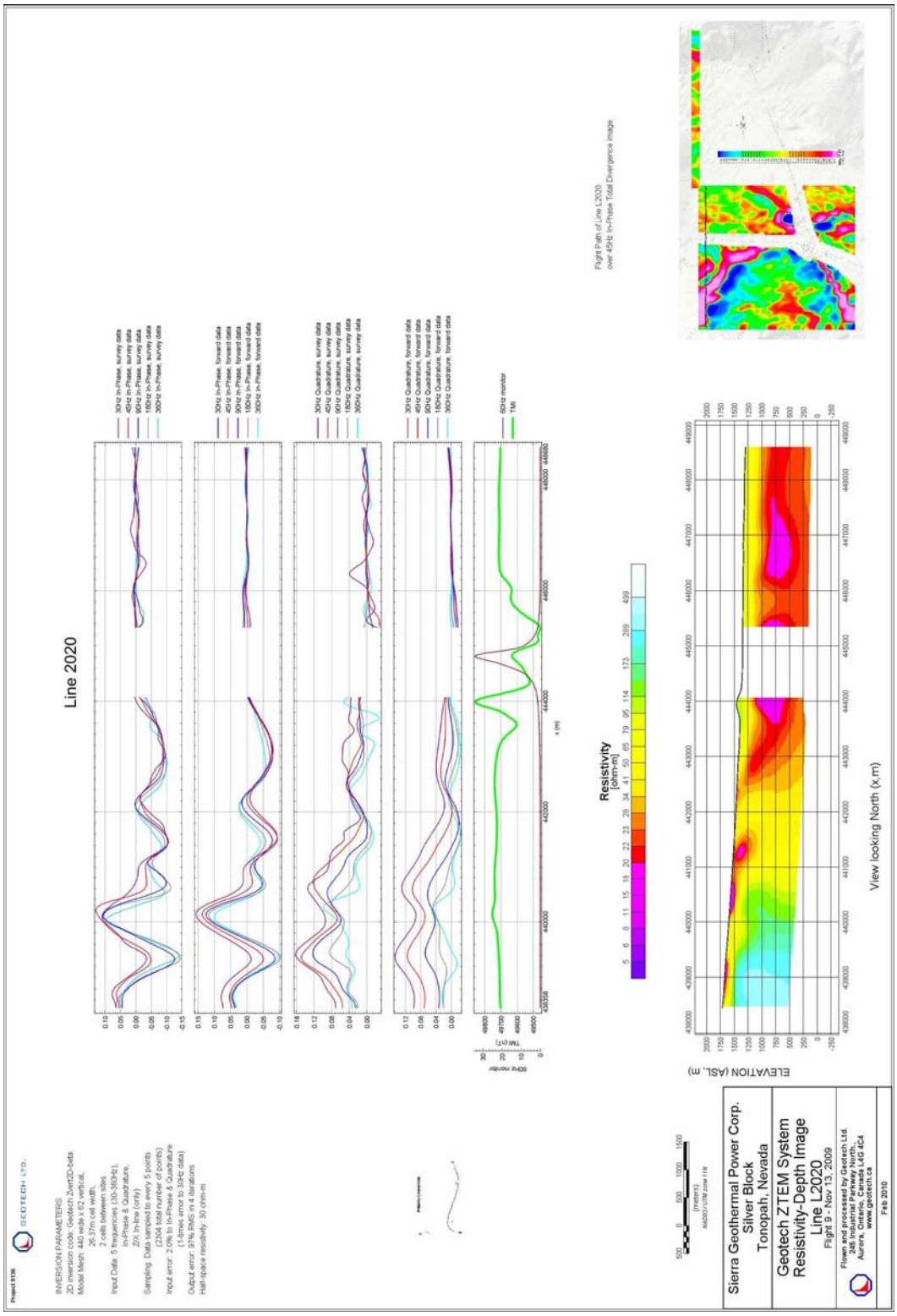

Silver Block Line 2020

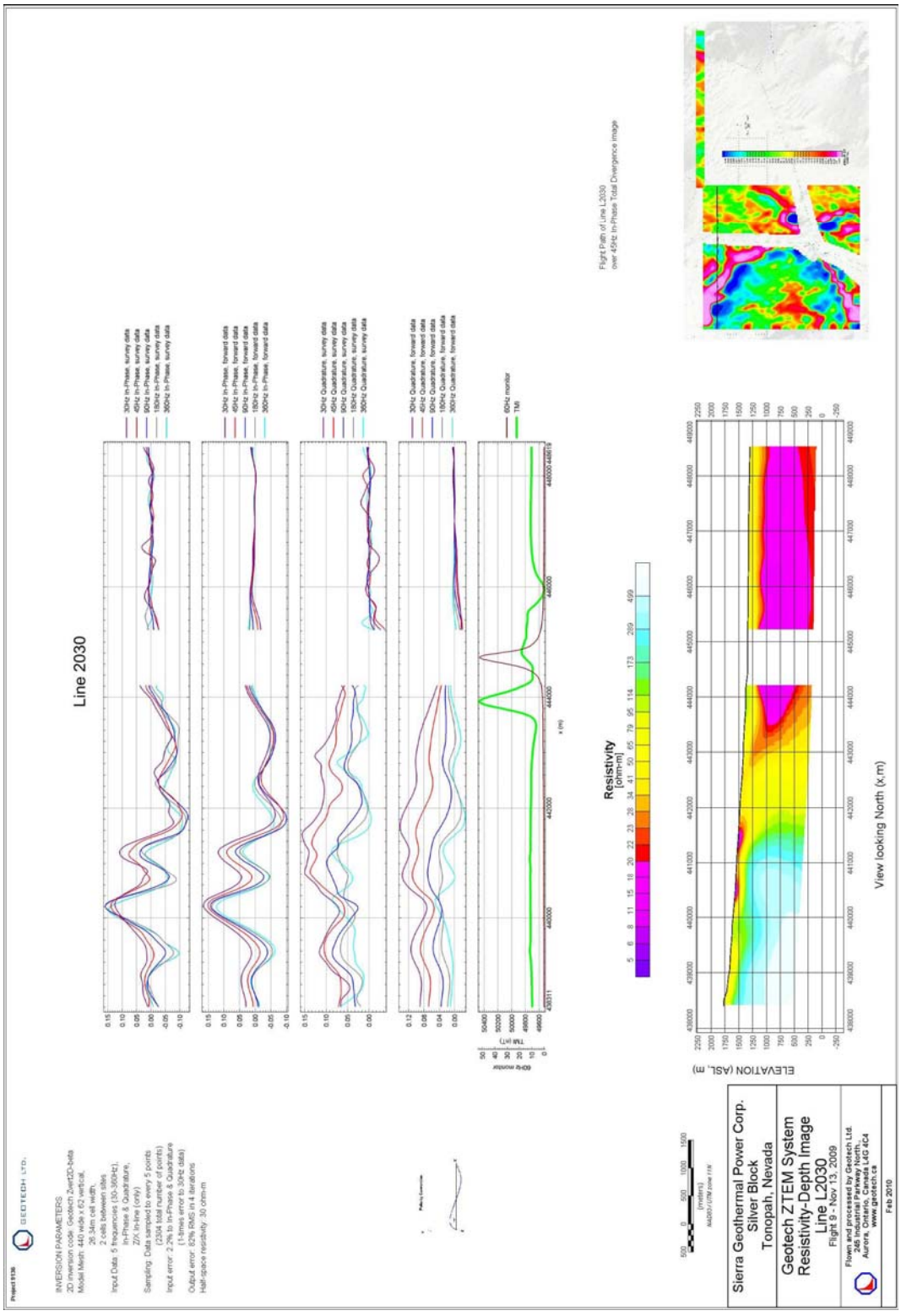

Silver Block Line 2030

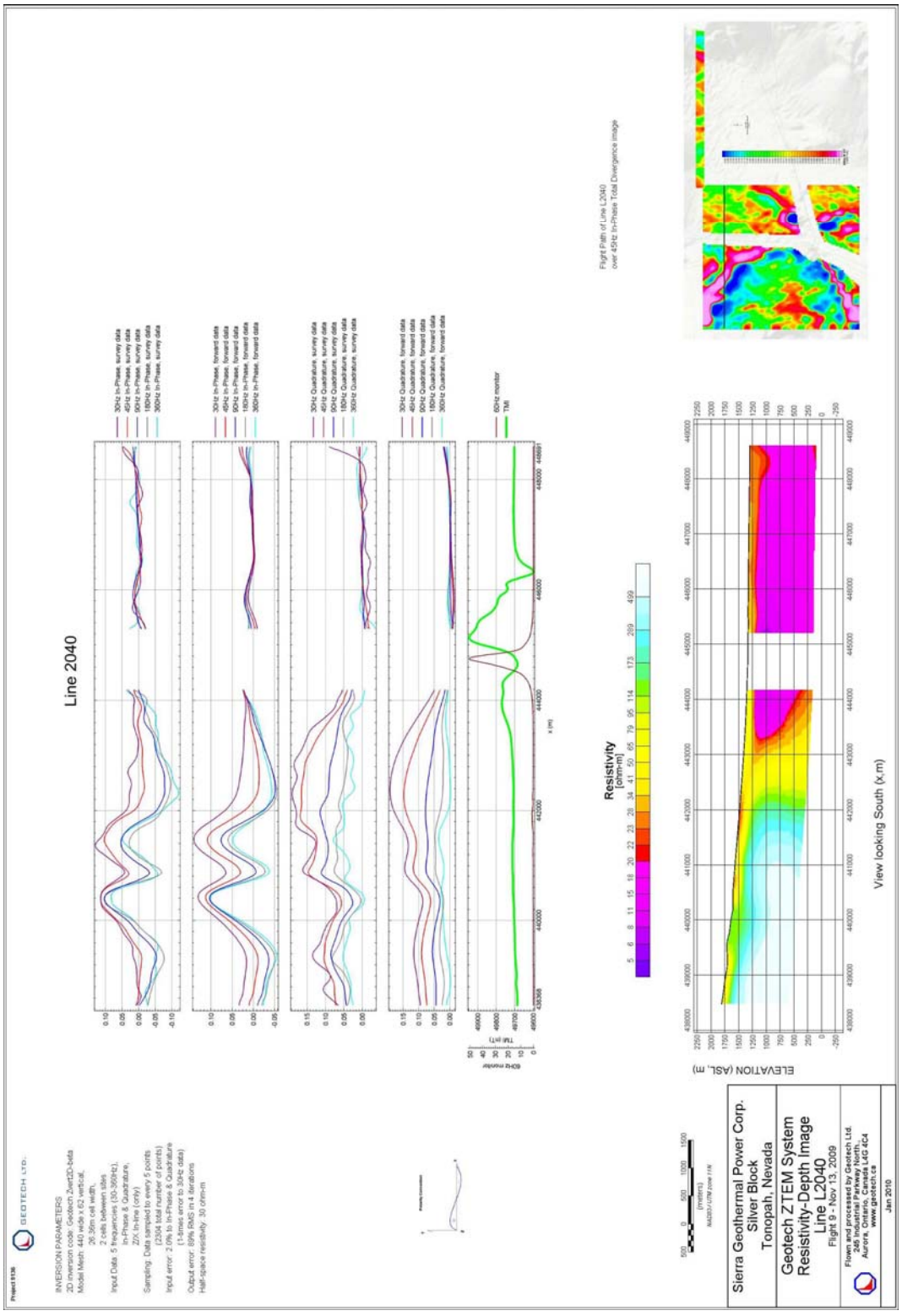

Silver Block Line 2040

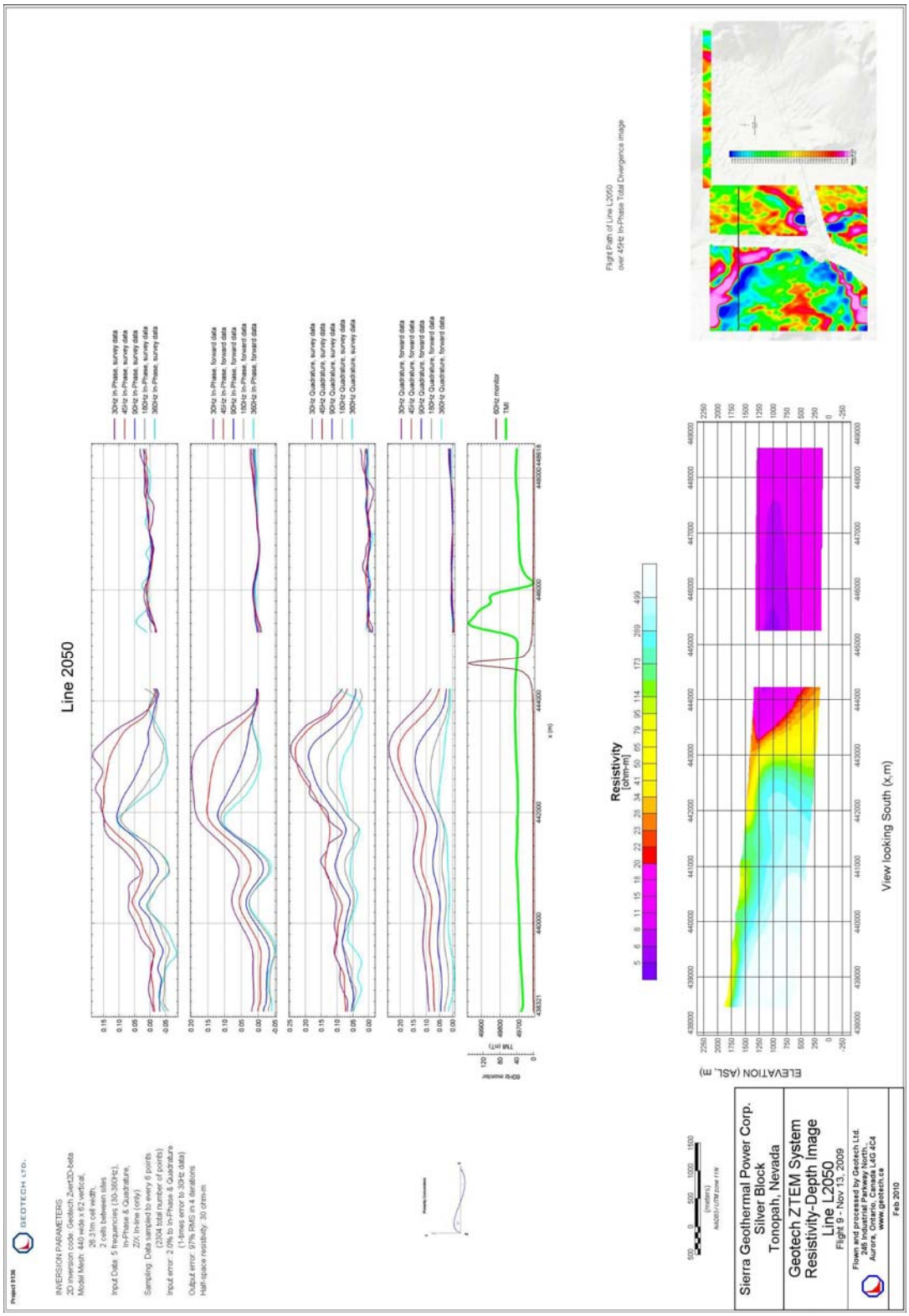

Silver Block Line 2050

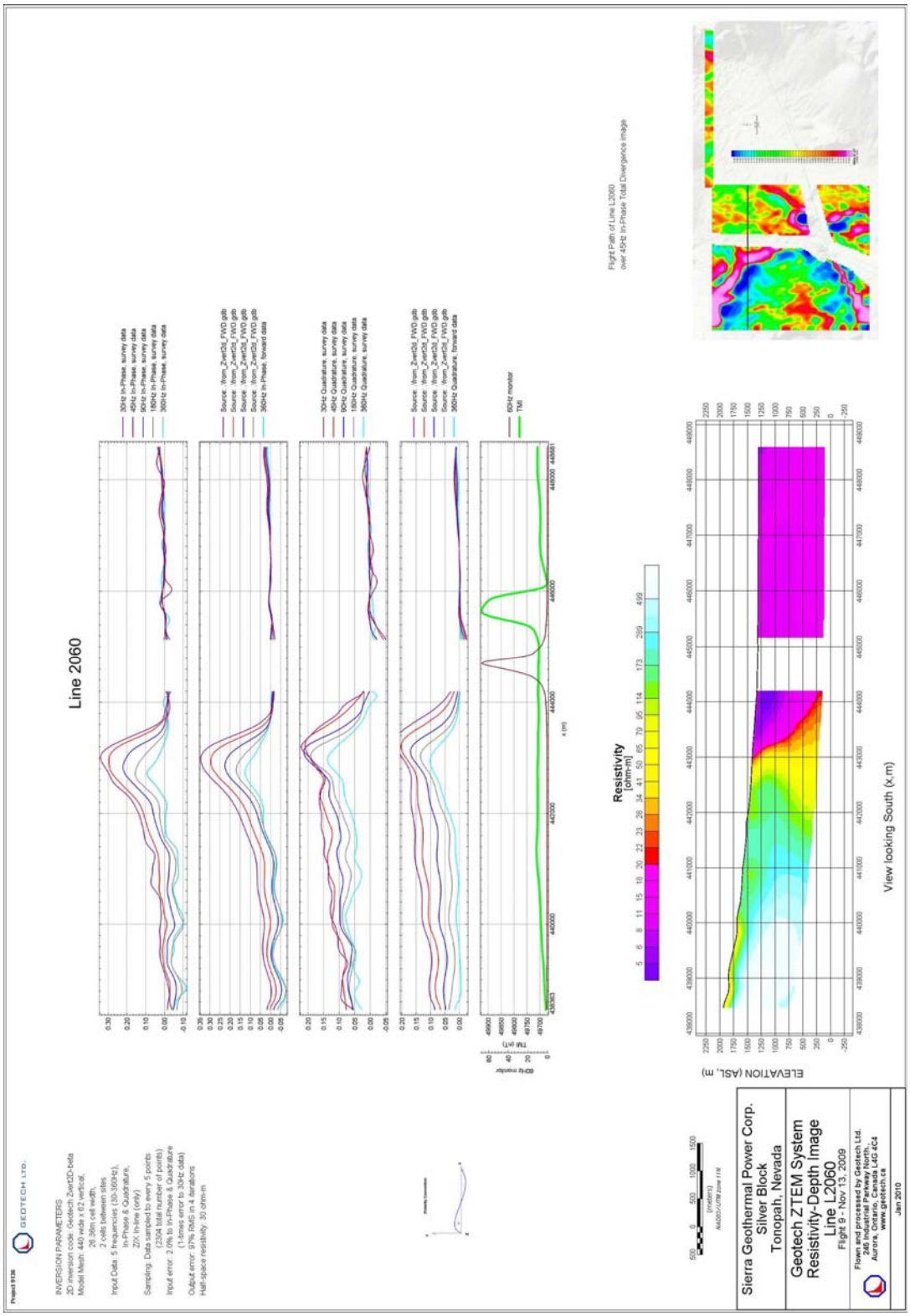

Silver Block Line 2060

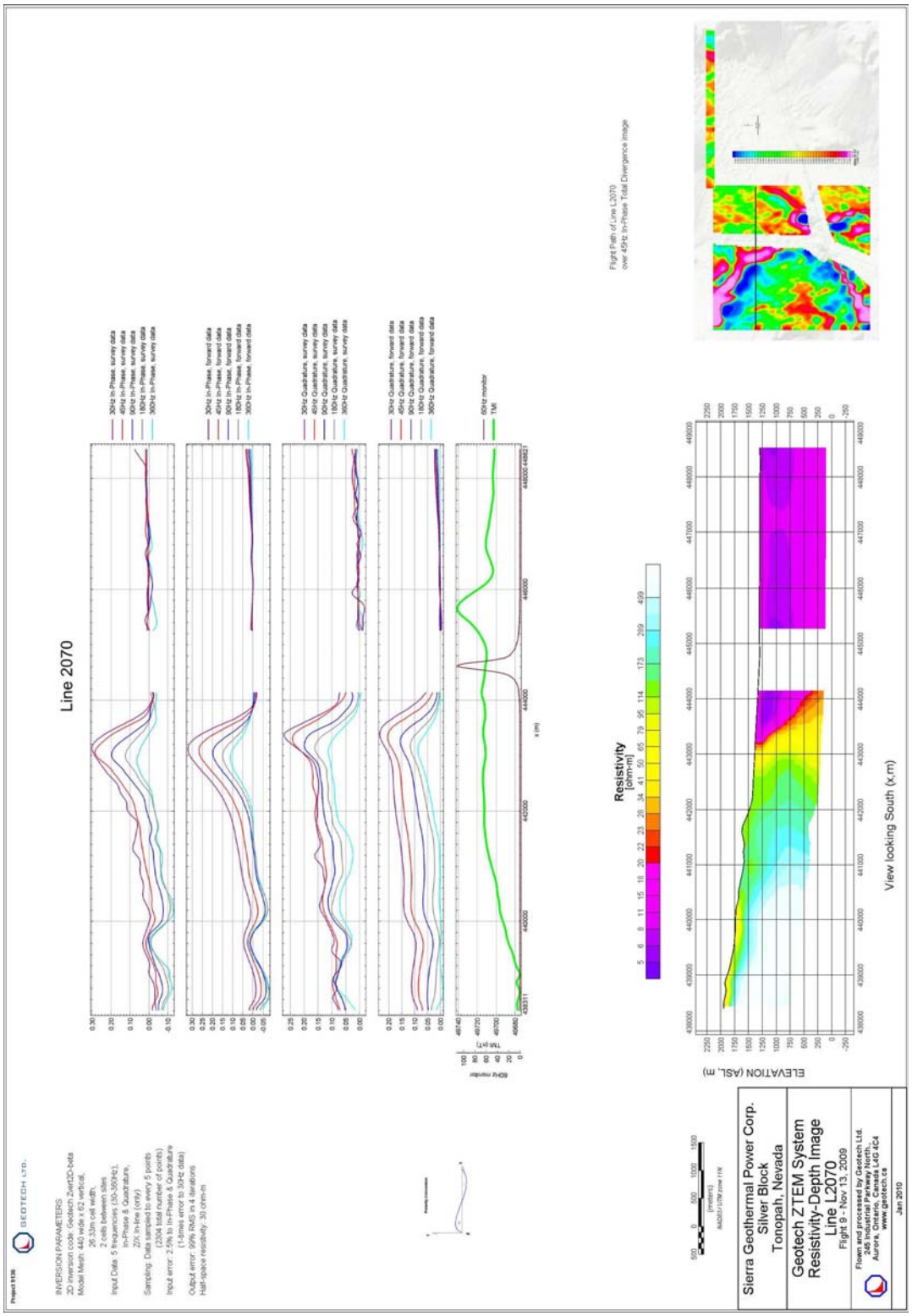

Silver Block Line 2070

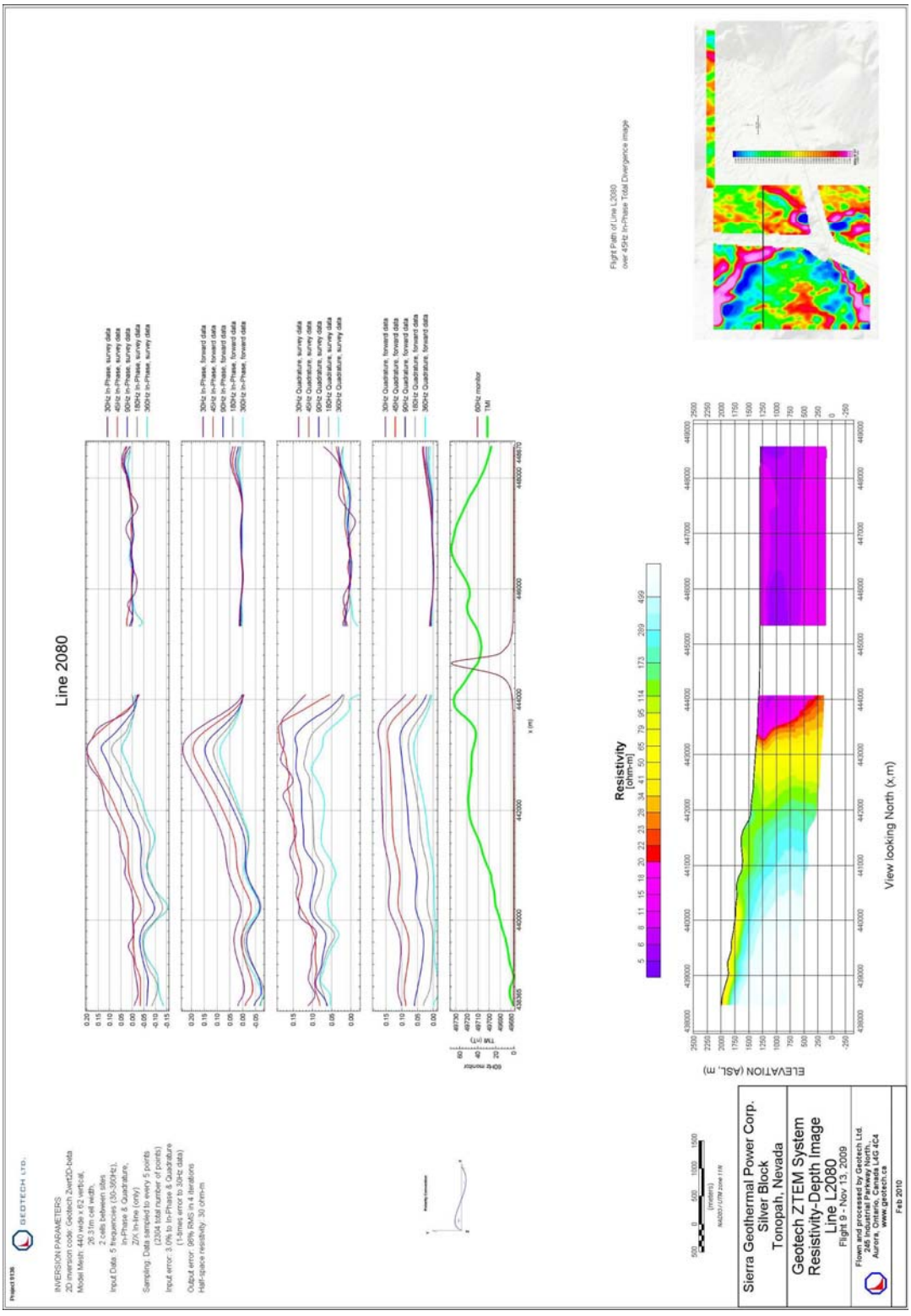

Silver Block Line 2080

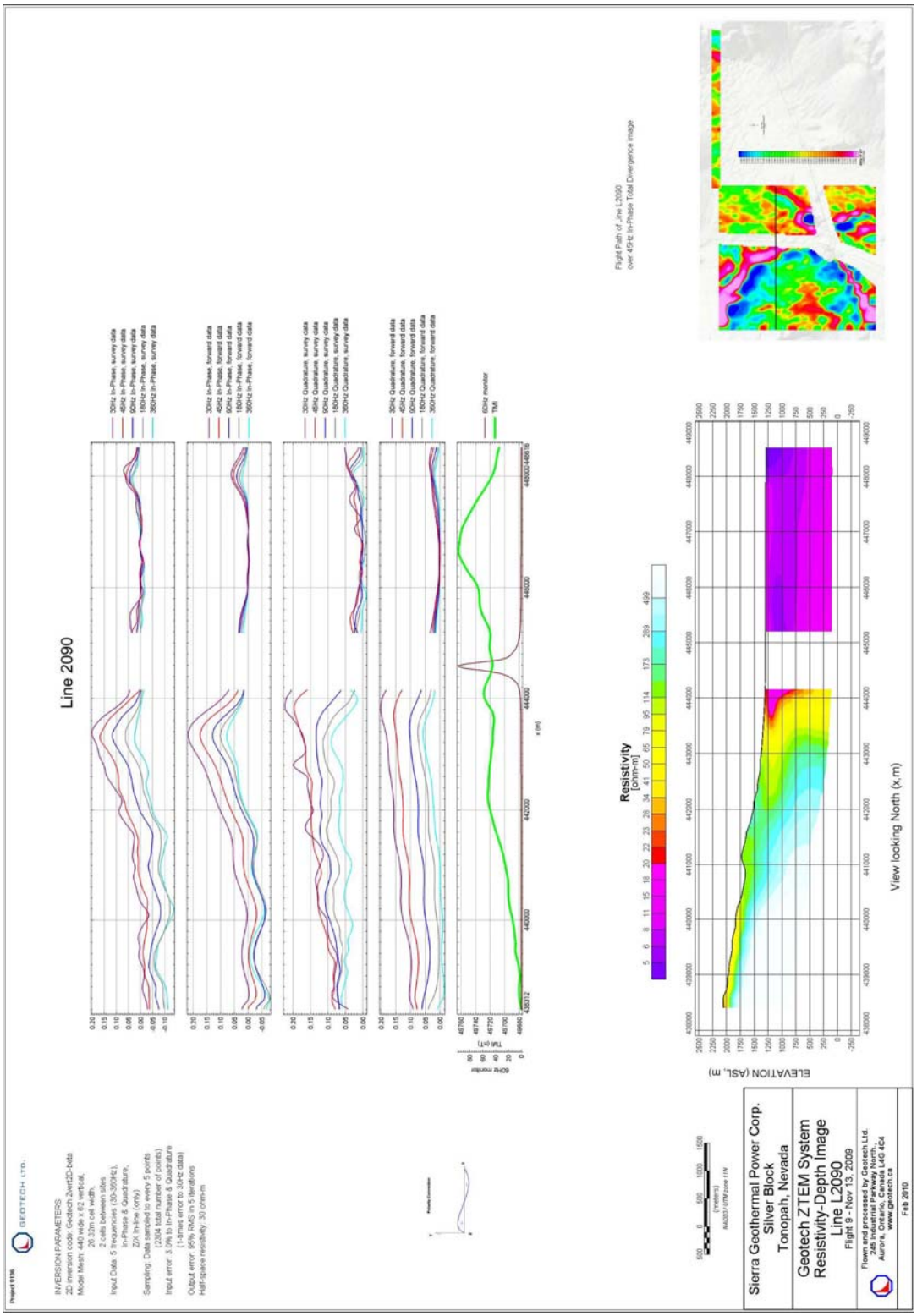

Silver Block Line 2090

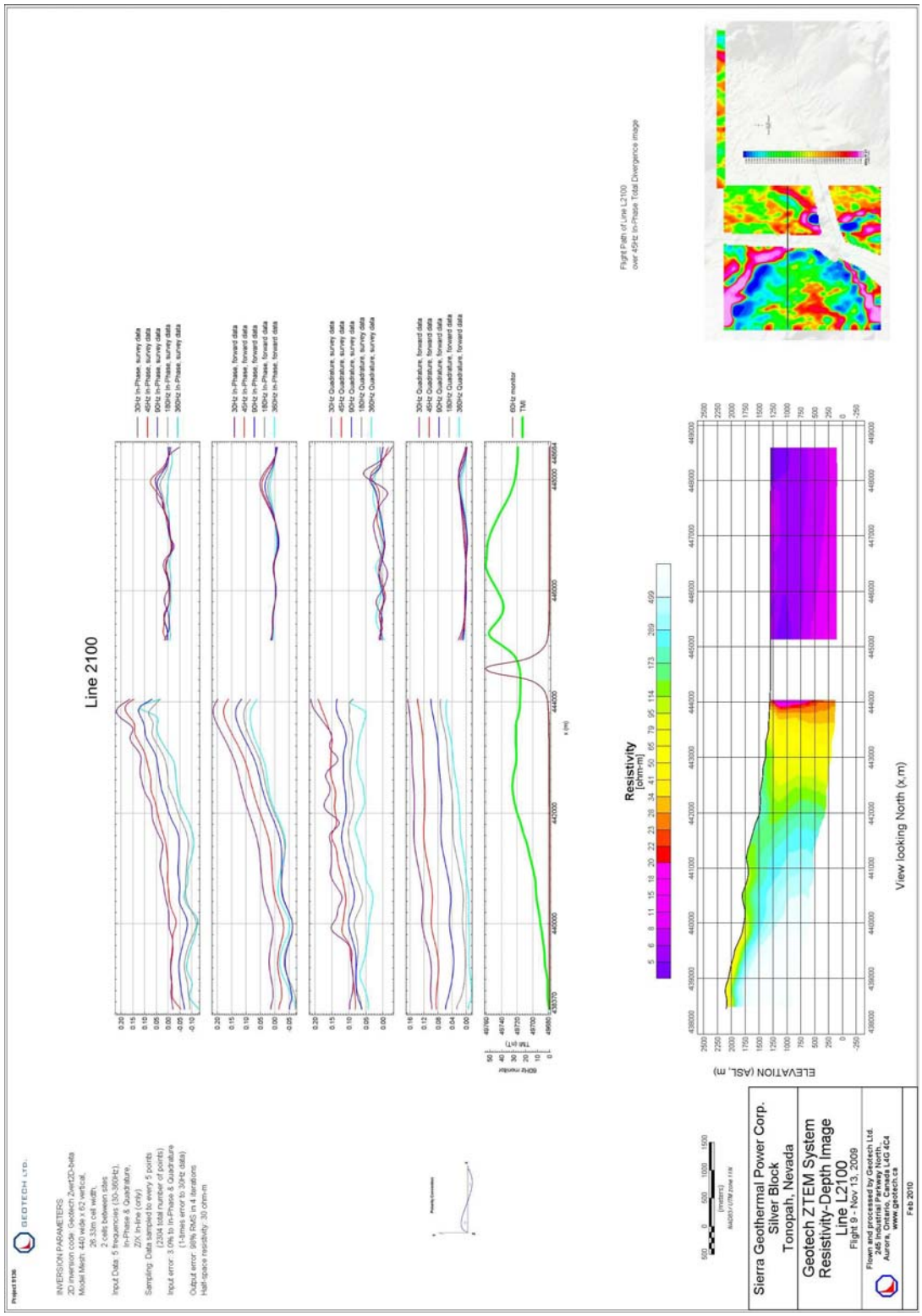

Silver Block Line 2100

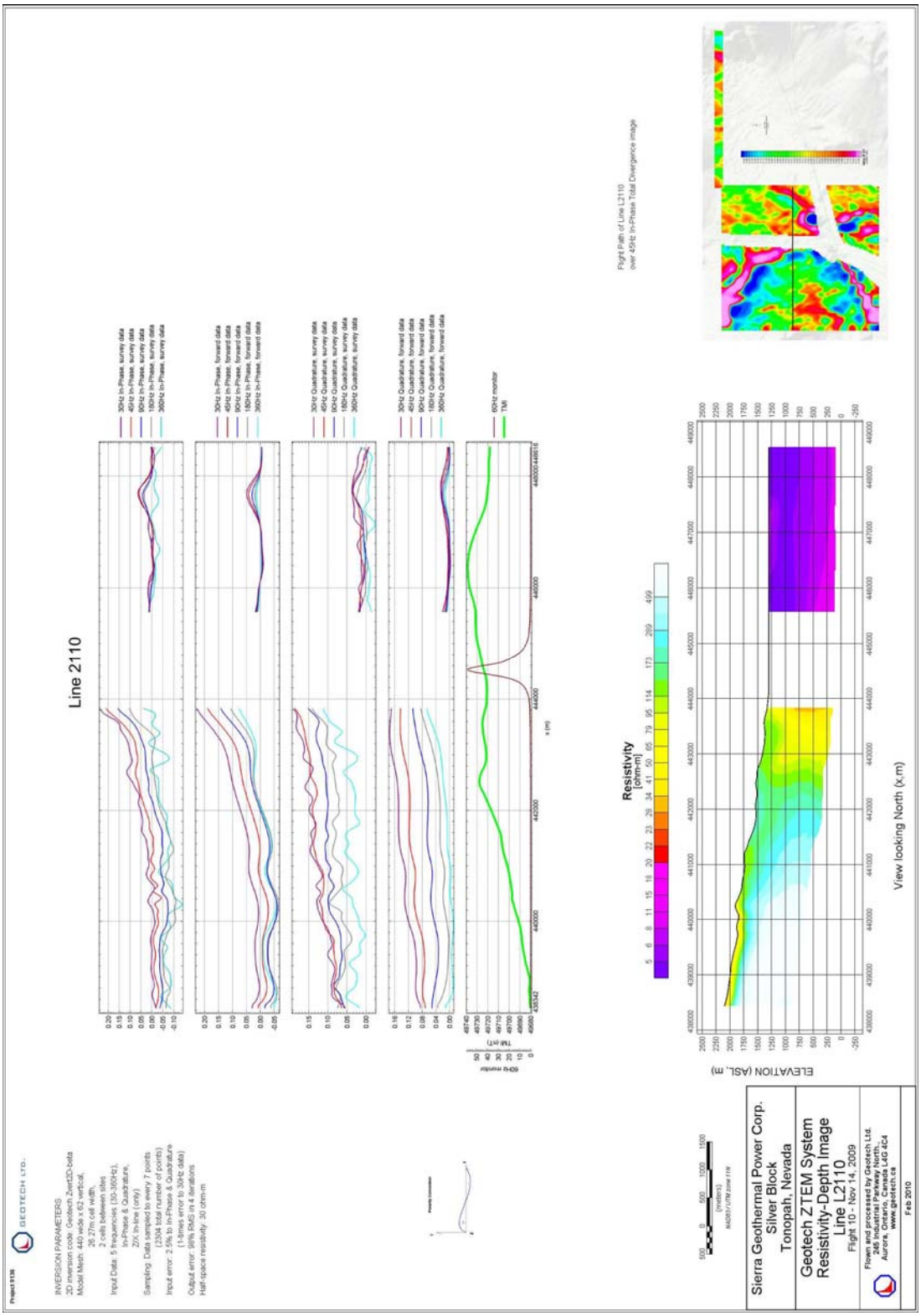

Silver Block Line 2110

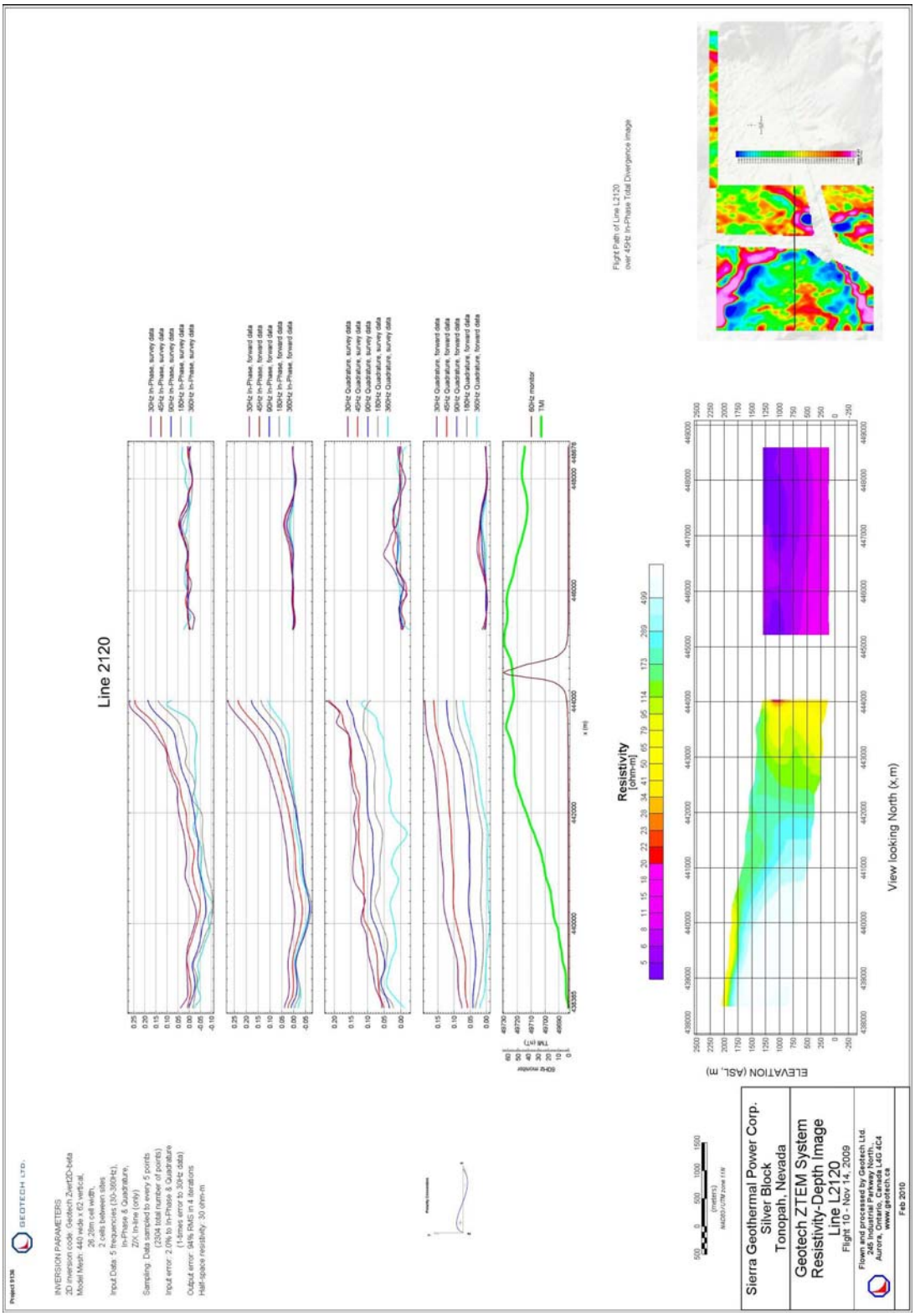

Silver Block Line 2120

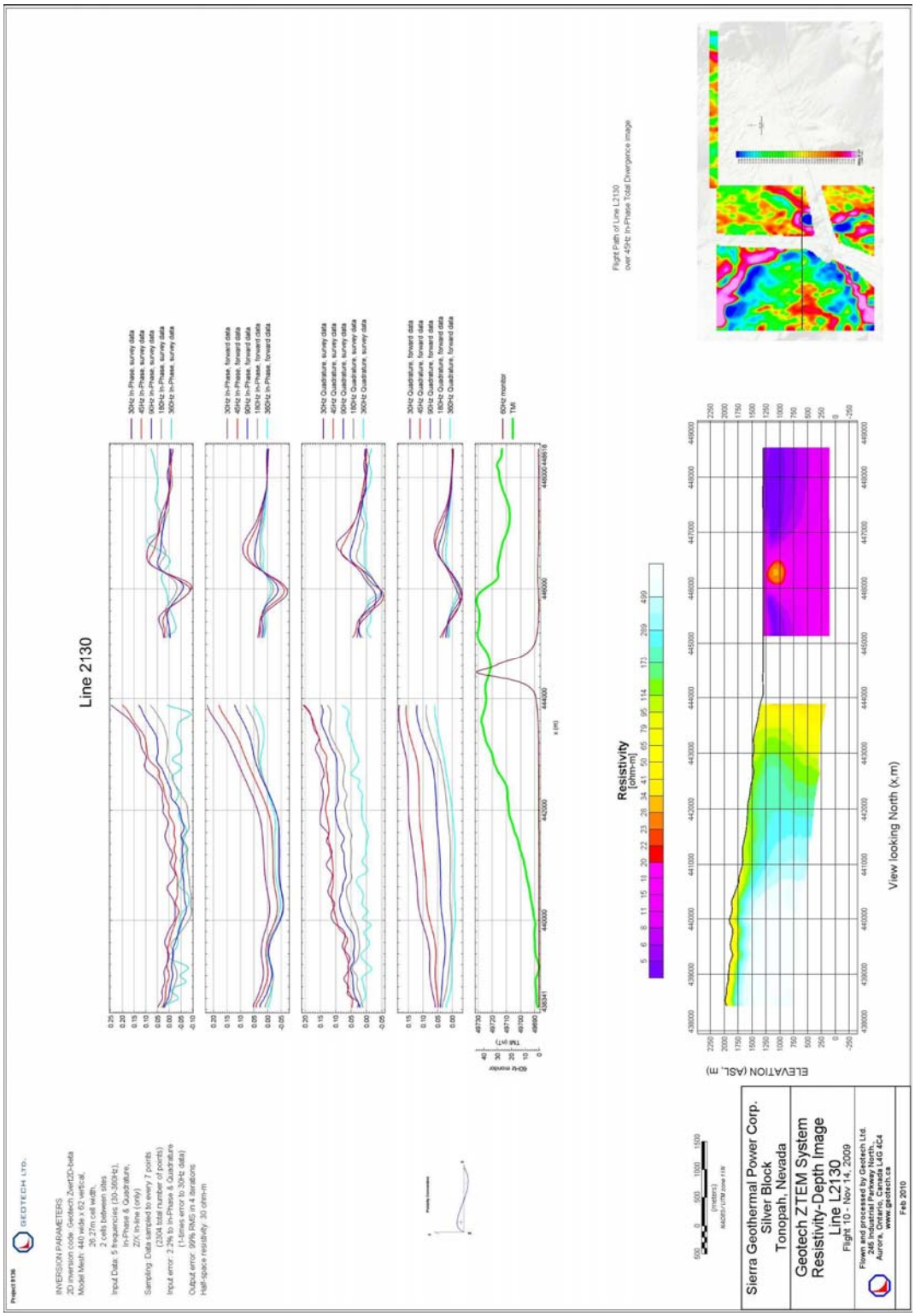

Silver Block Line 2130

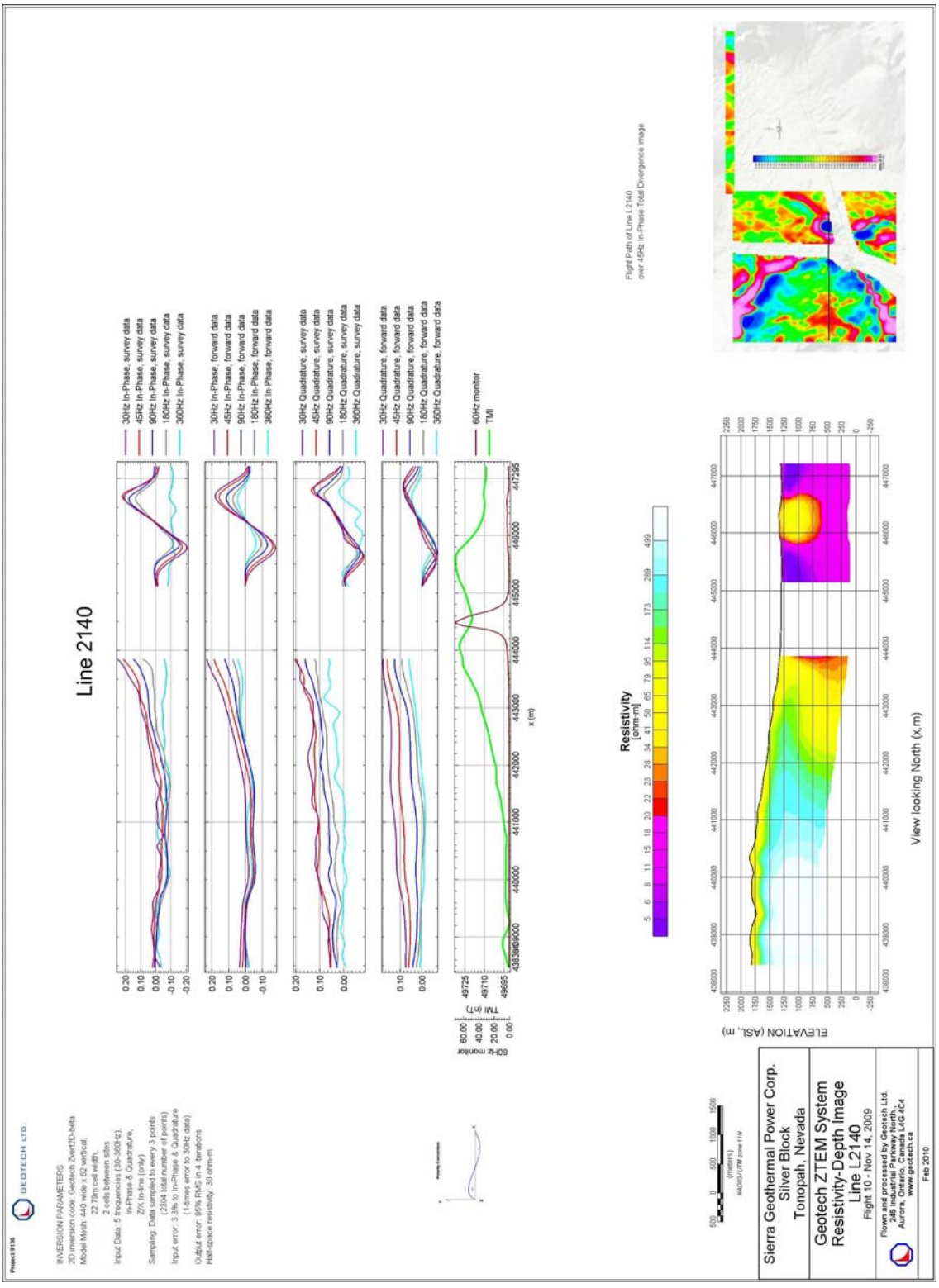

Silver Block Line 2140

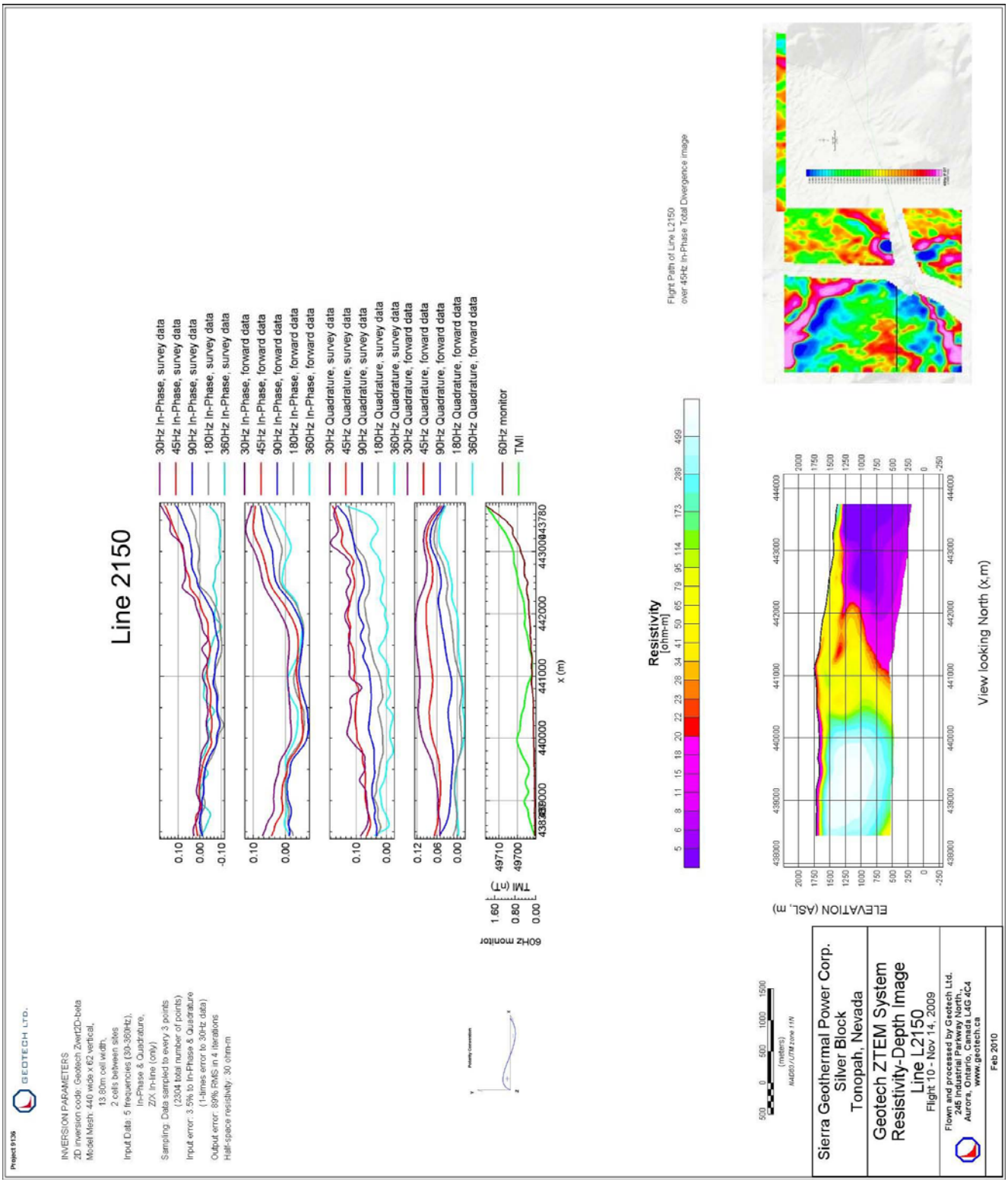

Silver Block Line 2150

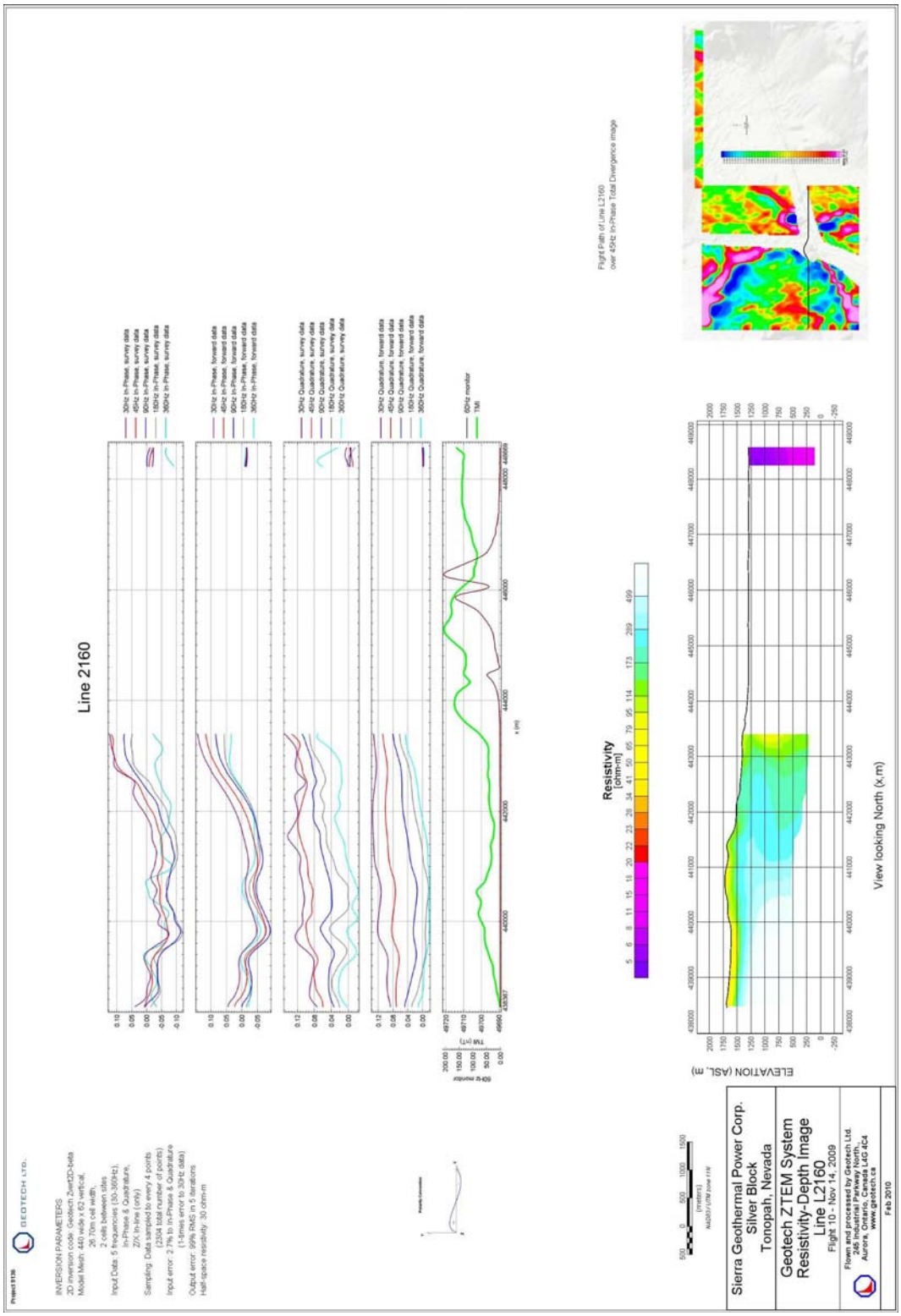

Silver Block Line 2160

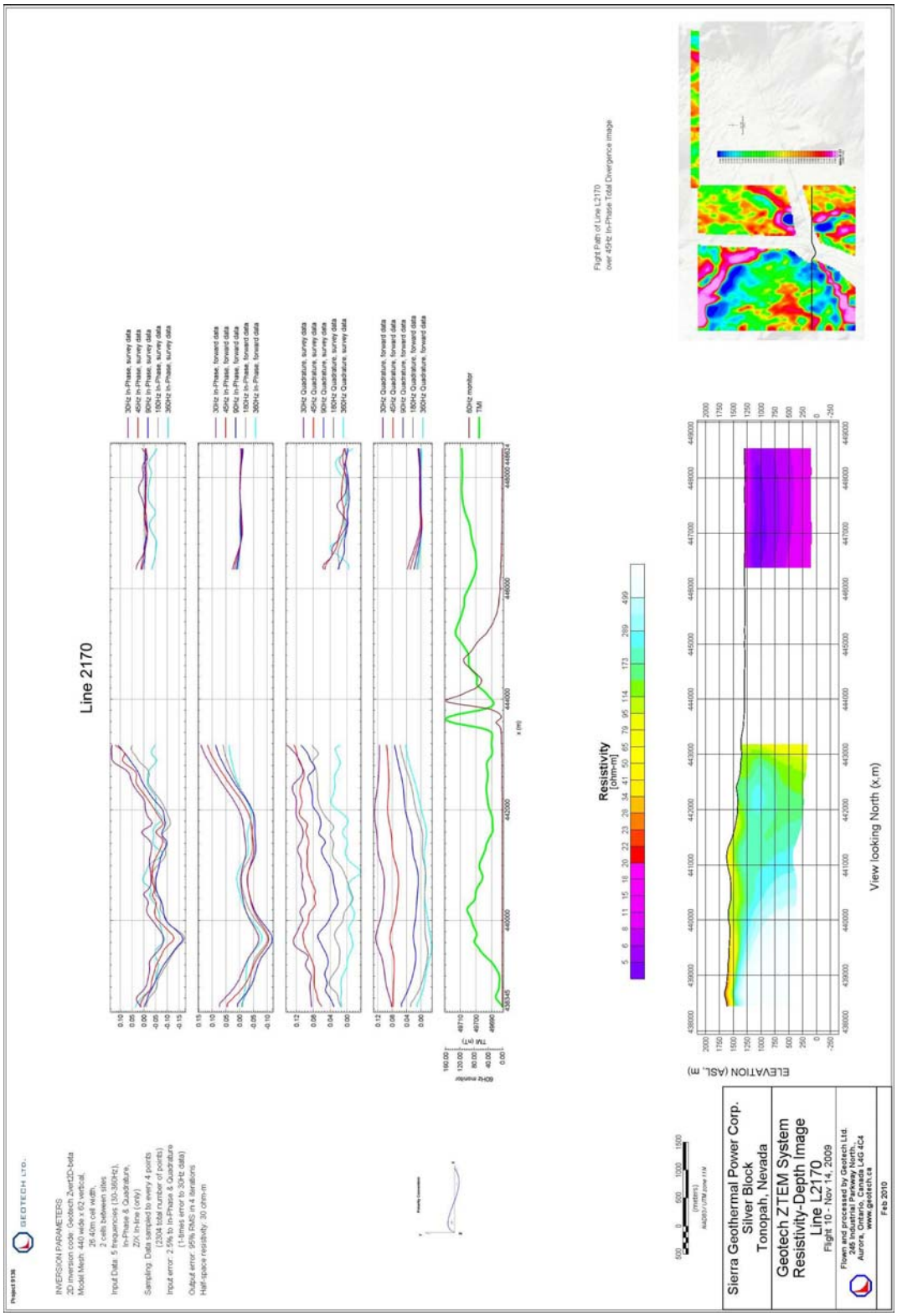

Silver Block Line 2170

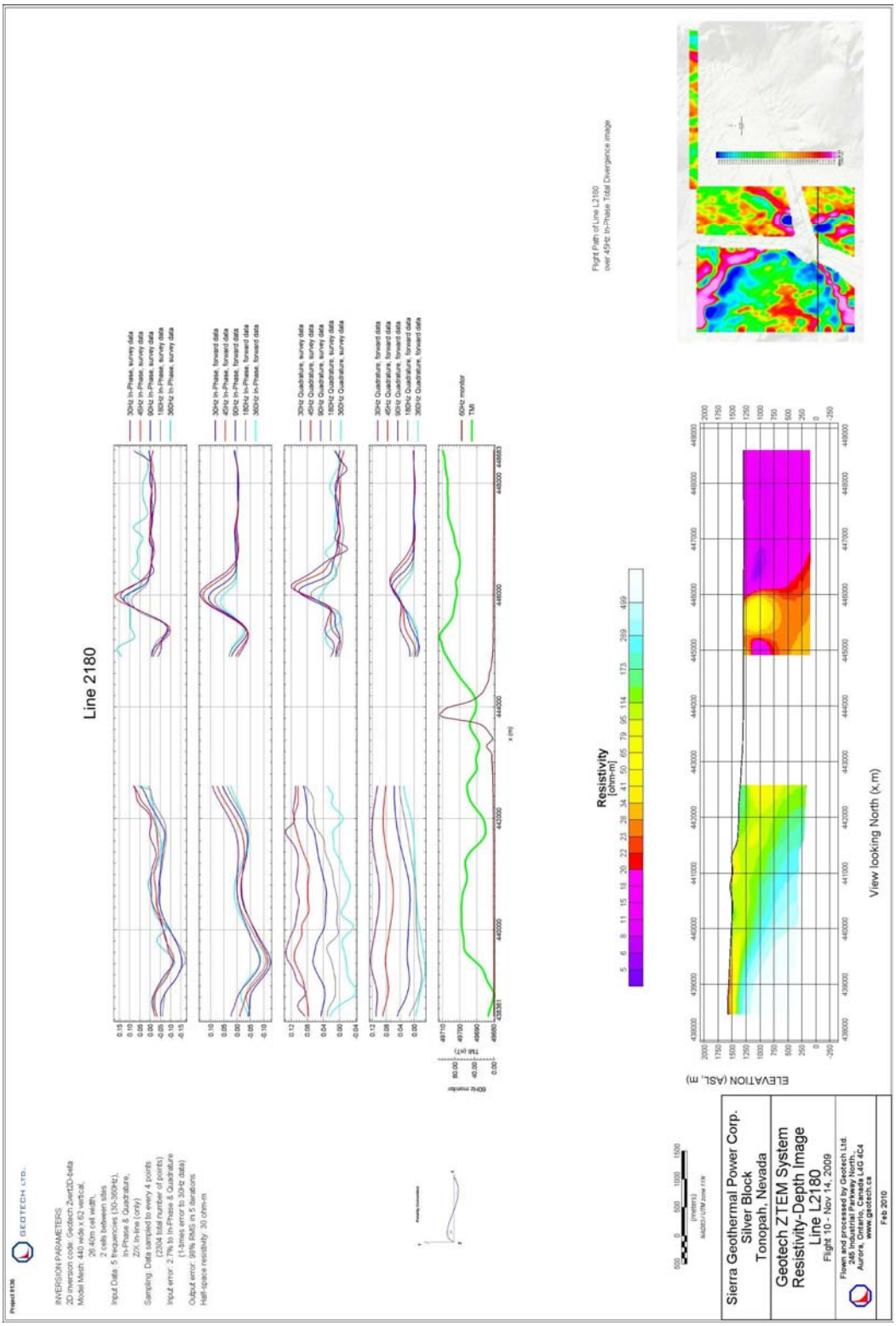

Silver Block Line 2180

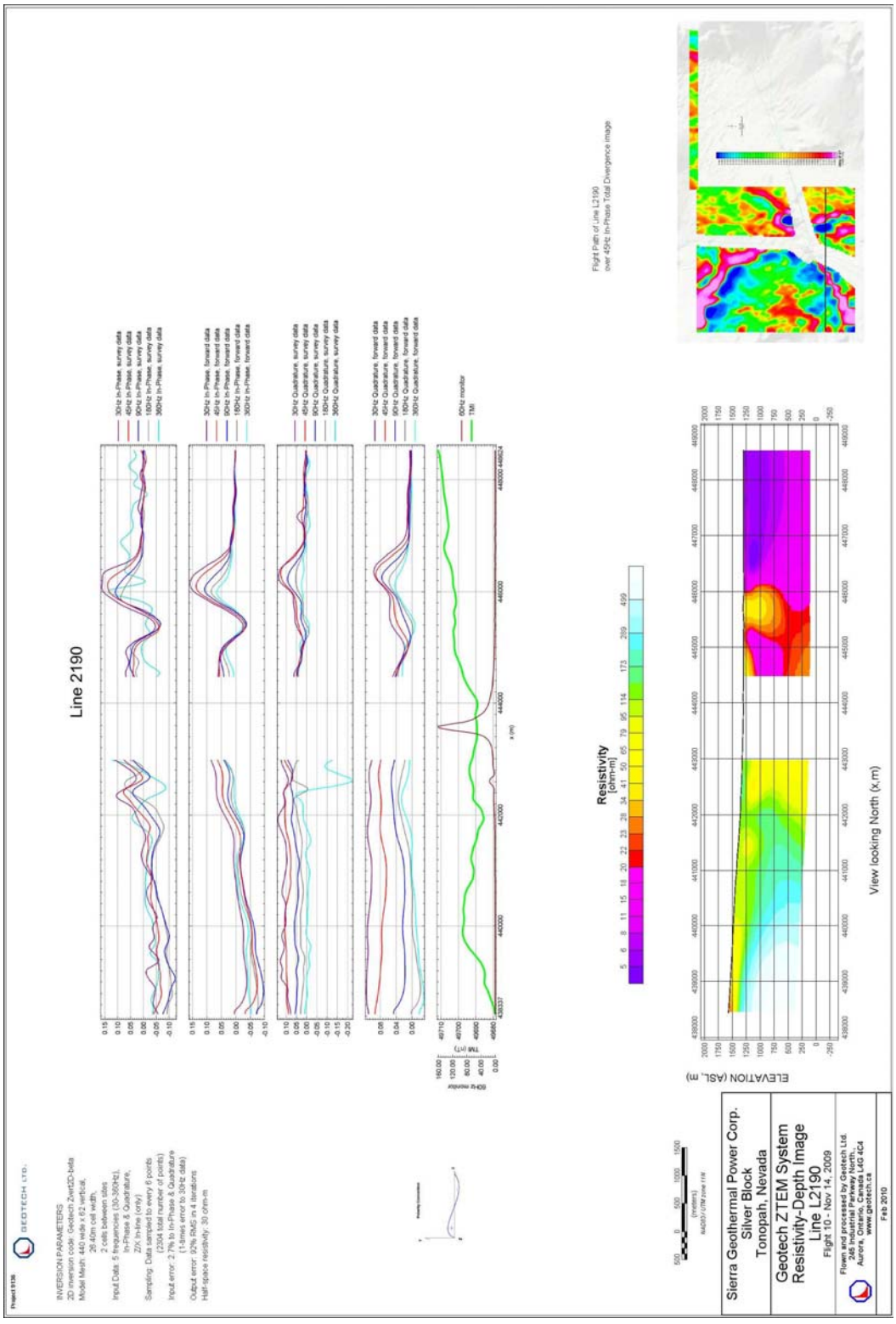

Silver Block Line 2190

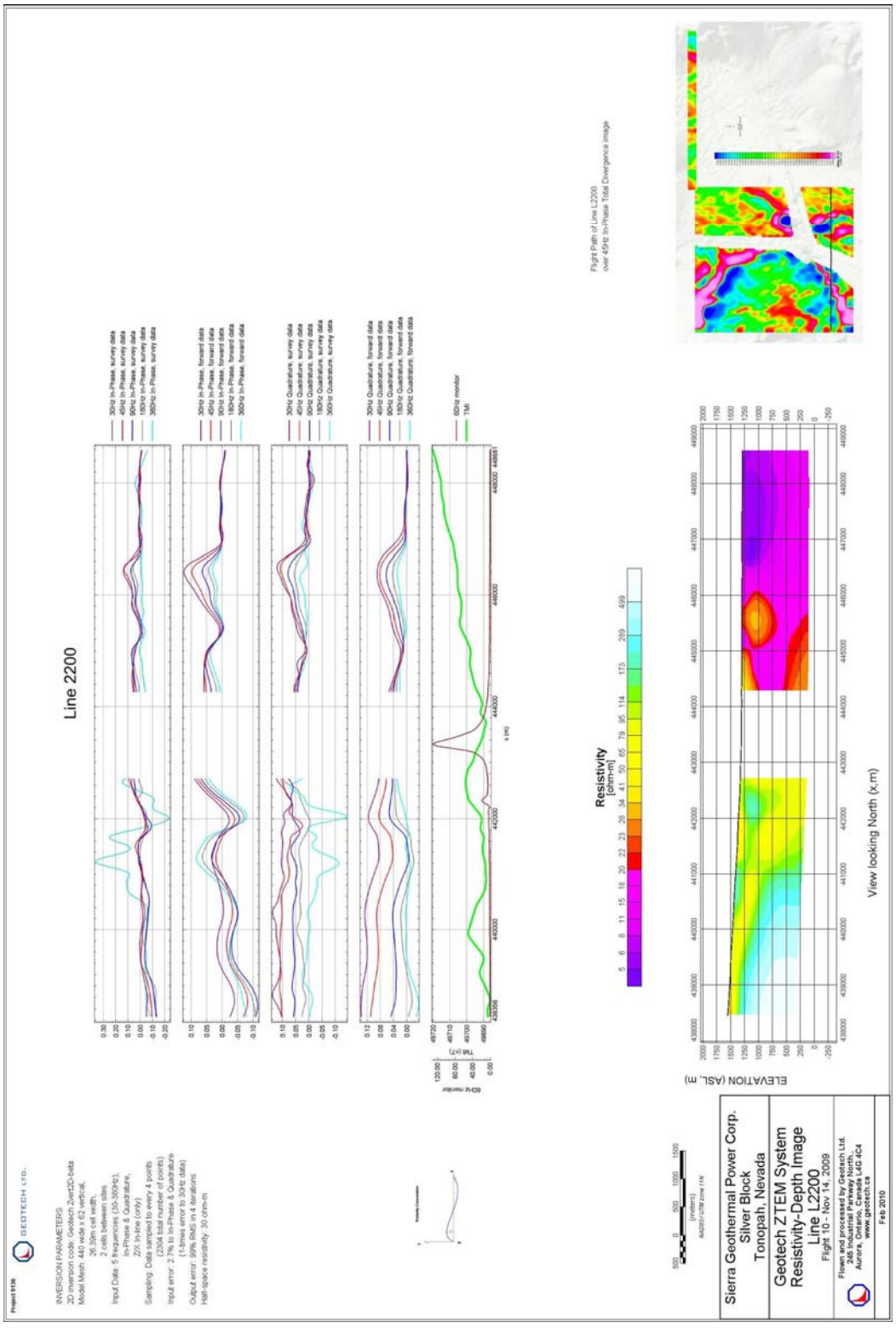

Silver Block Line 2200

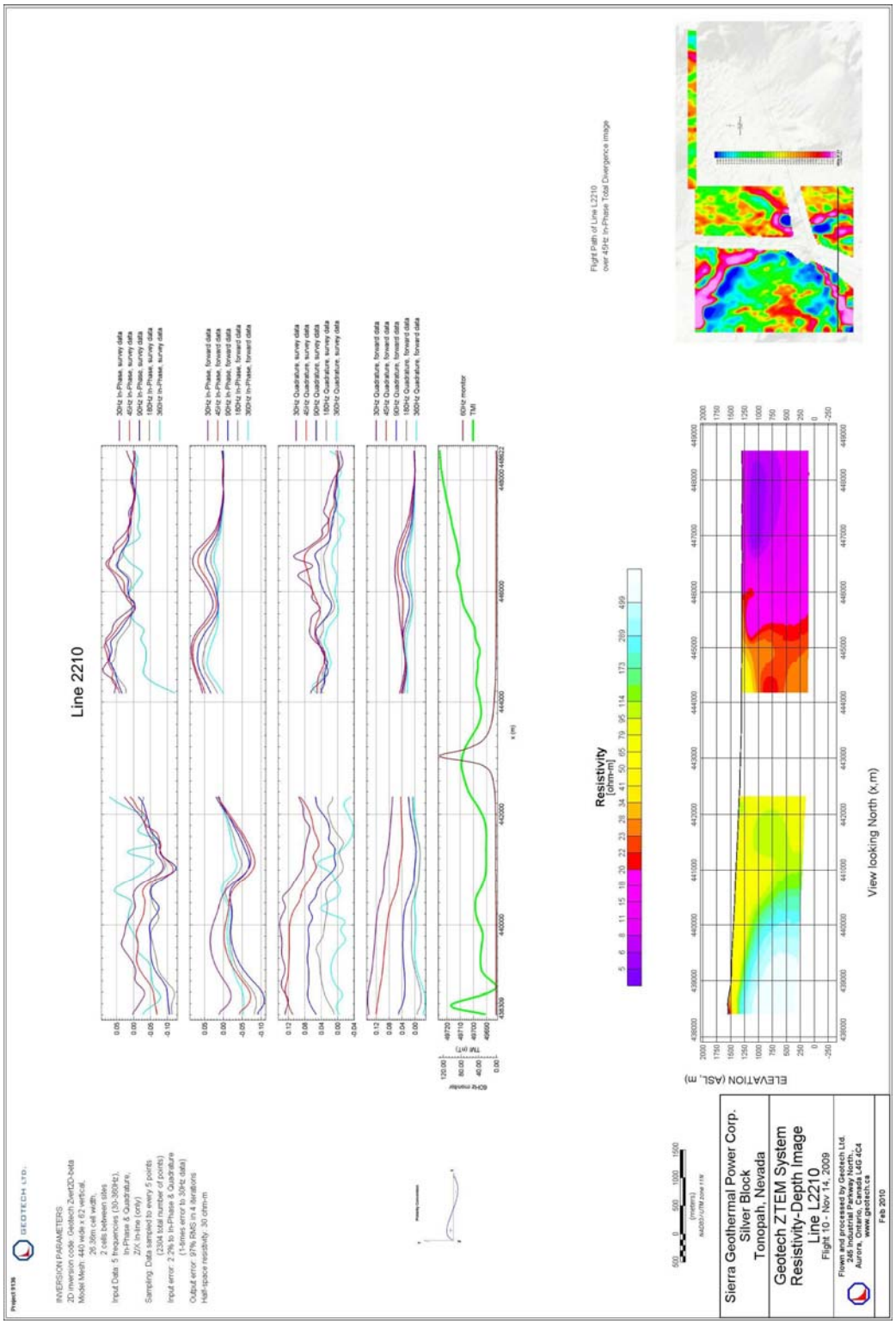

Silver Block Line 2210

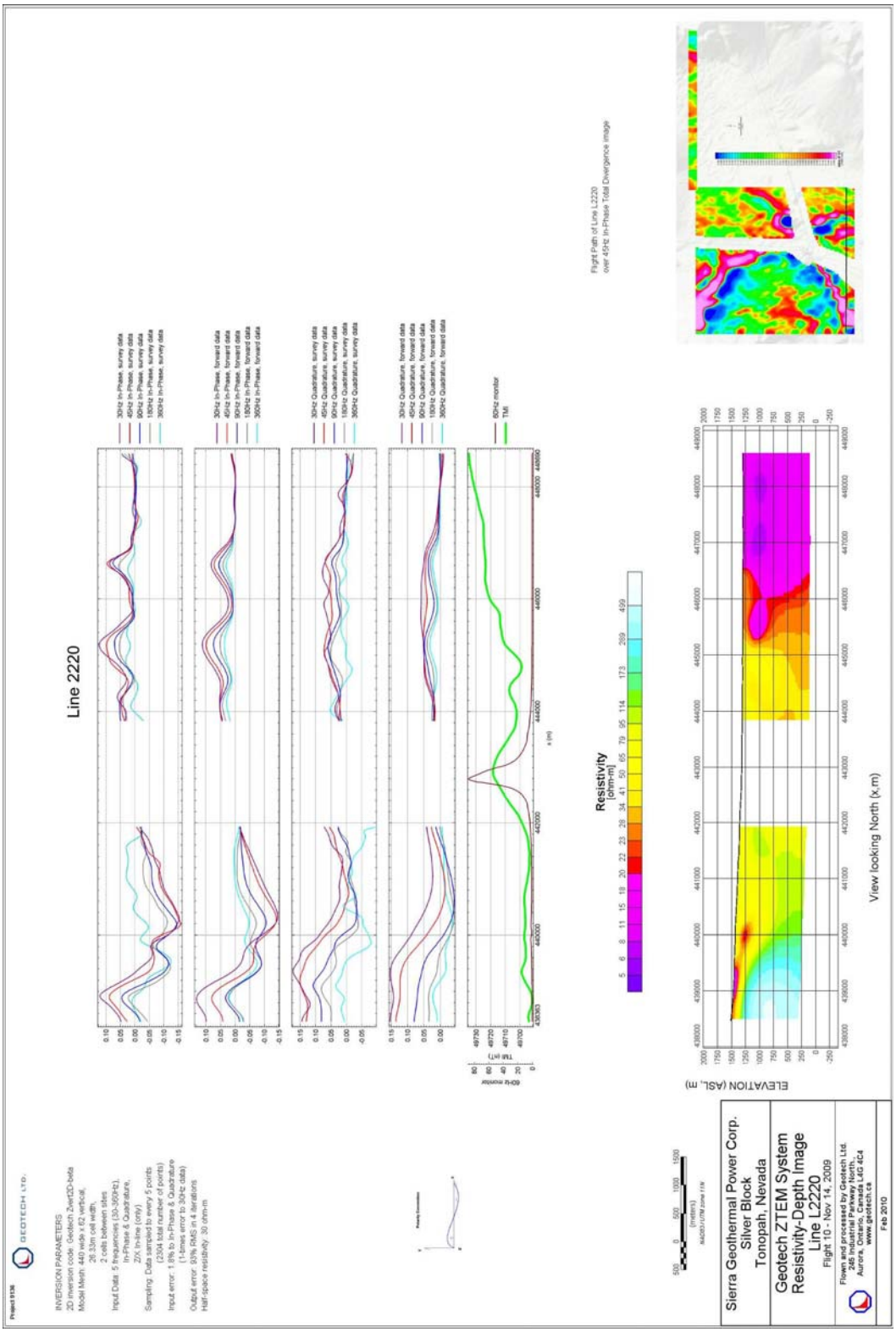

Silver Block Line 2220

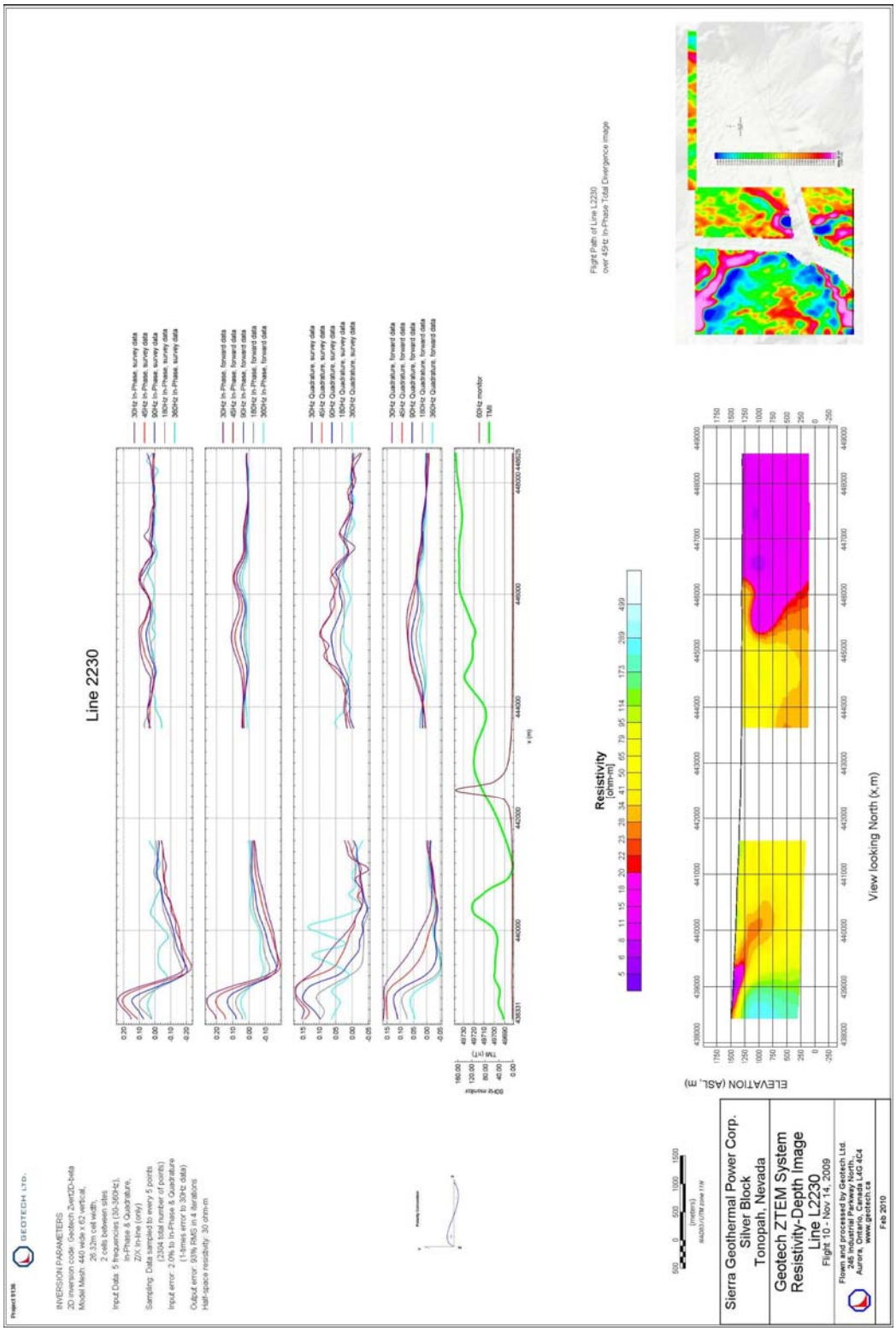

Silver Block Line 2230